(NASA-CR-158575) METALLIZATION OF LARGE SILICON WAFERS Final Report (Motorola, Inc.) 138 p HC A07/MF A01 CSCL 10A

N79-23517

Unclas
G3/44 25179

METALLIZATION OF LARGE SILICON WAFERS

MOTOROLA REPORT NO. 2344/4

FINAL REPORT

JPL CONTRACT 954689

PREPARED BY

ROBERT A. PRYOR

SUBMITTED BY

MOTOROLA INC. SEMICONDUCTOR GROUP

5005 EAST MCDOWELL ROAD

PHOENIX, ARIZONA 85005

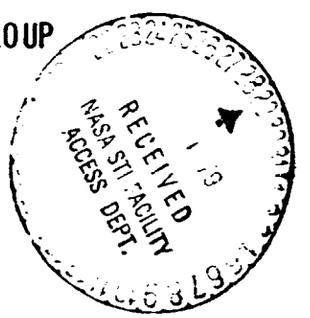

THE JPL LOW-COST SOLAR ARRAY PROJECT IS SPONSORED BY THE U.S. DEPARTMENT OF ENERGY AND FORMS PART OF THE SOLAR PHOTOVOLTAIC CONVERSION PROGRAM TO INITIATE A MAJOR EFFORT TOWARD THE LOW-COST SOLAR ARRAYS. THIS WORK WAS PERFORMED FOR THE JET PROPULSION LABORATORY, CALIFORNIA INSTITUTE OF TECHNOLOGY BY AGREEMENT BETWEEN NASA AND DOE.

PROJECT NO. 2364

DOE/JPL 954689-78/4
DISTRIBUTION CATEGORY UC-63

METALLIZATION OF LARGE SILICON WAFERS

MOTOROLA REPORT NO. 2344/4

FINAL REPORT

JPL CONTRACT 954689

PREPARED BY

ROBERT A. PRYOR

SUBMITTED BY

MOTOROLA INC. SEMICONDUCTOR GROUP

5005 EAST MCDOWELL ROAD

PHOENIX, ARIZONA 85005

THE JPL LOW-COST SOLAR ARRAY PROJECT IS SPONSORED BY THE U.S. DEPARTMENT OF ENERGY AND FORMS PART OF THE SOLAR PHOTOVOLTAIC CONVERSION PROGRAM TO INITIATE A MAJOR EFFORT TOWARD THE LOW-COST SOLAR ARRAYS. THIS WORK WAS PERFORMED FOR THE JET PROPULSION LABORATORY, CALIFORNIA INSTITUTE OF TECHNOLOGY BY AGREEMENT BETWEEN NASA AND DOE.

PROJECT NO. 2364

TABLE OF CONTENTS

SECTION	TITLE	PAGE
1.0	Summary	1
2.0	Introduction	3
3.0	Technical Discussion	5
3.1	Plated Metal Contact Systems	5
3.1.1	Electroless Nickel Plating	6
3.1.2	Palladium Silicide Formation	9
3.1.3	Palladium Plating	9
3.1.4	Combined Pd_2Si-Ni Contacts	10
3.2	Initial Nickel Palladium Metallization System (NPMS)	11
3.3	Pre-Plating Surface Preparation and Cleaning Experiments	17
3.4	Selective Metal Plating Review	26
3.4.1	Electroless Plating Reactions	26
3.4.1.1	Electroless Nickel	27
3.4.1.2	Electroless Palladium	29
3.4.2	Immersion Plating Reactions	30
3.5	Development of an Advanced Immersion Palladium Chemistry	31
3.5.1	Initial Immersion Palladium Studies: Fluoboric Acid Bath	31
3.5.2	Aqueous Bath with Hydrofluoric Acid	41
3.5.3	Aqueous Bath with Hydrochloric and Hydrofluoric Acids	42
3.5.4	Ammonium Fluoride Immersion Bath	45

SECTION	TITLE	PAGE
3.5.5	Immersion Plating Model	50
3.6	Plating Process Refinements	53
3.6.1	Ambient Light Level	53
3.6.2	Solution Temperature	55
3.6.3	Electroless Palladium Bath Composition	55
3.7	Heat Treatment Sequences for Silicide Formation	58
3.7.1	Heat Treatment Ambient	58
3.7.2	Heat Treatment Temperature	59
3.8	Recommended Palladium-Nickel-Solder Metallization Process	64
3.8.1	Process Sequence Outline	64
3.8.2	Plated Surface Characteristics	64
3.8.3	Typical Electrical and Mechanical Performance	74
3.9	NPMS Cost Estimates	80
3.9.1	Initial IPEG Price Analysis	83
3.9.2	Assumptions for Initial Cost Estimates	86
3.9.3	Detailed Expense Calculations	88
3.9.3.1	Steps 1a, 4a, and 6a: Acid Etch and Water Rinse	88
3.9.3.2	Step 1b: Immersion Palladium Coat and Water Rinse	93
3.9.3.3	Steps 1c, 4d, and 6c: Spin Dry	97
3.9.3.4	Steps 2 and 5: Heat Treatment and Palladium Silicide Formation	99
3.9.3.5	Step 3: High Pressure Scrub	100
3.9.3.6	Step 4b: Immersion Palladium Dip and Water Rinse	102
3.9.3.7	Step 4c: Electroless Palladium Plate and Water Rinse	102

SECTION	TITLE	PAGE
3.9.3.8	Step 6b: Electroless Nickel Plate and Water Rinse	104
3.9.3.9	Step 7: Solder Coat	107
3.9.4	Initial Price Analysis Results	110
3.9.5	Revised IPEG Price Analysis	118
4.0	Conclusions	123
5.0	Recommendations	125
6.0	New Technology	126
7.0	NPMS Annotated Bibliography	127

1.0 SUMMARY

A metallization scheme has been developed which allows selective plating of silicon solar cell surfaces. The system is comprised of three layers. Palladium, through the formation of palladium silicide at 300°C in nitrogen, makes ohmic contact to the silicon surface. Nickel, plated on top of the palladium silicide layer, forms a solderable interface. Lead-tin solder on the nickel provides conductivity and allows a convenient means for interconnection of cells.

To apply this metallization, three chemical plating baths are employed. Palladium is deposited with an immersion palladium solution and an electroless palladium solution, and nickel is deposited with an electroless nickel solution. Solder is applied with a molten solder dip. Extensive development work has been performed to achieve an effective immersion palladium solution formulation, leading to reproducible formation of the palladium silicide contact layer.

This metallization system has been repeatedly demonstrated to be extremely effective. Current-voltage characteristic curve fill factors of 78% are easily achieved. This has been done while maintaining metal contact adhesion at such a strength as to fail by fracturing silicon upon perpendicular pull testing rather than by delaminating the metal system.

Demonstrations have been performed on a laboratory scale using beakers, hot plates, and lots of 24 three inch diameter solar cells. On this basis, process specifications and procedures have been prepared. The laboratory process could be easily scaled to full production volume.

Although this metallization system has been shown to be cost effective in its present state of readiness, specific areas have been identified which

would profit from additional development, leading to appreciable further cost reductions which would make the metallization cost a minor factor in 50¢/watt solar cell economics.

A document, "Material, Supply, and Process Specifications and Procedures for Metallization of Large Silicon Wafers with the Palladium-Nickel-Solder Metallization System," has been prepared and will be available from JPL upon request.

2.0 INTRODUCTION

In pursuance of JPL Contract No. 954689, an advanced process for silicon solar cell metallization has been developed and demonstrated to be capable of permitting high reliability and large volume at low cost. The metallization, which has been demonstrated on a developmental laboratory scale, is discussed in this report.

This process is the forerunner of a production-ready process and requires advanced development in order to be entirely suitable for the high throughput, low cost technology required for long term goals. For example, chemical plating solutions are now contained and used in small volume beakers rather than in large volume, continuously replenished tanks, and heat treatments are performed in quartz tube lined, resistance heated furnaces rather than by using more appropriate belt furnaces. The fundamental process has, however been defined.

The metallization can be selectively plated to exposed silicon surfaces with no need to specially protect areas covered with a dielectric (such as an antireflection coating). The metallization scheme is comprised of three layers. Palladium, through the formation of palladium silicide at elevated temperatures, forms the ohmic contact to the silicon surface. Nickel, plated on top of the palladium silicide/palladium layer, forms a solderable interface. Lead-tin solder on the nickel provides high conductivity at low cost, allows a convenient means for interconnection of cells, and yields some additional degree of protection against deleterious effects resulting from moisture ingression.

The process discussed here is relatively complex and is considered to contain the maximum number of process steps required for assured metallization of n-on-p solar cells with n+ front surfaces and p+ back surfaces. It is probable that, in the future, this process may be altered, or steps be eliminated. To date, attempts to shorten the process have met with varying degrees of success. Such attempts have been sufficiently successful to show

feasibility, but not successful enough to guarantee a favorable outcome each and every time. This guarantee must be a prerequisite for a process sequence recommendation.

The process sequence reported here may require minor modifications to account for different types of solar cell substrates and to account for the previous processing history of substrates prior to metallization. For example, while an initial rinse in a dilute hydrofluoric acid solution is sufficient cleaning for most types of samples, some samples prepared in different fashion may require a more elaborate clean to ensure adequate plating to the silicon surface. This process does, however, assure a high quality metallization and cell performance on standard Motorola solar cells.

This report also discusses the technical details and background information which assist in understanding the principles and logic of a chemical plated, palladium-nickel-solder metallization system. The advanced development of palladium plating solutions is described, and process refinement are reviewed. In addition, a detailed exercise of the JPL IPEG price analysis is presented. This includes process equipment and throughput specifications.

Finally, conclusions are drawn and recommendations (including future advancements of the plated metal system process sequence) are given.

3.0 TECHNICIAL DISCUSSION

3.1 PLATED METAL CONTACT SYSTEMS

Plated contacts, particularly those incorporating electroless nickel, have been utilized in the past for solar cells as well as in other semiconductor metallization applications. While plated nickel contacts still find broad utilization in very deep junction devices, such as some silicon rectifier products, lack of plating control and rapid solid state diffusion of nickel into silicon have caused problems requiring plated nickel contacts for solar cells with shallow junctions to be largely supplanted by other metallization techniques. Experience in the solar cell industry has shown that it is difficult to control consistency of both the electroless nickel plating rate and adherence of the electroless plated nickel to the solar cell surface. A heat treating (sintering) cycle can be used to promote adherence of nickel to silicon, but solar cell current-voltage characteristic degradation can occur by diffusion of nickel into the p-n junction region, lowering cell fill-factor and efficiency.

Provided that control and reliability are good, however, plated contacts offer distinct advantages over all other metallization techniques for solar cells. The plated contact requires a relatively small capital investment, is amenable to both batch and continuous type processing, and is the most tolerant with respect to varying surface structure. Future solar cells will be fabricated on large area sheets of silicon which will be thin and may not be flat and smooth. In fact, it is anticipated that such future silicon substrates for solar cells will have varying degrees of curvature, taper, warpage, surface ripple, and surface texturing. A plated contact scheme which gives satisfactory performance today will be directly applicable to such future cells.

If a solderable metal film such as nickel is formed as part of the plating sequence, the contacts can be coated with a thick solder layer to provide both an inexpensive conductor and an additional degree of environmental protection.

To study and develop plated metal contact systems, the Motorola Solar Energy R&D Department has evolved solar cell fabrication processes designed to be compatible with plated metallization. Prior to metallization, an anti-reflection coating, which passivates the p-n junction perimeter and the silicon surface, is formed on the solar cell. The desired metal contact areas can then be exposed through the dielectric antireflection coating by patterning the coating with photolithographic, screen printing, printed wax, or shadow-masked plasma etching techniques. When metal plating reactions are selective, plating occurs only on the exposed silicon surface where the antireflection coating is removed, and no plating occurs on the remaining antireflection coating. Thus, the metal contacts are formed only where desired.

A literature search was conducted early in the program, and continual updating has been performed. It is included in this report as Section 7.0.

3.1.1 ELECTROLESS NICKEL PLATING

Nickel is a desirable contact because it is solderable and is capable of making ohmic contact to silicon. However, two major problem areas have

limited the use of electroless nickel for solar cell contacts. The first major problem area is uniformity control and repeatability of the plating process itself; the second problem area is ensuring good contact adherence, especially to shallow junction devices. Both of these problems contribute to questionable reliability.

The most appropriate electroless nickel bath for silicon contact application has been found to be the ammonia-type, basic (high pH) bath utilizing sodium hypophosphite as a reducing agent. On a bare silicon surface, the basic bath plates more readily, consistently, and uniformly than acid (low pH) baths. It has been observed, however, that the basic bath can chemically attack the silicon surface, forming a thin film between the silicon surface and the nickel layer. This film has been analyzed and found to be primarily SiO_2. It is postulated that, during plating of electroless nickel onto a bare silicon surface, some amount of this thin oxide layer is always formed and that its thickness and uniformity are the major variables in the control of electroless nickel plating on silicon. The formation of this film is dependent upon temperature, composition, degree of activation, and pH of the plating bath. The interrelations of these bath parameters are complex and not always predictable.

The rate of plating from common electroless nickel baths is highly dependent upon the type and (surface) concentration of the silicon dopant. Heavily boron doped surfaces, for example, plate at a much lower rate than lightly doped surfaces under some bath conditions. Bath components can be adjusted to essentially eliminate such plating rate differences, usually at the expense of bath life or efficiency, however.

As plated on silicon, electroless nickel may exhibit limited adherence and poor contact resistance, probably due (at least in part) to the presence of an oxide layer between the silicon and nickel. Normal procedure is to heat treat the solar cell to allow nickel diffusion to penetrate through any oxide layer and to form a nickel silicide layer. The silicide formation requires interdiffusion of the nickel and silicon.

Part of the difficulty in controlling nickel-silicon interdiffusion is that formation and growth of the nickel silicide interface is primarily a result of the movement of nickel atoms through the existing silicide and into the silicon. On the order of 95% of the atomic motion is contributed by the nickel [15].* Moreover, the first silicide formed is Ni_2Si, which will transform at temperatures greater than 350°C into NiSi. The NiSi region is initiated at the Ni_2Si-Si interface. This indicates that the binding energy of Ni_2Si is not particularly strong and that nickel diffusion may occur well beyond the Ni_2Si-Si interface.

If nickel penetrates to the region of a p-n junction, minority carrier lifetime near the junction decreases, junction characteristics degrade, and solar cell efficiency decreases. This phenomenon is seen primarily as an excess forward current which decreases the solar cell fill-factor. Too deep a nickel penetration can severely degrade solar cell efficiency.

On the other hand, nickel contact strength is strongly dependent upon adequate nickel silicide formation. In order to ensure this formation, a minimum time at an elevated temperature is required. In the case of very shallow junctions, formation of adequate nickel silicide for strength may

*Reference numbers cited, such as [15], are to be found in the NPMS Annotated Bibliography, Section 7.0 of this report.

automatically mean sufficient nickel diffusion in advance of the nickel silicide layer to degrade the p-n junction. As a result, a fine line exists between contact reliability and solar cell efficiency for electroless nickel plated contacts.

3.1.2 PALLADIUM SILICIDE FORMATION

Like nickel, palladium forms a silicide at temperatures as low as 200°C. However, the kinetics and mechanism of formation of the low temperature compound, Pd_2Si, are quite different from those of nickel silicides. First, marker experiments have shown that the interdiffusion of palladium and silicon occurs with nearly equal rates, silicon moving somewhat faster than paliadium [15]. Second, once Pd_2Si is formed, it is stable. Further time or increased temperature, at least up to 500°C, leave the layer unchanged [23]. This indicates a reasonably strong binding energy for the intermetallic compound and a self-limiting depth of palladium diffusion. Further, Pd_2Si grows epitaxially at all temperatures on <111> silicon surfaces, indicating minimal stress at the silicide-silicon interface [12]. These differences between palladium and nickel silicides give rise to the possibility that palladium contacts may provide excellent contact adherence while, at the same time, preserving p-n junction characteristics.

3.1.3 PALLADIUM PLATING

Palladium may be selectively plated from at least two separate types of plating baths: an electroless bath, similar in composition and action to the basic nickel electroless bath, and a displacement type (immersion) bath.

Performance of an electroless palladium bath is quite similar to its nickel counterpart, and it does present some difficulties when used to plate bare silicon surfaces. Just as for electroless nickel baths, the plating rate depends dramatically on the type and conductivity of the silicon surface--the p+ back of an n-on-p solar cell is much more difficult to plate than the n+ front. Good electroless palladium plating on both solar cell surfaces has not yet been readily obtained without some surface preparation step, such as sensitizing with a displacement palladium (immersion) solution.

3.1.4 COMBINED Pd_2Si-Ni CONTACTS

Since palladium is more expensive than nickel, palladium may be utilized to form a Pd_2Si ohmic contact layer with a subsequent nickel layer providing a solderable contact surface. Electroless nickel will plate readily to both palladium and Pd_2Si. Plating occurs at relatively equal rates on Pd_2Si formed on silicon with different doping concentrations and types, eliminating the need to modify nickel baths in order to plate n+ and p+ regions simultaneously.

In addition to being relatively inexpensive, nickel provides a solderable surface which has very low rates of dissolution into lead-tin solders. This characteristic allows for a wide control range of solder time and temperature, both in solder coating the solar cell metallization and in any subsequent reflow (or other high temperature interconnection) operation.

3.2 INITIAL NICKEL PALLADIUM METALLIZATION SYSTEM (NPMS)

Drawing upon observations of the previous Section, a particular plating system was proposed for applying metal contacts to all exposed silicon on solar cell surfaces. The application is selective, in that metal is applied in additive fashion, only to those areas of the cell where bare silicon is exposed and a contact grid pattern is desired. There is no need to remove any metal later in the process sequence.

The proposed system is the "nickel-palladium metallization system" (NPMS). This system consists of three "layers" upon the silicon substrate: a palladium silicide/palladium first layer, a nickel second layer, and a lead-tin solder third layer.

In developing a feasible NPMS process sequence, care must be exercised at any step where a nickel layer undergoes a high (i.e., greater than approximately 250°C) temperature cycle. If the palladium/palladium silicide layer is not totally continuous, nickel can penetrate the junction, the amount of penetration depending on the time and temperature of sinter.

Experiments with solar cells have shown that extremely adherent contacts can be made by forming a layer of Pd_2Si upon which nickel is plated and soldered with no additional heat treatments after the Pd_2Si formation. Cells fabricated with this technique have been subjected to metal layer pull tests which resulted in failure due to silicon substrate fracture rather than lack of metal layer adhesion.

Listed in Table 3.2-1 is an outline of process steps which constituted the initial NPMS sequence. This sequence was shown to be feasible, and provided a starting point for investigation of individual process steps and process variables. In developing a production-worthy process, some steps in the baseline NPMS sequence were changed or even eliminated. Times and temperatures for chemical cleaning and plating steps and for thermal

TABLE 3.2-1

INITIAL NPMS (NICKEL-PALLADIUM METALLIZATION SYSTEM)

STARTING POINT: a) Solar Cell with AR Coat,

b) Metal Pattern Etched Through Front Dielectric,

c) Back Dielectric Totally Etched Away.

STEP	PROCESS
1	Immersion Plate, Thin Pd Layer
2	Sinter 5 Minutes @ 600°C
3	Scrub Back to Remove Free Pd
4	Electroless Plate, Thin Pd Layer
5	Sinter 30 Minutes @ 600°C
6	Electroless Plate, Thick Ni Layer
7	Bake 30 Minutes @ 220°C
8	Solder Dip 60-Sn/40-Pb Solder

All "Sinter" and bake steps to be in forming gas.

treatment cycles are certainly primary variables. Control limits for chemical plating solution operation and bath constituents are also important.

Immersion palladium, electroless palladium and electroless nickel plating solutions which work with the baseline NPMS process of Table 3.2-1 are listed in Tables 3.2-2, 3.2-3, and 3.2-4. The electroless formulations are taken from Modern Electroplating [3], which references the original studies in the literature by Brenner and Riddell [44] and by Pearlstein and Weightman [56].

Success of the NPMS depends critically on performance of the immersion palladium plating step, and considerable effort was devoted to its understanding and control. The immersion palladium bath must consist essentially of $PdCl_2$ in a solution which permits effective plating of silicon surfaces while simultaneously attacking any native silicon oxides present to enhance generalized plating.

TABLE 3.2-2

INITIAL IMMERSION PALLADIUM SOLUTION*

BATH CONSTITUENTS		
Water	H_2O	500 mℓ
Fluoboric Acid	HBF_4	500 mℓ
Hydrochloric Acid	HCl (38%)	2.5 mℓ
Palladium Chloride	$PdCl_2$	0.050 g

OPERATING TEMPERATURE: ROOM TEMPERATURE

*This table gives the initial, proposed formulation. For the final, recommended formulation, see page 53.

TABLE 3.2-3

INITIAL ELECTROLESS PALLADIUM PLATING BATH*

Bath Constituents

Palladium Chloride	$PdCl_2$	2 g/l
Hydrochloric Acid	HCl (38%)	4 ml/l
Ammonium Hydroxide	NH_4OH (25% NH_3)	160 ml/l
Ammonium Chloride	NH_4Cl	27 g/l
Sodium Hypophosphite	$NaH_2PO_2 \cdot H_2O$	10 g/l

MAXIMUM OPERATING TEMPERATURE: $55^{\circ}C$

*REFERENCE NO. 3, Page 740.
This table gives the initial, proposed formulation. For the final, recommended formulation, see page 56.

TABLE 3.2-4

ELECTROLESS NICKEL PLATING BATH*

Bath Constituents

Nickel Chloride	$NiCl_2 \cdot 6H_2O$	30 g/l
Sodium Hypophosphite	$NaH_2PO_2 \cdot H_2O$	10 g/l
Sodium Citrate	$Na_3C_6H_5O_7 \cdot 2H_2O$	84 g/l
Ammonium Chloride	NH_4Cl	50 g/l

ENOUGH NH_4OH IS ADDED TO MAINTAIN BATH pH BETWEEN 8 AND 10

MAXIMUM OPERATING TEMPERATURE: $95^{o}C$

*REFERENCE NO. 3, page 713
This is both the intial and final formulation.

3.3 PRE-PLATING SURFACE PREPARATION AND CLEANING EXPERIMENTS

Pre-plating cleans of silicon wafer surfaces have been deemed to be of special importance for insuring repeatable and consistent selective plating depositions. In particular, in forming the initial NPMS palladium layer with an immersion palladium plating, the silicon must be clean to guarantee an adherent and uniform palladium deposition.

Over the course of the NPMS process sequence development, several investigations have been performed to assess the effectiveness of various cleaning and surface preparation techniques. These experiments were conducted by first preparing solar cells by using the particular cleaning technique under consideration, and then attempting to deposit a palladium layer on the silicon surface using one of several formulations of immersion palladium solutions. The outcome of each experiment was evaluated by SEM (scanning electron microscope) examination of the plated surface. Some plated layers were abraded with cellulose swabs to test metal adhesion.

The first group of experiments utilized the fluoboric acid immersion palladium solution (HBF_4ImPd) to study the benefits of various pretreatments which attack silicon, silicon dioxide, or miscellaneous organic contaminants. These pretreatments may be used alone or in sequential combinations. Five sequences studied are diagrammed in Tables 3.3-1 and 3.3-2.

If the silicon surface as-received for plating is already reasonably clean, then silicon dioxide etches using dilute hydrofluoric acid (HF) solutions, such

TABLE 3.3-1

PRECLEANS BASED ON THE ACID ETCHING OF OXIDES

CLEAN A

10:1 H_2O:HF etch

↓

DIH_2O rinse

↓

HBF_4 ImPd

↓

SEM

CLEAN B

10:1 H_2O:HF etch

↓

50:1 H_2O:HF rinse

↓

HBF_4 ImPd

↓

SEM

TABLE 3.3-2

PRECLEANS BASED ON SHALLOW ETCHING
OF THE SILICON SURFACE

CLEAN C

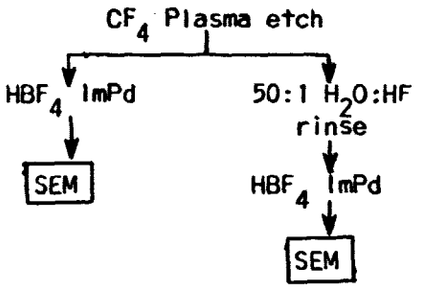

CLEAN D

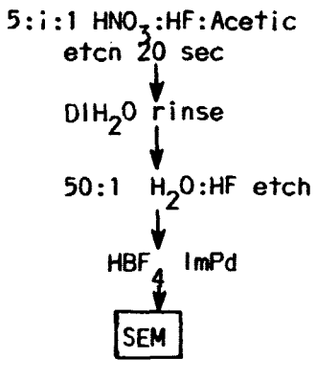

CLEAN E

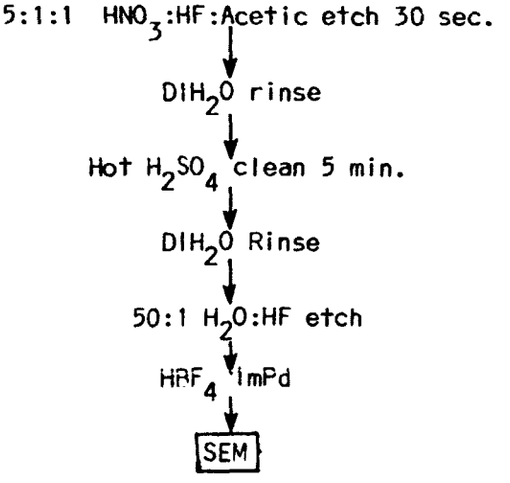

as outlined in cleans A and B of Table 3.3-1, are reasonably effective. However, more positive overall results were obtained with cleans C, D, and E which were capable of lightly etching the silicon surface in the solar cell ohmic contact areas. Clean C used a dry plasma etch (CF_4) technique while cleans D and F used wet nitric-hydrofluoric-acetic acid etch solutions. In addition, clean E incorporated a hot sulfuric acid clean, expected to attack organic contaminants.

Clean E, in particular, showed some promise of improved plating performance, and so a second group of experiments was performed to further investigate variations of this clean by using different silicon etch compositions and to establish whether a hot sulfuric acid clean would be sufficient without using the silicon etch. Cleans F and G in Table 3.3-3 use different ratios of nitric acid, hydrofluoric acid, and acetic acid in the silicon etch solution. If the silicon etch step is deleted, the clean H of Table 3.3-4 is obtained. Clean I of Table 3.3-4 is a simplification of clean H.

Cleans F, G, H, and I were evaluated with the immersion palladium solution which contains fluoboric acid (HBF_4 ImPd) and also with a solution in which the fluoboric acid was eliminated and the HCl content was increased. This particular solution (HCl ImPd) closely resembles the well known solution of palladium chloride, hydrochloric acid, and water used to "sensitize" various metals and non-metals for subsequent electroless plating.

This second group of experiments (Tables 3.3-3 and 3.3-4) indicated that sulfuric acid treatment is of some advantage in promoting improved plating. It also showed that a silicon etch greatly improves the immersion palladium layer plating uniformity.

Unfortunately, there are some major drawbacks to using a silicon etch. When working with shallow solar cell junctions, there is not much room for error while etching the silicon surface. The silicon etch rate must be precisely

TABLE 3.3-3

ADDITIONAL SILICON ETCH CLEANING PROCEDURES

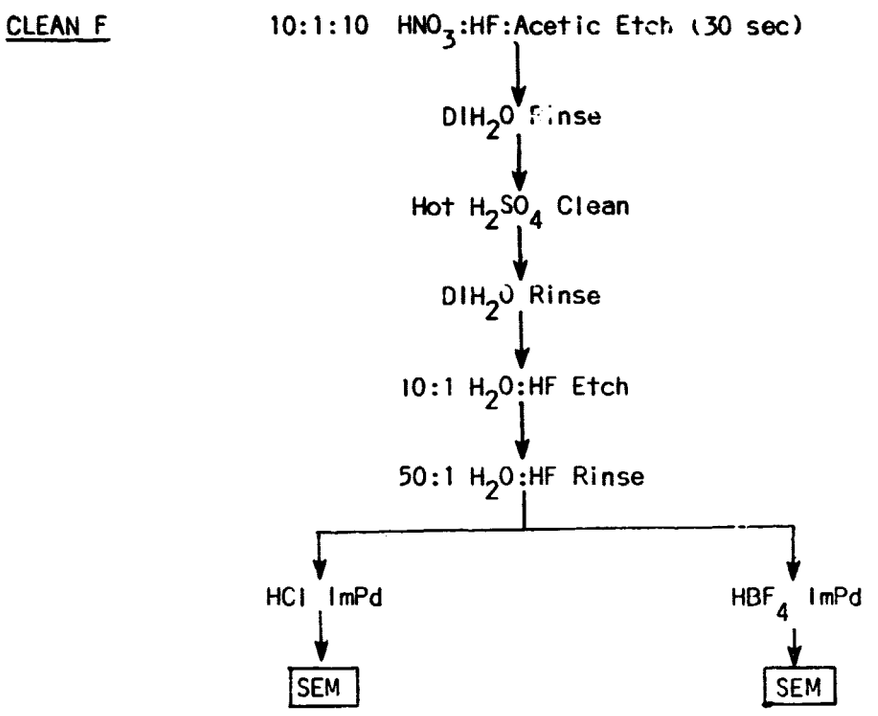

TABLE 3.3-3 (continued)

CLEAN G

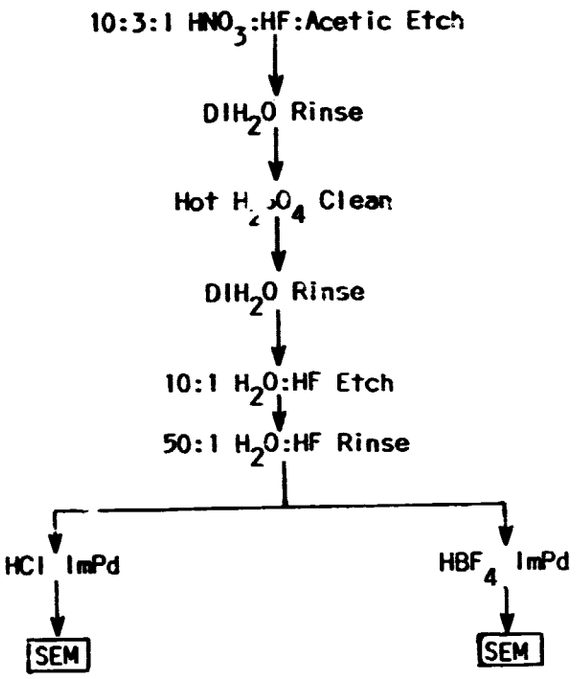

TABLE 3.3-4

PRECLEANS DESIGNED TO REMOVE ORGANIC CONTAMINANTS

CLEAN H

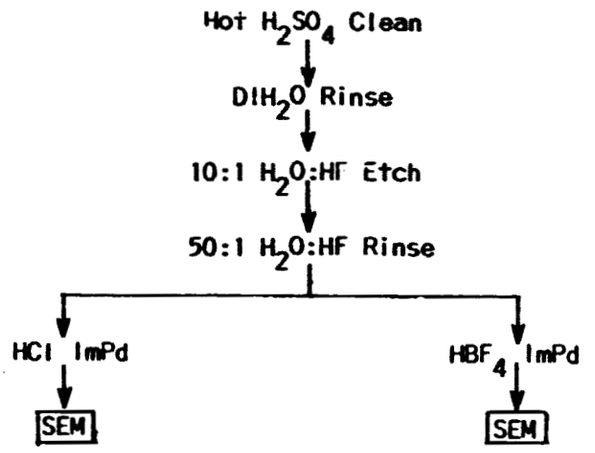

CLEAN I

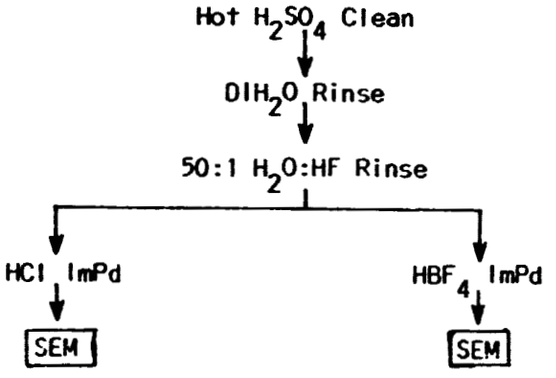

controlled or the junction is quickly penetrated and the device ruined; in fact, this effect was experienced. However, since plating occurred more evenly when the surface was lightly etched, there probably are contaminants present, during normal semiconductor processing, which tend to interfere with uniform plating initiation.

One type of impurity which might interfere with good plating behavior is a metallic impurity. Since test solar cell substrates are prepared for metallization by photolithographic patterning of the silicon nitride anti-reflection coating, and since photoresist is notorious for metallic contaminants, it is not unreasonable that metallic impurities may be left behind. For this reason, a cleaning approach which includes a metal etchant has been considered to be useful.

In particular, an approach has been studied whereby solar cells to be plated are first given a plasma "ash" which oxidizes the silicon surface with an oxygen plasma. Any organic contaminants present during this step will be oxidized and volatilized. After chemically etching the silicon dioxide formed during the plasma clean, the cells are immersed in a metal etchant such as a hydrochloric acid solution or an aqua regia solution (HCl and HNO_3). Immediately before the immersion palladium bath step, the cells are rinsed in a dilute HF solution to guarantee an oxide-free surface. An example of this sequence is diagrammed in Table 3.3-5.

This type of pre-clean procedure has given consistent initiation of immersion palladium deposits with various solar cell test samples which have been fabricated. In the future, when photolithographic etching of metal contact patterns is replaced by more economical techniques, a less involved cleaning procedure may suffice.

TABLE 3.3-5

PRECLEAN SEQUENCE INCORPORATING BOTH
PLASMA REMOVAL OF ORGANICS AND
CHEMICAL ETCHING OF METAL IMPURITIES

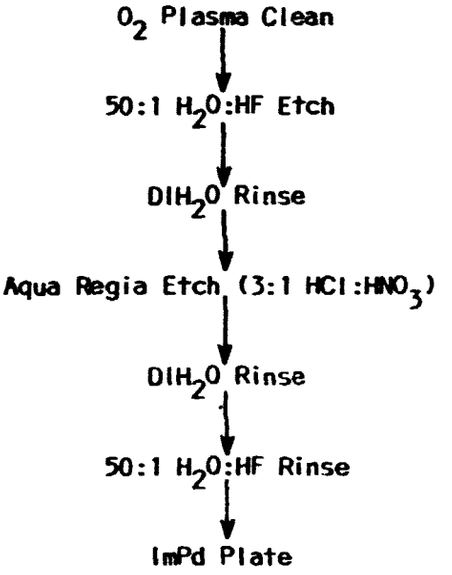

3.4 SELECTIVE METAL PLATING REVIEW

A number of the advantages of the NPMS process sequence are derived from the fact that the metal plating processes used are selective. That is, metal is plated only onto exposed areas of silicon where metal contact is desired. Areas protected by dielectrics or other masks are not plated. This results in an additive metallization system which minimizes materials waste. In addition to being selective, the plating processes chosen for the NPMS are non-electrolytic. Being self-initiating, they require no electrical connections to the solar cell and do not require external potentials or electric currents to initiate and maintain the plating reactions. Three types of non-electrolytic plating solutions are employed for the NPMS process. They are an immersion palladium solution, an electroless palladium solution, and an electroless nickel solution. A brief review of the fundamentals of the chemistry and behavior of these solutions is presented below.

3.4.1 ELECTROLESS PLATING REACTIONS

In electrolytic plating processes, electrons are supplied from a D.C. power source to convert metal ions in a plating solution to metallic form at the surface of the part being plated. However, with electroless plating processes, metal deposition occurs by immersion of the part in solution with no electrical connections or D.C. power supply attached. Necessary electrons are supplied by a chemical reducing agent dissolved in the solution. Simultaneous with the reduction of a metal salt to the metal, the reducing agent is oxidized. To

prevent spontaneous decomposition of the plating solution, electroless plating baths are formulated to have concentrations of the metal salt and the reducing agent, and the solution pH, such that metal reduction occurs only in the presence of a catalyst.

In fact, electroless deposition is defined as the autocatalytic chemical reduction of metal from solution. Hence, the metal being deposited serves as its own catalyst for the continuation of the reaction. In this manner, deposits may be built up as thick as desired. All that is necessary is that the initial surface to be plated be catalytic as well.

One characteristic of the electroless reaction is that elements of the reducing agent are incorporated into the metallic deposit. Thus, the metal layer built up by the electroless solution is not pure but contains a small percentage (3% to 15%) of other elements. This may or may not be of advantage to the characteristics of the metal layer.

3.4.1.1 ELECTROLESS NICKEL

Electroless nickel plating was discovered by Brenner and Riddell in 1944 and first reported in 1946 [44]. Since then it has become the most familiar and widely used electroless plating process in industry. Numerous electroless nickel solution formulations are available in both acid and alkaline form, employing several different reducing agents and at least two different nickel salts. These nickel salts are nickel chloride ($NiCl_2$) and nickel sulfate ($NiSO_4$), and a very common reducing agent is sodium hypophosphite (NaH_2PO_2).

The most probable reactions which occur in electroless nickel plating when sodium hypophosphite is the reducing agent are given in the following equations [48]:

$$[H_2PO_2]^- + H_2O \xrightarrow{\text{catalyst } (Ni^o)} H^+ + [HPO_3]^{--} + 2\,H_{catalyst} \quad (1)$$

$$Ni^{++} + 2\,H_{catalyst} \rightarrow Ni^o + 2H^+ \quad (2)$$

$$[H_2PO_2]^- + H_{catalyst} \rightarrow H_2O + OH^- + P \quad (3)$$

$$[H_2PO_2]^- + H_2O \xrightarrow{\text{catalyst } (Ni^o)} H^+ + [HPO_3]^{--} + H_2\uparrow \quad (4)$$

In the presence of water, hypophosphite anions are dehydrogenated by the nickel catalytic surface, shown in equation (1). The active hydrogen atoms are adsorbed or loosely bonded on the nickel surface, as indicated by the symbol $H_{catalyst}$ in equations (1), (2) and (3). The nickel ions in solution are reduced to metallic nickel by these active hydrogen atoms, shown in equation (2). In equation (3), a small proportion of the hypophosite anions are reduced by the active hydrogen to yield elemental phosphorous. It is this phosphorous which is incorporated into the deposited nickel layer, amounting to between 3% and 15% of the deposit. Finally, equation (4) indicates that additional hypophosphite anions are catalytically oxidized to acid orthophosphite anions which results in the evolution of gaseous hydrogen.

As shown by equations (2) and (4), as the reactions proceed, hydrogen ion concentration increases, thus reducing solution pH. Since the plating rate will decrease as pH decreases, periodic additions of alkali may be necessary

during operation. In addition, chemical additives may be used in the plating solution formulation to serve both as buffers which help stabilize pH, and as complexing agents which promote bath stability.

An electroless nickel solution is inherently unstable, requiring only the presence of a catalyst to initiate a reaction. Complexing agents are used to prevent the formation of insoluble nickel phosphite precipitates. Should such precipitates form, they may act as catalysts, causing spontaneous reduction of the remaining nickel ions throughout the solution. However, with the proper chemical additives, nickel ion complexes are formed which are readily soluble and remain in solution, eliminating precipitates. Examples of chemicals which serve both as buffering agents and complexing agents are sodium citrate ($Na_3C_6H_5O_7$), ammonium chloride (NH_4Cl), and ammonium hydroxide (NH_4OH).

3.4.1.2 ELECTROLESS PALLADIUM

Electroless palladium solutions have been formulated using either hydrazine or sodium hypophosphite as the reducing agent. For the case of sodium hypophosphite, the behavior of the plating solution is very similar to that discussed in Section 3.4.1.1 for electroless nickel. Palladium is entered into solution in the form of a palladium salt such as palladium chloride ($PdCl_2$). Obtaining a solution of palladium chloride in water usually requires the presence of small amounts of hydrochloric acid (HCl) to promote solubility. Once again, chemical additives are used to help buffer pH and to act as complexing agents to promote solution stability. Both ammonium chloride and ammonium hydroxide are used. Unfortunately, electroless palladium solutions tend to be even more unstable than electroless nickel solutions. This limits their working temperature to a maximum of 70°C [56] whereas nickel plating baths may be operated to 95°C.

3.4.2 IMMERSION PLATING REACTIONS

In the electroless plating techniques discussed above, electrons are supplied by a reducing agent to convert metal ions to metallic deposits. If, instead, electrons are supplied by another element going into solution, then immersion (displacement) plating occurs. In immersion deposition, the reaction depends upon the relative electrode potentials of the substrate and deposited metal. When the metal is more noble than the substrate, the immersion process replaces the surface of the substrate with a thin coating of essentially pure metal. This occurs as the substrate surface is dissolved and goes into solution as anions, yielding electrons which can reduce the metal ions already in solution. Therefore, the immersion plating reaction will continue as long as new reaction sites on the substrate are available. In this manner, the deposit thickness is self limiting. When the substrate is completely covered, the reaction must cease.

How well the displacement deposition occurs depends upon the ability of the solution to dissolve the substrate. However, if the substrate is attacked too vigorously this can lead to undercutting and pitting of the immersion deposit, limiting adhesion. It is also possible for a displacement coating not to form continuously, and therefore not stop further reaction; in this case, a much thicker, porous deposit can be obtained.

3.5 DEVELOPMENT OF AN ADVANCED IMMERSION PALLADIUM CHEMISTRY

3.5.1 INITIAL IMMERSION PALLADIUM STUDIES: FLUOBORIC ACID BATH

The baseline NPMS process outlined in Table 3.2-1 provides for the use of three chemical plating solutions. The first solution deposits a layer of elemental palladium (or a palladium compound) by means of a chemical displacement reaction at the silicon surface. The chemical bath used to achieve this reaction is a solution containing palladium chloride ($PdCl_2$) and is called an immersion bath since the displacement reaction is initiated merely by immersing the silicon substrate into the bath.

A primary purpose of the immersion palladium layer is preparation of the silicon surface for subsequent deposition of the electroless palladium layer. Without such preparation, the silicon surfaces of solar cells have proven very difficult to plate in electroless palladium plating solutions. This difficulty is compounded by the high impurity concentrations and opposite conductivity types of the front and back cell surfaces, in order to provide a more catalytic surface, and to minimize electroless plating rate difference between n-type and p-type surfaces, a thin immersion palladium layer is deposited first.

Several types of palladium chloride solutions were initially considered for use as the immersion palladium bath. Differences between the solutions manifest themselves as differences in plating rates on silicon surfaces of various conductivities and conductivity types. One thing various baths considered initially have in common is the fundamental structure of the palladium deposits. Scanning electron microscope photographs show that the palladium is deposited in somewhat hemispherical clumps (grains) of metal (or metal compounds) scattered across the surface of the silicon.

In one experiment, for example, fluorinated solutions of palladium chloride ($PdCl_2$) were prepared with different $PdCl_2$ concentrations: 0.5 standard, standard, 2 standard and 5 standard. The standard solution is that given earlier in Table 3.2-2. Silicon wafers were immersed for 75 seconds and 150 seconds into each of these solutions. The results are shown in the SEM photographs of Figures 3.5-1, 3.5-2, 3.5-3, and 3.5-4.

Observed grain sizes of the deposits from these baths vary from much less than 0.1 micron diameter to as large as 0.5 micron diameter. Grain size, as well as the spacing between grains, is strongly dependent on the concentration of $PdCl_2$ in solution as well as the length of time for which the silicon is plated. As seen in Figures 3.5-1 through 3.5-4, as $PdCl_2$ concentration was increased, the size of the largest grains deposited became greater As plating time was increased there seemed to be a tendency to obtain greater coverage of the silicon surface by depositing small grains in the spaces between the large grains.

The deposits observed in Figure 3.5-1 through 3.5-4 are nowhere near optimum. However, once heat treated (sintered), these deposits provide nucleation sites for the catalytic formation of electroless palladium films. It is believed that electroless palladium will adhere only to the grains deposited in the immersion step. Thus, a major requirement on the initial immersion palladium layer is that it provide an adherent formation of grains. A shortcoming of the particular deposits shown in Figures 3.5-1 through 3.5-4 is that, even after sintering, a substantial portion of the grains can be removed by mechanical abrasion or scrubbing, indicating that adherence is probably not adequate. This is illustrated in Figure 3.5-5 which shows an SEM shot of a solar cell surface after the first three steps of Table 3.2-1. Scrubbing (in this case with a cellulose tissue) has removed a considerable amount of the grains, and shows some smearing of metal.

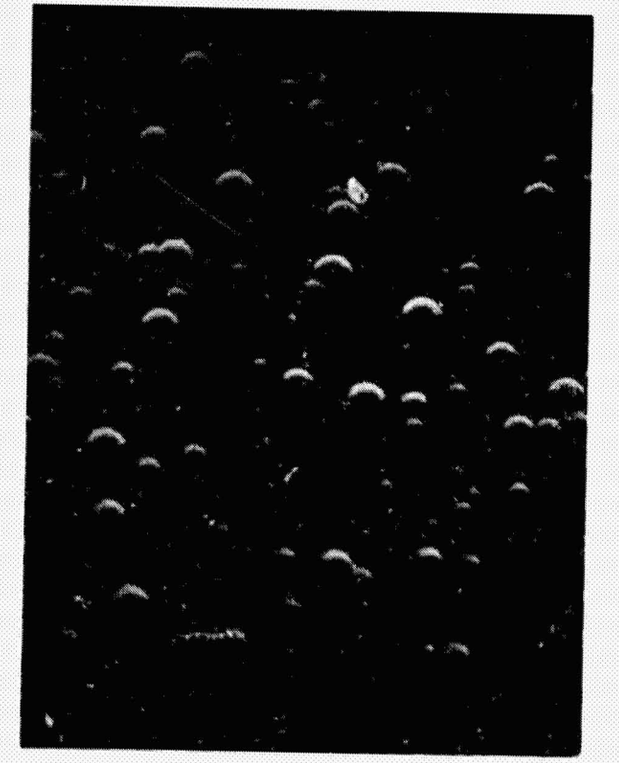

(a) 75 sec. immersion

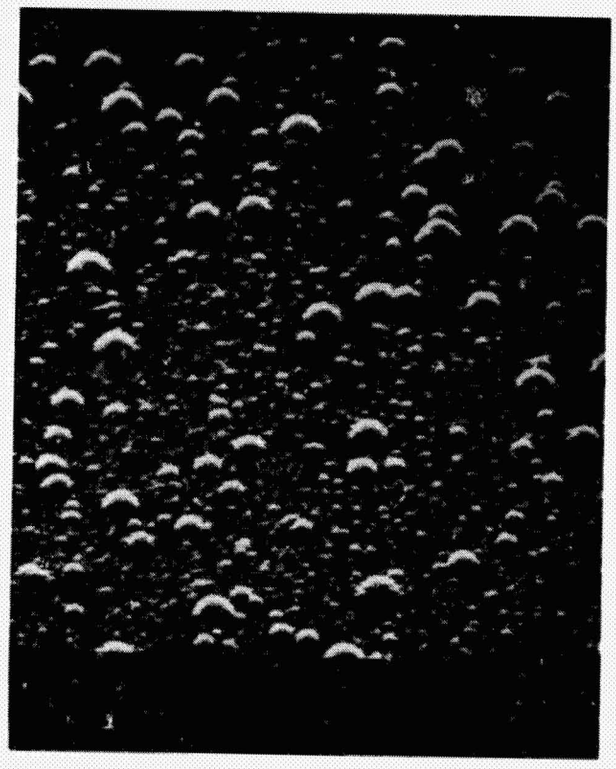

(b) 150 sec. immersion

FIGURE 3.5-1: Immersion palladium plating at one half standard palladium chloride concentration.

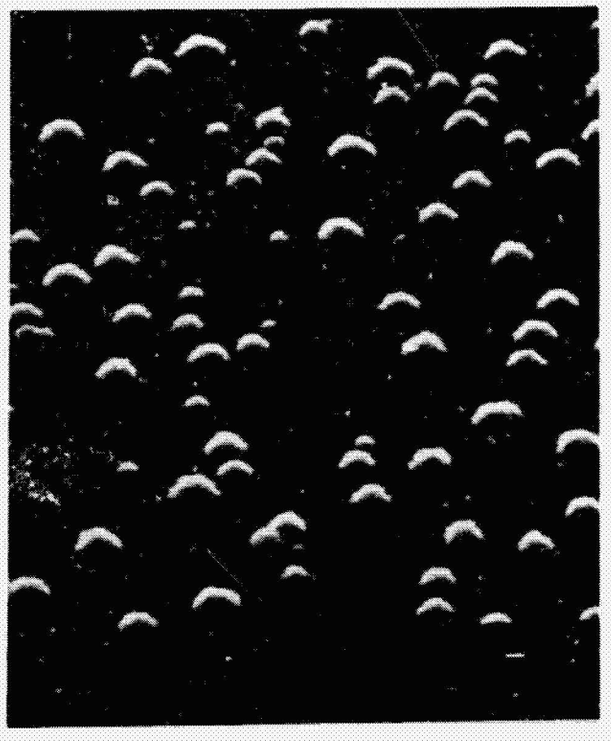

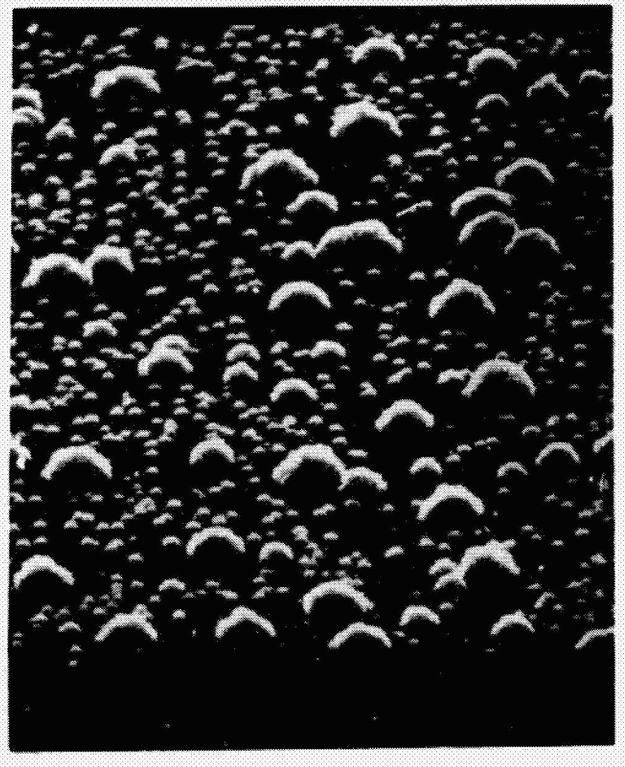

(a) 75 sec. immersion

(b) 150 sec. immersion

FIGURE 3.5-2: IMMERSION PALLADIUM PLATING AT STANDARD PALLADIUM CHLORIDE CONCENTRATION.

(a) 75 sec. immersion

(b) 150 sec. immersion

FIGURE 3.5-3: Immersion palladium plating at twice standard palladium chloride concentration.

(a) 75 sec. immersion

(b) 150 sec. immersion

FIGURE 3.5-4. Immersion palladium plating at five times standard palladium chloride concentration.

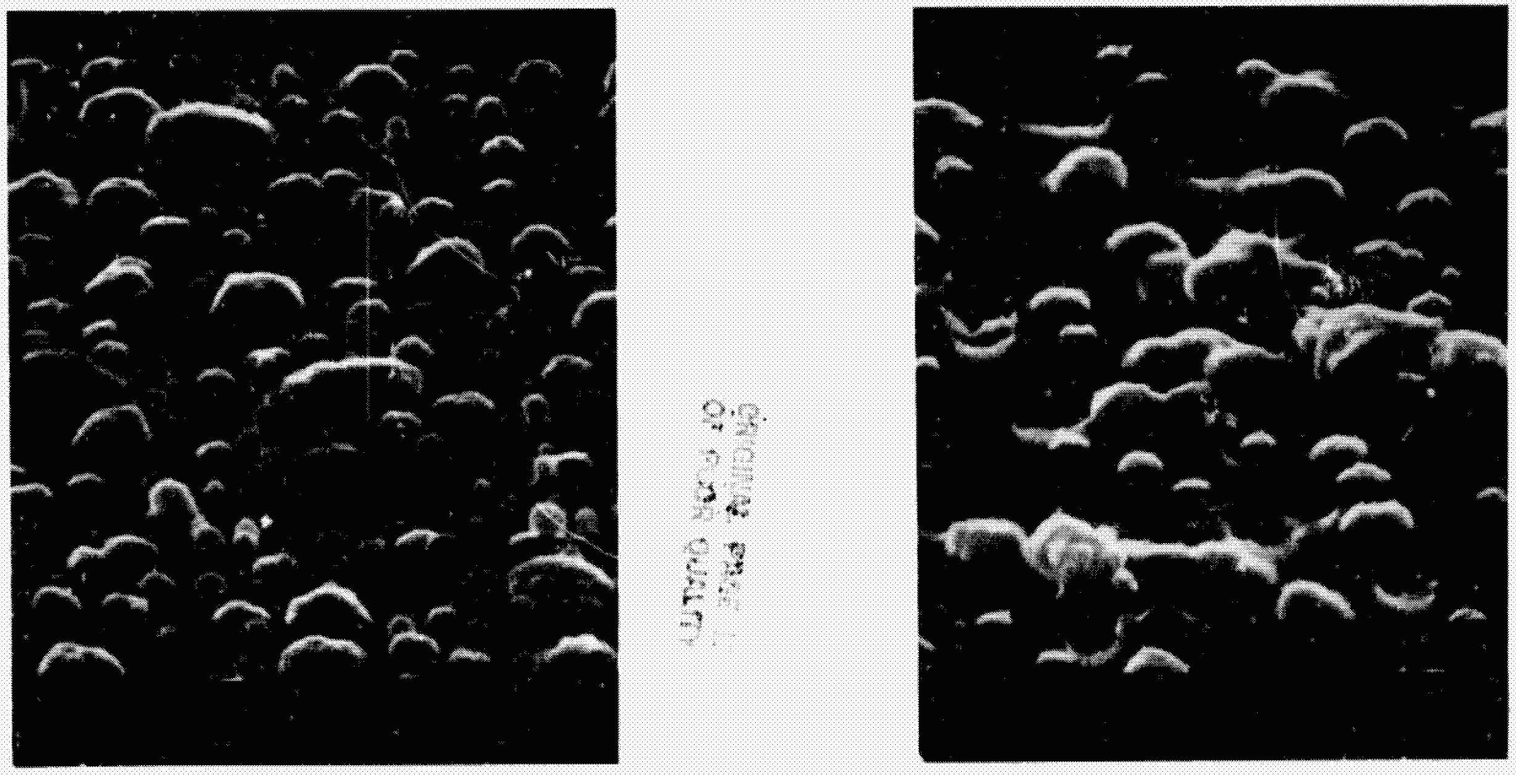

(a) 150 sec. immersion, after sinter, before scrubbing.

(b) after sinter, after scrubbing

FIGURE 3.5-5: Immersion palladium plating at five times standard palladium chloride concentration after sintering 15 min. at 700°C, before and after scrubbing.

The initial NPMS process sequence (Table 3.2-1) incorporated Step #3 for removal of any nonadherent palladium after the initial immersion deposit and sinter. This scrubbing step appears to promote adherence of subsequently deposited metal on the back surface. However, the inability of effectively scrubbing the patterned front surface metal, particularly with texture etched wafers, and the expense of scrubbing, make elimination of this step highly desirable.

Several difficulties with the behavior of the fluoboric acid immersion palladium bath suggested removing it from consideration for further development even though some improvements had been achieved by using reduced $PdCl_2$ concentrations. For example, the growth of palladium nodules (See Figure 3.5-6) does not really agree with the assumption of a displacement reaction mechanism, even though this growth is to be expected with this bath since literature references allude to plating activation sites instead of depositing a continuous palladium film. Since a potential mechanical failure mode is separation at the silicon-palladium interface, this plating mechanism is especially subject to adhesion control problems. Examination of a silicon surface after a palladium layer has been separated gives the appearance of "pits" where the nodules were plated. The problem is not simply one of mechanical fracture, however, because these areas resemble etched (or chemically attacked) regions rather than mechanically fractured spots. This is illustrated in Figure 3.5-7. Another troublesome observation has been a heavy buildup of a dark residue, analyzed as silicon, around the end of the metal sintering furnace quartz tube. This is especially prevalent at the higher sintering temperatures of 600°C and 700°C.

(a) 5 minute immersion

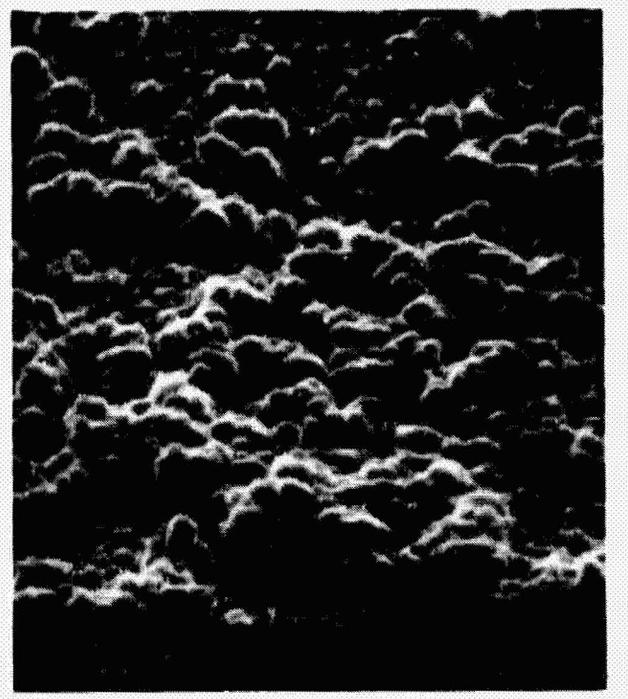

(b) 5 minute immersion, rinse, second immersion for 30 sec.

FIGURE 3.5-6: GROWTH OF IMMERSION PALLADIUM "NODULES" ON SILICON WAFER SURFACE USING HBF_4 TYPE IMMERSION PALLADIUM SOLUTION.

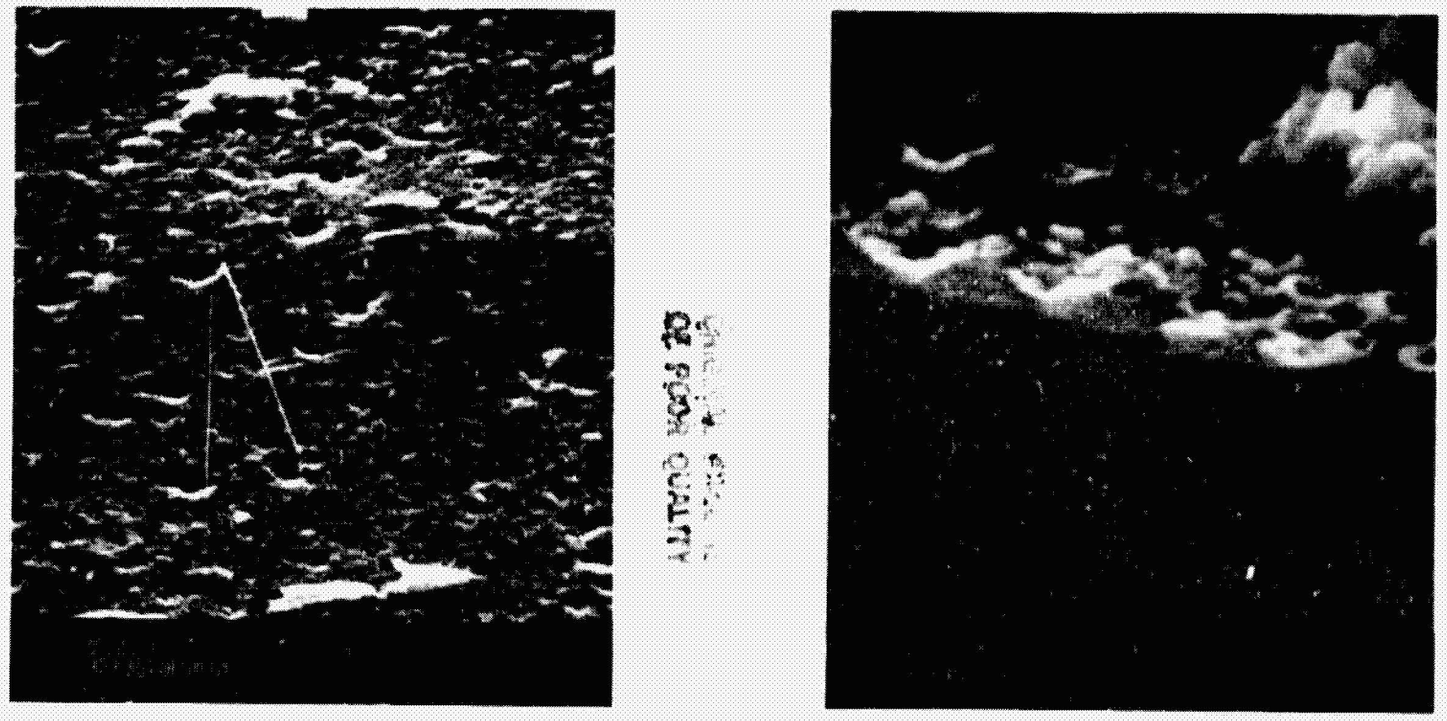

(a) after mechanically scrubbing immersion palladium layer from surface.

(b) after peeling metal layers from surface. Photo shows a sectioned sample.

FIGURE 3.5-7: APPEARANCE OF PITTING ON SILICON SURFACE WHICH HAS BEEN PLATED IN HBF_4 TYPE IMMERSION PALLADIUM SOLUTION.

From the above observations, it may be concluded that plating is initiated at existing surface sites or at only localized displacement sites. At these sites the nodules grow rapidly by a closed system electrolytic mechanism or by the formation of palladium salt complexes (palladium chlorides) which coplate with palladium. A coplating of palladium salts may explain the formation of the pitted surface after sintering and poor as-plated strength. Etching of silicon by chlorine freed at 600°C during sintering may form a volatile silicon compound which would redeposit silicon when cooled. This would account for the silicon deposit on the quartz liner in our sintering furnace. These observations, combined with the continual problem of obtaining constant metal plating rates for the front (n-type) and back (p^- type) surfaces, have forced a re-evaluation of the immersion bath chemistry.

3.5.2 AQUEOUS BATH WITH HYDROFLUORIC ACID

Assuming that a high HCl concentration may complex palladium chloride ions into more stable ions (which could also be deposited), HCl was eliminated from the immersion bath. Since palladium chloride is slightly soluble in water, a very dilute aqueous solution was made with approximately 0.01 g/liter of $PdCl_2$. Since we had experienced a stability problem with fluoboric acid and had doubts concerning the activity of the bath, hydrofluoric acid was substituted for the fluoboric.

The solution evaluated was

CONSTITUENT		AMOUNT
Water	H_2O	3 ℓ
Palladium Chloride	$PdCl_2$	0.02g
Hydrofluoric Acid	Hf	30 mℓ

The palladium chloride was dissolved at 70°C for 30 minutes, then allowed to cool to 30°C. Any undissolved residue was filtered, and the HF was added. Wafers were then plated for 10 to 15 minutes at 30°C.

The results were very encouraging; a thin palladium layer was plated, although palladium clusters were still present. (See Figure 3.5-8 for a scanning electron micrograph.) A great improvement in adherence was produced, with an undetectable amount of material being removed by vigorous swabbing. The $PdCl_2$ concentration was varied within the solubility limits with no apparent change in deposition rate. This should be expected with a true displacement reaction [50]. However, slight variations in HF concentration did affect the plating rate. The generalized observations are illustrated in Figure 3.5-9.

Even though this bath did give the desired displacement layer, the bath was not acceptable. It had a slow deposition rate, and the low constitutent concentrations made reproducibility difficult. An even more serious problem was the tendency to form anodic "oxide" films. This tendency could be reduced at higher temperatures (40°C), but at this temperature HF etching of the anti-reflection layer was accelerated.

3.5.3 AQUEOUS BATH WITH HYDROCHLORIC AND HYDROFLUORIC ACIDS

In an attempt to reduce bath sensitivity to variations in palladium chloride concentration, a small amount of hydrochloric acid was added. It was found that a molar concentration of HCl no greater than that of $PdCl_2$ was necessary to reduce the probability of forming complex ions. The bath has the same constituents of those listed in the literature[26] but at quite different concentrations. A typical bath used in these experiments consisted of:

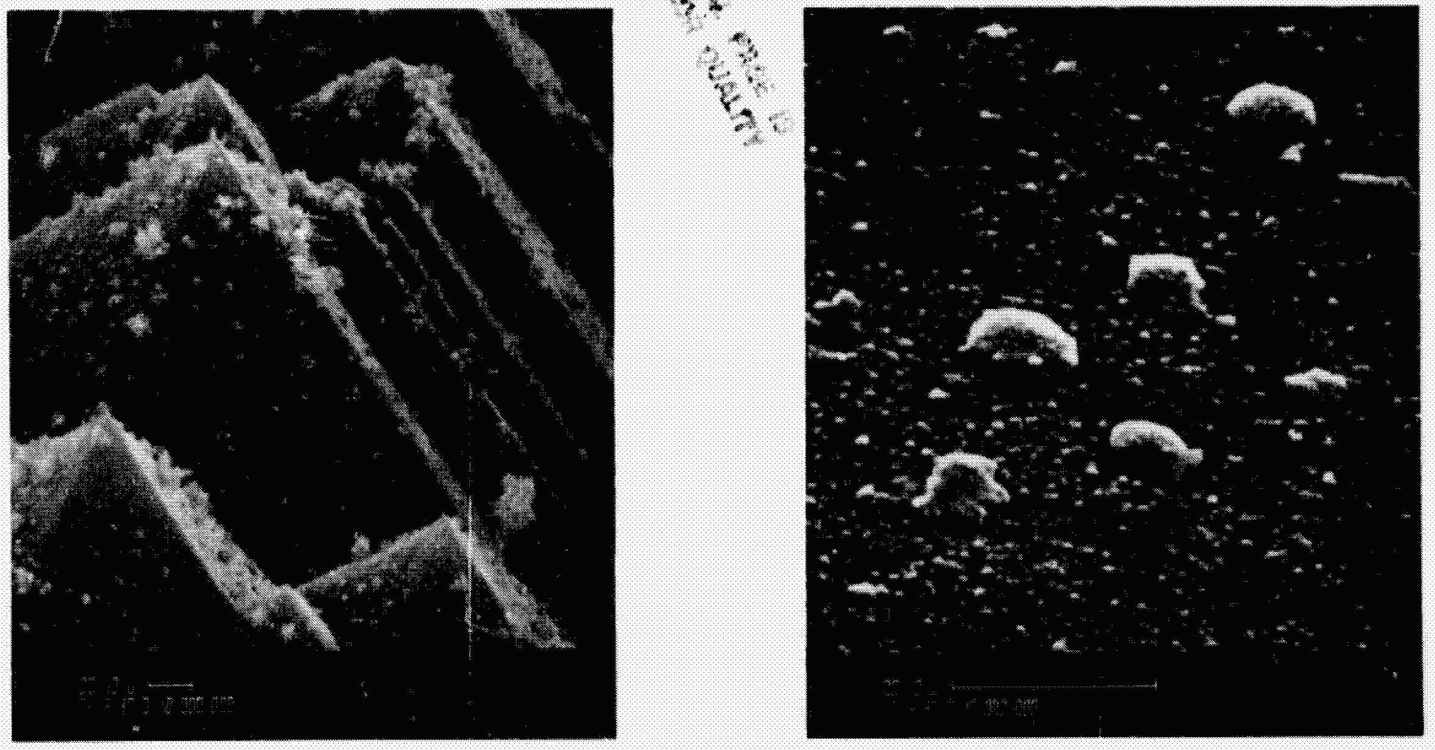

(a) n+ front textured surface showing large Pd clusters on top of fine grained Pd layers.

(b) p+ back surface.

FIGURE 3.5-8: IMMERSION PLATED PALLADIUM LAYERS USING AQUEOUS, HF TYPE IMMERSION PALLADIUM SOLUTION.

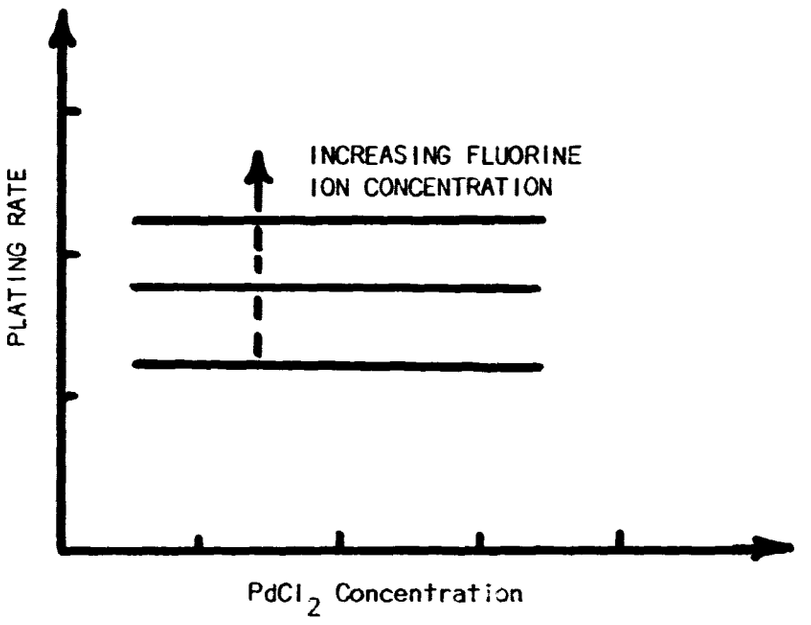

FIGURE 3.5-9: GENERALIZED REPRESENTATION OF THE DISPLACEMENT PLATING MECHANISM; RATE VERSES $PdCl_2$ CONCENTRATION. THE EFFECT OF FLUORINE CONCENTRATION IS DENOTED AS A RATE CHANGE.

CONSTITUENT		AMOUNT
Water	H_2O	3 ℓ
Palladium Chloride	$PdCl_2$	0.06g
Hydrochloric Acid	HCl (38%)	3mℓ
Hydrofluoric Acid	HF	10mℓ

With addition of the slight amount of HCl, the bath could be used at room temperature. Plating rate was increased, but the displacement layer had some loose nodules that could be swabbed off. The remaining layer was as good as the one produced from the bath with no HCl. The faster plating seemed to control oxide formation noted in Section 3.5.2. By plating the wafers, swabbing off the loose material, and plating again, a thick continuous layer could be deposited. The bath, however, still etched the AR dielectric layer at an unacceptable rate.

3.5.4 AMMONIUM FLUORIDE IMMERSION BATH

When experimentation with hydrofluoric baths had reached the point of diminishing return, a concentrated bath consisting of $PdCl_2$ dissolved in a strong HCl solution similar to that preferred for metal (copper) substrates was tried. This was done to evaluate the role of HF in plating silicon. A reference for $SnCl_2/PdCl_2$ immersion plating of semiconductor material [57] suggested use of a fluorine acid predip to remove any oxides. This was evaluated to determine if a predip would be sufficient without producing etching of the antireflection layer. The immersion palladium bath consisted of the following:

CONSTITUENT		AMOUNT
Water	H_2O	800 mℓ
Palladium Chloride	$PdCl_2$	0.25 g
Hydrochloric Acid	HCl (38%)	100 mℓ

A concentrated hydrofluoric acid predip was attempted with no success; plating did not initiate well, and the antireflection layer etched too quickly. However, an ammonium fluoride predip did initiate plating at a few spots, although the plated material was not very adherent. Addition of ammonium fluoride to the bath gave the desired immersion plating, but it also produced simultaneous plating of a thick nodular layer. This layer could be easily swabbed off leaving behind the adherent, thin immersion layer. By repeating this plating procedure, the immersion layer could be built up, but only after plating a considerable amount of extra material. This led to a series of experiments where the palladium and HCl concentrations were reduced by factors of two. The generalized relation which was determined for deposition rate versus Pd concentration is illustrated in Figure 3.5-10. The result of these experiments was a solution which gave an adherent, uniform immersion plated layer with reduced nodule formation (see Figure 3.5-11) with little or no visible residue removed by mechanical swabbing (see Figure 3.5-12). However, an effective layer for consistent initiation of electroless palladium was best obtained by using two plating steps and by swabbing before the second step. This ammonium fluoride bath did not etch the silicon nitride antireflection coating, but the plating time was rather long for an efficient process. To minimize plating time, the ammonium fluoride concentration was increased; this resulted in a corresponding increase in plating rate. A slight temperature dependence has been noted but has not yet been evaluated. The current bath formulation is:

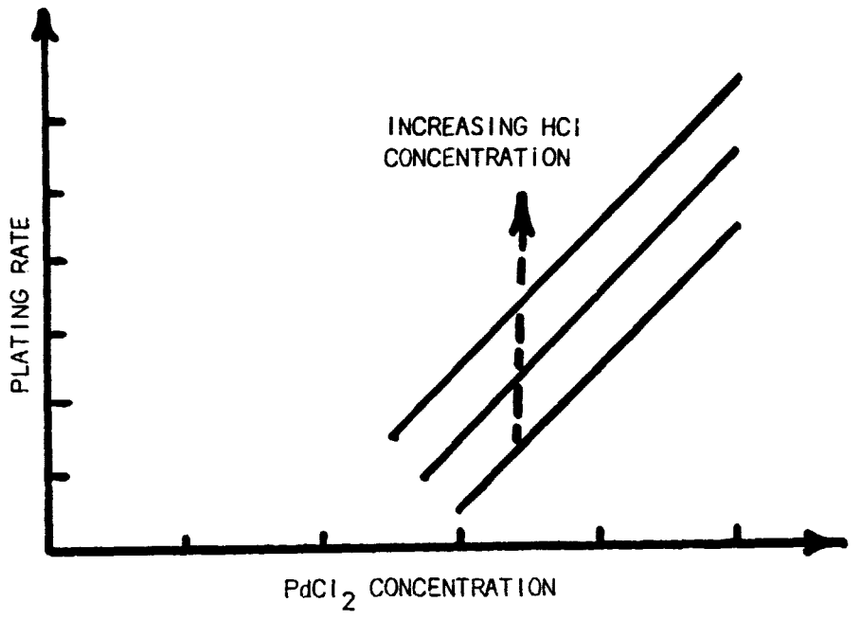

FIGURE 3.5-10: GENERALIZED REPRESENTATION OF NODULE PLATING MECHANISM RATE VERSES $PdCl_2$ CONCENTRATION. THE EFFECT OF HCl CONCENTRATION IS DENOTED AS A RATE CHANGE.

(a) N+ front textured surface showing large Pd grains on top of continuous, fine-grained Pd layer.

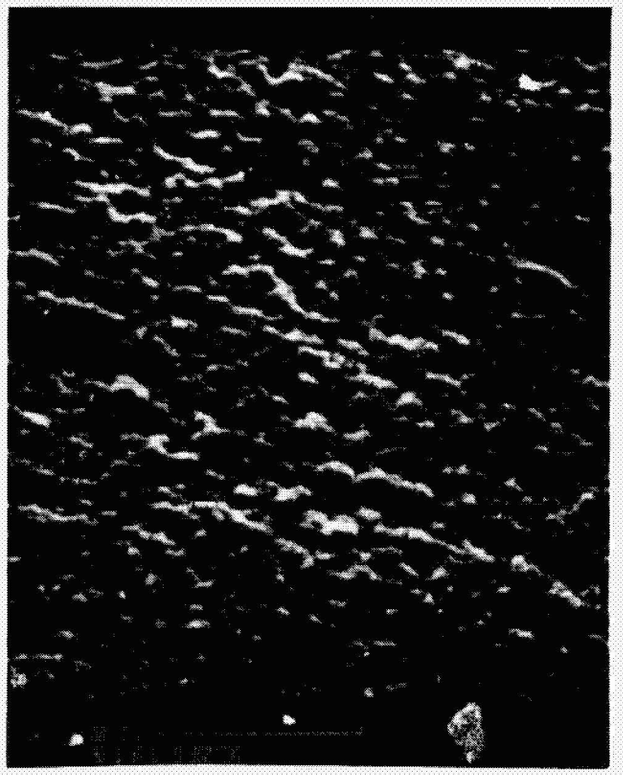

(b) P+ back smooth surface showing continuous, fine-grained Pd layer.

FIGURE 3.5-11: IMMERSION PALLADIUM PLATING FROM AMMONIUM FLUORIDE TYPE IMMERSION PALLADIUM SOLUTION.

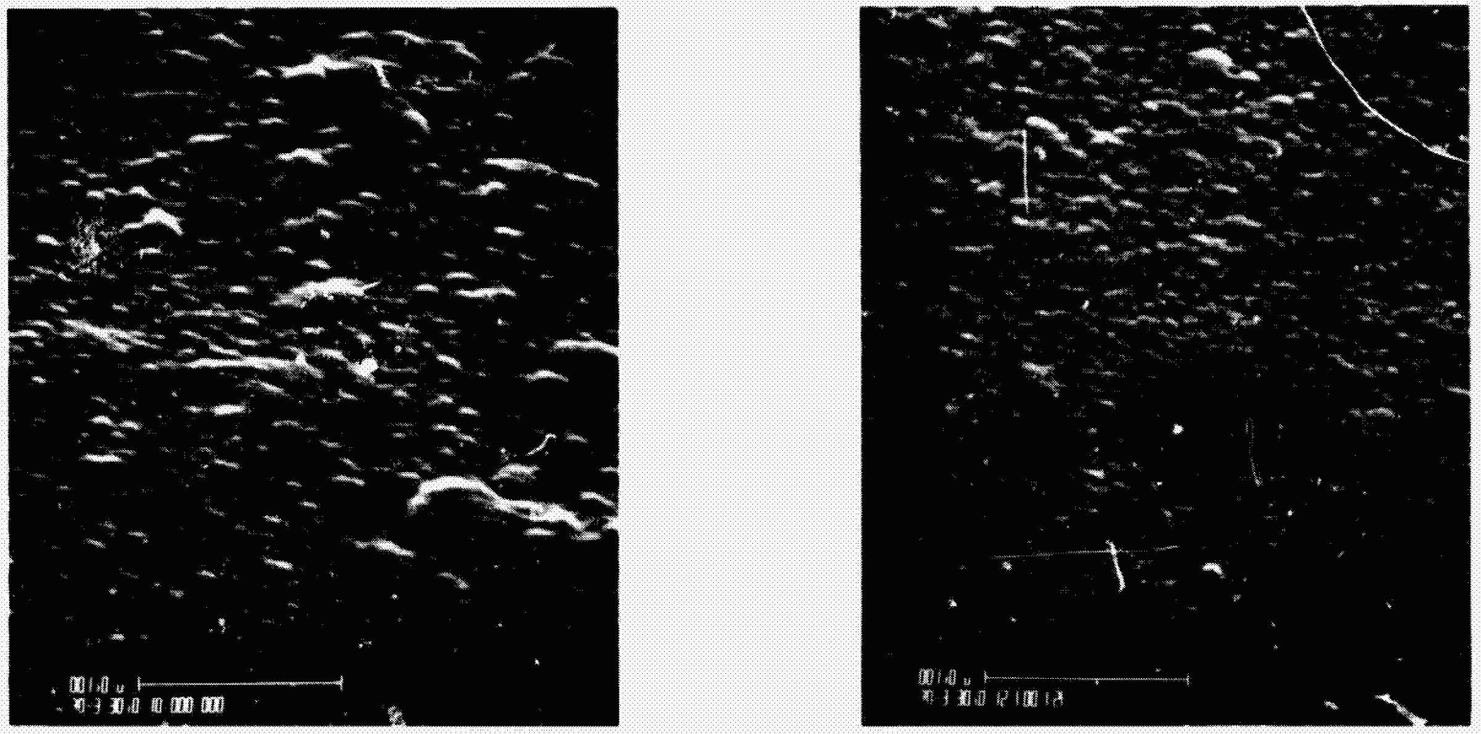

(a) before mechanical scrubbing.

(b) after mechanical scrubbing

FIGURE 3.5-12: EFFECTS OF MECHANICAL SWABBING OR SCRUBBING ON IMMERSION PALLADIUM PLATING FORMED WITH AMMONIUM FLORID" TYPE IMMERSION PALLADIUM SOLUTION.

CONSTITUENT		AMOUNT
Water	H_2O	3 ℓ
Palladium Chloride	$PdCl_2$	0.08 g
Hydrochloric Acid	HCl	10 mℓ
Ammonium Fluoride	NH_4F	200 mℓ

This bath plates a thin metallic immersion layer with little or no loose nodule formation. The plated layer will withstand a vigorous mechanical swab with a Q-tip and will consistently initiate electroless plating.

3.5.5 IMMERSION PLATING MODEL

Observations from all of the experiments performed can be summarized by a generalized model of the mechanisms involved in immersion plating with the palladium chloride bath. This model is graphically represented in Figure 3.5-13. For the very dilute aqueous bath (Region A), a true displacement reaction occurs from the Pd+ ions in solution. The rate in this region is strongly affected by temperature and somewhat less by HF concentration. In Region C, the "loose nodule" mechanism is predominant. Although not entirely understood, this mechanism may be due to colliodal ionic complex radicals plating along with the metal. Several studies of the Sn-Pd solutions for activating dielectrics have shown that large complexes, Pd_xCl_y and $Sn_xPd_yCl_z$ molecules, exist in a colloidal [45, 54, 57]. These colloidal complexes can also become ionic and participate in a cathodic plating mechanism. Reducing the HCl concentration should reduce this complexing, and, as expected, deposition rate was observed to decrease with lowered HCl concentration.

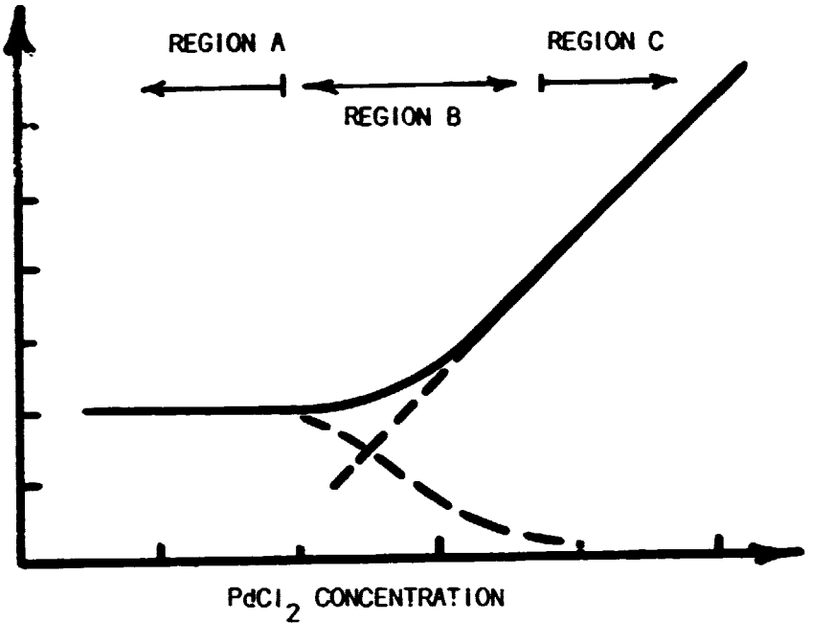

FIGURE 3.5-13: GENERALIZED DEPOSITION MODEL

Region A: Aqueous Solution Displacement Mechanism

Region B: Simultaneous Nodule and Displacement Mechanism (Current Process Solution)

Region C: Nodule Plating Mechanism with Little to No Displacement Plating.

The simultaneous formation of both a displacement layer and nodules over a wide range of concentrations occurs in Region B, Figure 3.5-13. Beyond some point, the displacement plating rate, which is usually independent of concentration, begins to decrease with increasing $PdCl_2$ concentration. This is denoted by the lower dashed curve. In this region, nodule formation seems to proceed at a faster rate, and so the displacement reaction is reduced by some mechanism such as a surface masking effect or localized depletion of the reaction species. Some additional detailed research would be required to fully understand the process, but the proposed model can be used as a guide for the development of an optimized immersion palladium solution.

3.6 PLATING PROCESS REFINEMENTS

3.6.1 AMBIENT LIGHT LEVEL

It was found, in the plating of solar cells, that ambient light level is important. The open circuit voltage generated by a cell, even while immersed in a plating solution, may be sufficient to initiate an electrolytic plating reaction, even in an electroless plating bath.

For example, an n-on-p solar cell may generate from 0.3 to 0.6 volt in ambient light conditions. This negative potential at the n-type front surface will cause the front to act as a cathode in the electroless solution and plate more rapidly than expected. (In some situations this may be desirable, but ordinarily it is not.) Electroless nickel and electroless palladium solutions tend inherently to plate n-type regions faster than p-type regions. A high ambient light level would accentuate this effect and cause an n-type solar cell front to plate much more heavily than a p-type back. This is undesirable since the front metal thickness must be carefully limited to be able to control metal penetration at the front junction and prevent junction punch-through; if the back plates much more slowly, its palladium thickness could be unacceptably thin. Consequently, the electroless palladium plating of solar cells should be done in a very low ambient light level.

To the contrary, the ammonium fluoride type immersion palladium bath developed in Section 3.5.4 has been found to benefit from a high ambient light level. Table 3.6-1 details the formula for the recommended immersion palladium solution. With this solution, the best uniformity between solar cell front n+ surface and back p+ surface plating rates has been obtained when a high intensity quartz-halogen lamp (type ENH) was positioned about two feet above the immersion palladium bath container. The resulting high

TABLE 3.6-1

IMMERSION PALLADIUM SOLUTION

CONSTITUENT		AMOUNT
Water	H_2O	1000 mℓ
Ammonium Fluoride	NH_4F	67 mℓ
Hydrochloric Acid	HCl (38%)	3 mℓ
Palladium Chloride	$PdCl_2$	0.027 g

light intensity promotes equal front and back plating. This effect would be consistent with the supposition that negatively charged palladium chloride complexes are the primary bearers of palladium in the immersion solution.

3.6.2 SOLUTION TEMPERATURE

It was previously noted that the electroless nickel solution could be operated at temperatures as high as 95°C and that the electroless palladium solution might possibly work as high as 70°C. However, these temperatures are not necessarily optimum for use with the NPMS process sequence.

While the electroless nickel solution can be maintained at 95°C, reducing the temperature will improve bath stability and slow the evaporation of ammonia from solution. This provides for more consistent operation of the bath, at least on a laboratory scale. The penalty for reducing the temperature is a simultaneous reduction in plating rate. However, since the desired nickel layer is relatively thin (say, 5000 Å), a plating rate reduction will not impact the process unduly. As a result of numerous trials, it has been found that 80°C is a reasonable temperature compromise for electroless nickel bath operation.

Although in theory the electroless palladium solution might work at 70°C, in practice this bath is too unstable for reasonable operation at this temperature. It has been determined that operation at 50°C provides a good compromise between plating rate and bath stability.

3.6.3 ELECTROLESS PALLADIUM BATH COMPOSITION

Table 3.6-2 details the recommended formula for the electroless palladium solution. The preferred electroless palladium solution differs from the solution originally given in Table 3.2-3 by an 86% reduction in sodium hypophosphite concentration. This reduction has resulted in a more stable and controllable deposition of electroless palladium.

TABLE 3.6-2

ELECTROLESS PALLADIUM SOLUTION

CONSTITUENT		AMOUNT
Hydrochloric Acid	HCl (38%)	4 mℓ/ℓ
Palladium Chloride	$PdCl_2$	2 g/ℓ
Ammonium Chloride	NH_4Cl	27 g/ℓ
Sodium Hypophosphite	$NaH_2PO_2 \cdot 2H_2O$	3.75 g/ℓ
Ammonium Hydroxide	NH_4OH (58%)	160 mℓ/ℓ

The operating stability of the electroless palladium solution is very much dependent on the manner in which the solution is prepared. To guarantee a stable solution which will not spontaneously decompose, it is best to mix the solution constituents in the order recommended in the process specification found in the document "Material, Supply, and Process Specifications and Procedures for Metallization of Large Silicon Wafers with the Palladium-Nickel-Solder Metallization System". This document is available from the Jet Propulsion Laboratory LSA Project upon request. When these instructions for electroless palladium solution preparation are followed, there should be no difficulty with palladium bath instability.

3.7 HEAT TREATMENT SEQUENCES FOR SILICIDE FORMATION

The initial NPMS process sequence discussed in Section 3.2 and outlined in Table 3.2-1 required two heat treatment cycles for the reliable formation of an adherent palladium silicide (Pd_2Si) contact layer. These heat treatments have been routinely performed in a resistance heated furnace using tubular quartz sleeves, although it is expected that, in the long term, belt furnaces may be more appropriate. The original NPMS process sequence stipulated that heat treatment cycles be performed at 600°C in forming gas -- a mixture of 96% nitrogen and 4% hydrogen. Over the course of work on this contract, both the heat treatment temperature and ambient have been altered.

3.7.1 HEAT TREATMENT AMBIENT

Forming gas was originally chosen for the heat treatment ambient to prevent oxidation of the palladium layers during the silicide formation steps. However, the fact that hydrogen is known to quickly diffuse through palladium has presented some questions about potential palladium-hydrogen interactions. Any penetration and absorption of hydrogen into the palladium layer may effect palladium silicide formation at the palladium/silicon interface. If oxidation of the palladium surface were not a major problem, nitrogen alone may be a suitable annealing ambient. Hutchins and Shepela [20] have reported that a thin film of PdO was detected on Pd_2Si films grown in the temperature range of 550°C to 700°C. The thin PdO films that were formed could be etched in a dilute HF solution. However, Pd_2Si films grown at 350°C did not show the PdO surface film.

To determine the suitability of a nitrogen anneal, studies were performed to compare nitrogen (N_2) and forming gas ($N_2 + H_2$) ambients at three different annealing temperatures. The temperatures considered were 500°C, 600°C, and 700°C. Test solar cells were plated in an immersion palladium bath using the fluoboric acid (HBF_4) type solution. (This plating deposits a thin, granular layer of palladium on the exposed silicon surfaces.) Scanning electron microscope photos were obtained for the plated palladium films before and after heat treatment. Six different anneals were tested, combining the three temperatures and two ambients.

In general, no problem was encountered in those tests where hydrogen was eliminated and only nitrogen was used. Where forming gas was used, there seemed to be a tendency for palladium grains to deform or to flow and "bead-up" rather than to be converted to adherent palladium silicide. Mechanically abrading the plated surfaces after heat treatment by using cellulose swabs indicated that, qualitatively, annealing in N_2 gave better adhesion than annealing in $N_2 + H_2$.

In other experiments, no difficulty was encountered during subsequent processing of samples annealed only in nitrogen. Pretreatments in dilute HF solutions (such as 10:1 H_2O:HF and 50:1 H_2O:HF) were sufficient to prepare the palladium silicide surface of the samples for additional plating. Therefore, a forming gas ambient has been eliminated in favor of using a nitrogen ambient for the metallization heat treatment steps where palladium silicide is formed.

3.7.2 HEAT TREATMENT TEMPERATURE

Experience with the HBF_4 immersion palladium bath had indicated that heat treatment temperatures between 500°C and 700°C were most satisfactory for obtaining adhesion of the immersion palladium and electroless palladium layers.

At lower temperatures, silicide formation did not seem to be adequately strong. These observations, however, are not supported by observations from the technical literature.

Hutchins and Shepela [20] have studied the rate of formation of Pd_2Si layers as a function of temperature and time. From their empirical data, they developed an analytical expression for the thickness (X) of the Pd_2Si formation for any given temperature (T) and time (t). The relation is

$$X^2 = K(T) \cdot t \tag{1}$$

where

$$K(T) = 7 \times 10^{-2} \exp\left(-\frac{29{,}200 \text{ cal/mol}}{RT}\right) \frac{cm^2}{sec} \tag{2}$$

R is the gas constant, 1.987 cal mol^{-1} $^oK^{-1}$. Solving these equations for X, substituting the value of R, and converting the dimensions from centimeters to microns,

$$X(\mu) = \left\{7 \times 10^6 \, t(sec) \exp\left[-\frac{14{,}694}{T(^oK)}\right]\right\}^{1/2} \tag{3}$$

Equation (3) gives the thickness of the Pd_2Si layer formed after annealing a film of palladium on a silicon surface. It is assumed that the palladium film is sufficiently thick to act as a Pd source for the duration of the annealing time.

Computations made by using equation (3) are presented in Figure 3.7-1. This figure can be used to estimate the various combinations of time and temperature which should be sufficient to form a Pd_2Si layer of a given thickness. For example, if a Pd_2Si layer which is 0.5 μ thick is desired, an anneal of 10 minutes at 350°C should be sufficient. However, an equivalent anneal cycle would be 82 minutes at 300° C. Of course, such a 0.5 μ layer of Pd_2Si can be obtained only if enough palladium (approximately 0.3 μ or 3000Å) is present. In forming that layer, less than 0.2 μ of the silicon surface will be consumed.

FIGURE 3.7-1: Pd_2Si layer thickness as a function of heat treatment time and temperature.

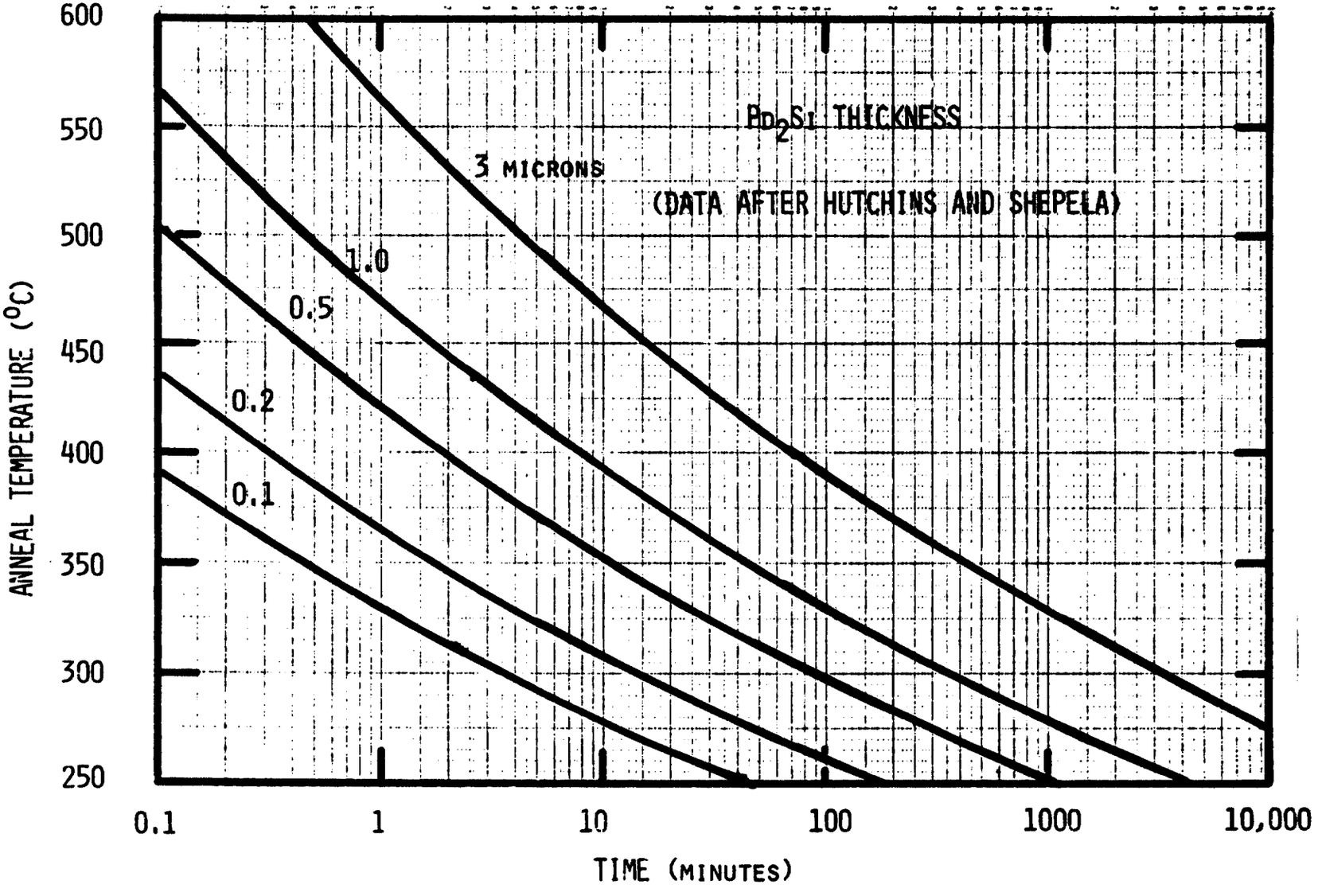

The curves of Figure 3.7-1 imply that there should be adequate palladium silicide formation rates at temperatures as low as 250 - 300°C. The discrepancy between the implication of these curves and the difficulty experienced in obtaining adhesion with a low temperature anneal may be due to the nature of the plated palladium layer. If, as hypothesized in previous sections, the immersion palladium layer formed in a HBF_4 type bath contains a significant amount of palladium salt as well as palladium, this may account for slower silicide formation. The small percentage of phosphorus present in an electroless palladium layer may also impede rapid silicide formation, especially if the prior immersion layer has not been reacted sufficiently.

These discrepancies have been reconciled substantially by using the newly developed NH_4F immersion palladium solution rather than the HBF_4 solution. In fact, it has been confirmed that when using the NH_4F solution, annealing temperatures as low as 300°C are sufficient both for the anneal after immersion palladium and for the anneal after electroless palladium. Excellant adhesion is obtained. These results are apparently due to the improved nature of the palladium layer obtained with the new immersion solution. As plated, the thin film of palladium is very adherent and probably forms an intimate contact with the silicon surface in true displacement fashion. Furthermore, inclusion of palladium salts in the immersion Pd layer is minimized, if not eliminated.

Since the palladium layers in the nickel-palladium metallization system are limited to thin films intentionally, satisfactory heat treatments could be performed at almost any temperature between 300°C and 700°C. This is because the source of Pd on the silicon surface is limited, and therefore the thickness of the Pd_2Si layer (and its penetration into the silicon surface) will be limited. However, there are numerous benefits to be obtained by using the lowest practical annealing temperature. A lower temperature means that there

will be less oxidation of the palladium surface should some oxygen be present in the furnace atmosphere during the anneal; thus, subsequent plated layers may be applied with more control. At lower anneal temperatures, there will be substantially less possibility of palladium punch-through to the junction at silicon surface defects or areas of excessively thick palladium deposits. Furthermore, a lower temperature annealing furnace will consume less power and provide lower cost operation.

3.8 RECOMMENDED PALLADIUM-NICKEL-SOLDER METALLIZATION PROCESS

3.8.1 PROCESS SEQUENCE OUTLINE

The metallization process sequence developed through work on this contract is outlined in Table 3.8-1. The sequence consists of six basic steps, four of which are for metal application and two of which are for heat treatments. As will be demonstrated in following sections, this sequence has met the objectives of the contract. It is capable of being implemented in high volume production, it provides a reliable ohmic contact which does not degrade solar cell electrical performance, it has consistently great mechanical strength, and it is capable of low cost application.

The individual process sequence steps will be discussed in more detail in the next section.

3.8.2 PLATED SURFACE CHARACTERISTICS

In the first step of the process sequence a thin palladium layer is established on the bare silicon surface. This is accomplished by placing the patterned solar cells into an immersion palladium solution. The purpose of this step and the following heat treatment (step number 2) is to prepare an adherent foundation for the subsequent build-up of a thicker palladium silicide layer. Figure 3.8-1 shows SEM photographs of the immersion palladium layer resulting from step 1. Both a smooth, chemically etched back surface of approximately <100> silicon orientation and a texture etched front surface with <111> silicon facets are shown. In both cases, a very fine-grained, thin palladium layer is interspersed with somewhat larger grains or nodules of palladium. These nodules are a consequence of the plating reaction. It is the fine grain, very thin layer that is desired. This layer is probably no more than 50 to 100Å thick.

TABLE 3.3-1

PROCESS SEQUENCE OUTLINE

PALLADIUM-NICKEL-SOLDER METALLIZATION SYSTEM

Starting Point: a) Solar cell with dielectric AR coat

b) Pattern of desired metal contact etched into dielectric

(Back surface may be totally bare or may be patterned.)

STEP	PROCESS
1	Immersion palladium coat (displacement reaction), room temperature solution.
2	Heat treatment (silicide formation), 300°C in nitrogen.
3	Electroless palladium plate (autocatalytic reaction), heated solution.
4	Heat treatment (additional silicide formation), 300°C in nitrogen.
5	Electroless nickel plated (autocatalytic reaction), heated solution.
6	Solder coat, lead-tin solder.

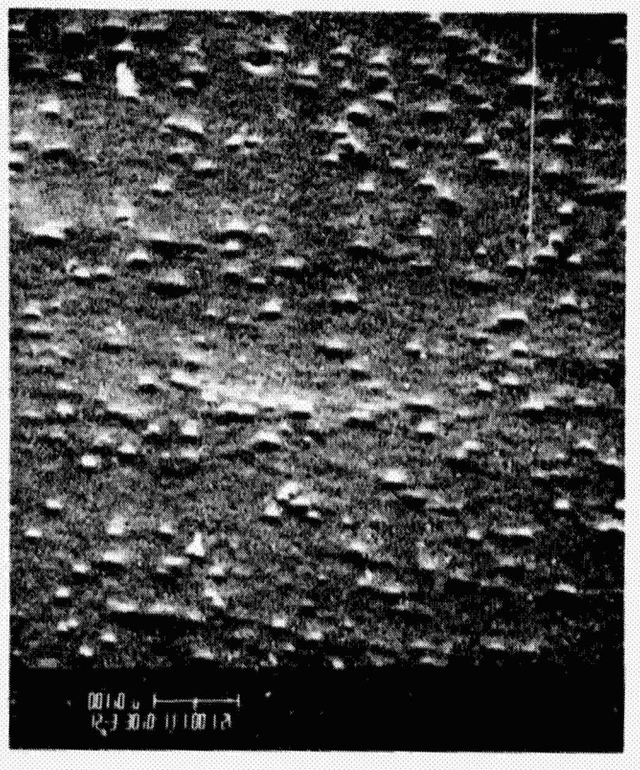

a) Smooth, chemically etched back surface, 12,000 X

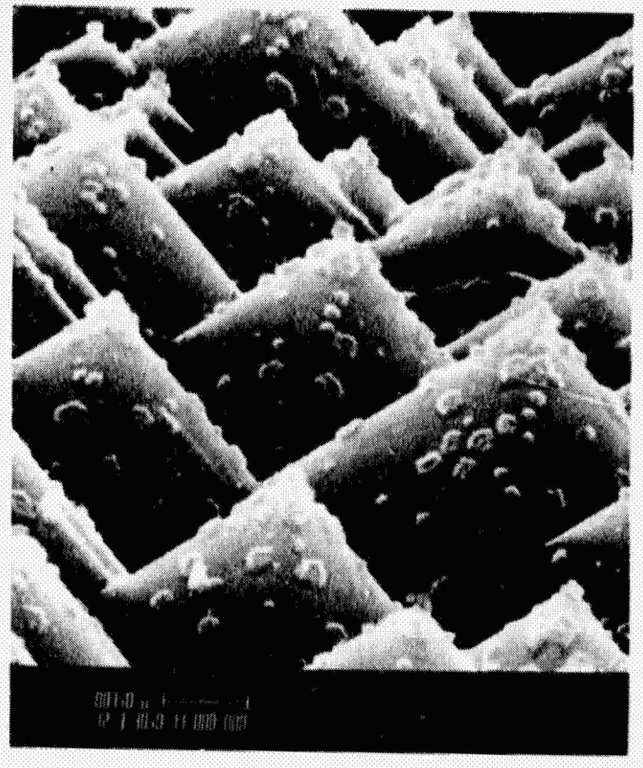

b) Texture etched front surface, 12,000X

FIGURE 3.8-1: PLATED SURFACE RESULTING FROM STEP 1 OF THE PROCESS SEQUENCE. A VERY FINE GRAINED SURFACE FILM OF PALLADIUM IS INTERSPERSED WITH LARGE GRANULAR PALLADIUM FORMATIONS.

In step 3 of the process sequence a moderately thick layer (approximately 1000Å) of palladium is plated from an electroless palladium solution. This plated layer is shown in Figures 3.8-2 and 3.8-3. The electroless plating process gives a continuous palladium layer with rather large palladium grain size. Incorporated into this layer is a small percentage of phosphorus because of the sodium hypophosphite reducing agent used in the electroless bath.

In step 4 the palladium layer is reacted at 300°C in nitrogen ambient to form palladium silicide, Pd_2Si. Photos of the surface after this step are shown in Figure 3.8-4 at moderate magnification and in Figure 3.8-5 at high magnification. Pd_2Si is known to form epitaxially on (111) silicon. Indeed, Figures 3.8-4 b) and 3.8-5 b) show a smoothing of the palladium film on the surface of the textured silicon facets compared to the as-deposited palladium films of Figures 3.8-2 and 3.8-3. The back surface palladium silicide layer can be seen to be substantially rougher than the as-deposited layer of palladium. It is probably not apparent in the reproduced photograph of Figure 3.8-5 a), but there is a tendancy to produce some fine, vertical whiskers during the palladium silicide growth.

In step 5, an electroless nickel plating solution is used to plate a moderately thick (approximately 5000Å) layer of nickel over the palladium silicide/palladium layer previously formed. This nickel layer also contains a small percentage of phosphorus because of the sodium hypophosphite reducing agent. SEM photographs of the nickel surface are shown in Figure 3.8-6. Considerable rounding of the textured surface contours can be observed because of the thick nickel deposit.

Figure 3.8-7 shows a photograph of the front of a completed cell. Although difficult to see, the nickel layer has been solder coated by a dip solder process with 60/40 Sn/Pb solder.

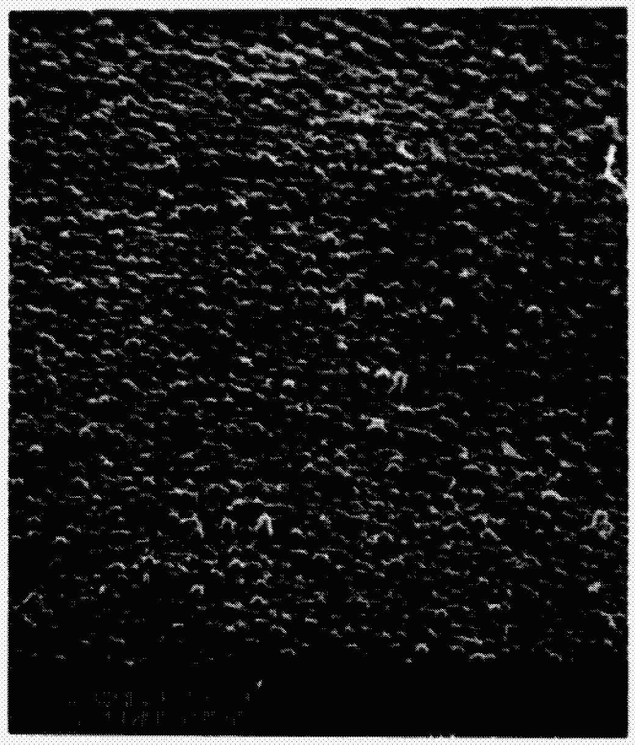

a) Smooth, chemically etched back surface, 12,000 X

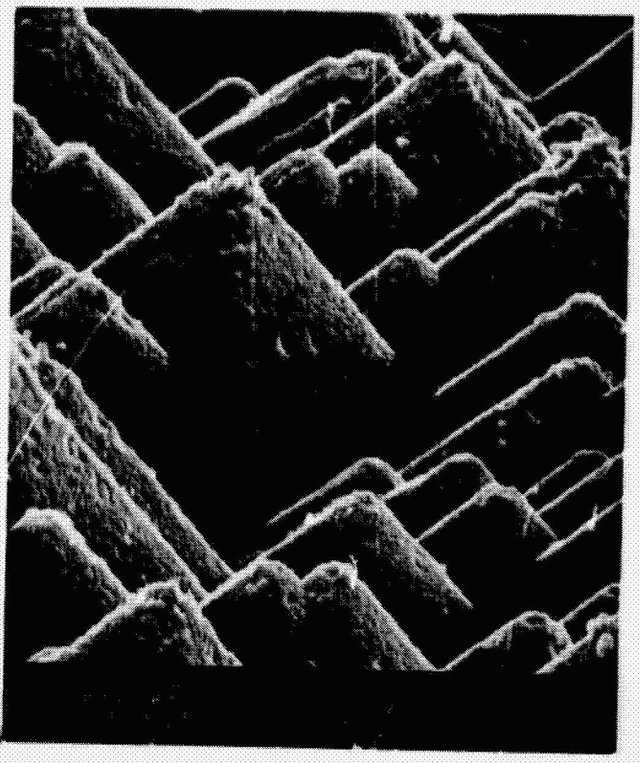

b) Texture etched front surface, 12,000 X

FIGURE 3.8-2: 12,000X MAGNIFICATION OF ELECTROLESS PLATED PALLADIUM LAYERS RESULTING FROM PROCESS SEQUENCE STEP 3.

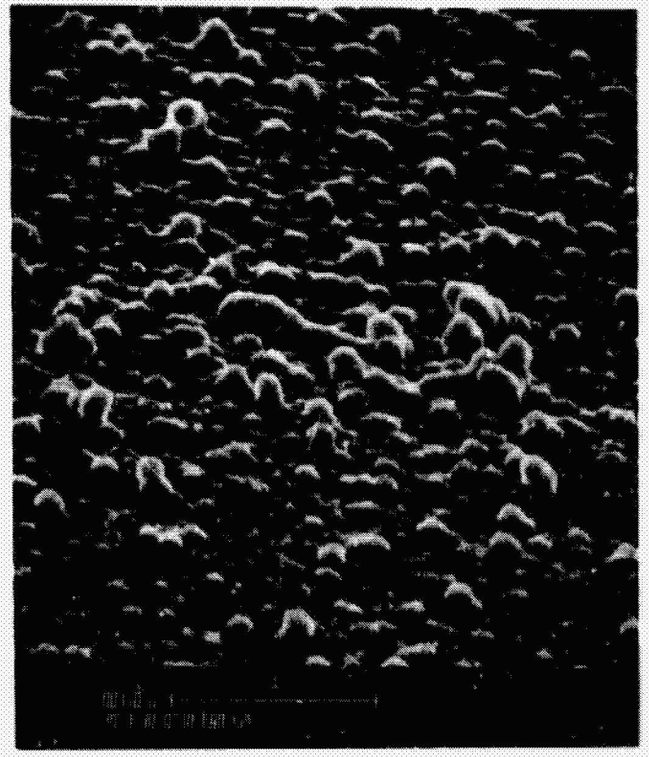

a) Smooth, chemically etched back surface, 30,000X

b) Texture etched front surface, 30,000X

FIGURE 3.8-3: 30,000X MAGNIFICATION OF ELECTROLESS PLATED PALLADIUM LAYERS RESULTING FROM PROCESS SEQUENCE STEP 3.

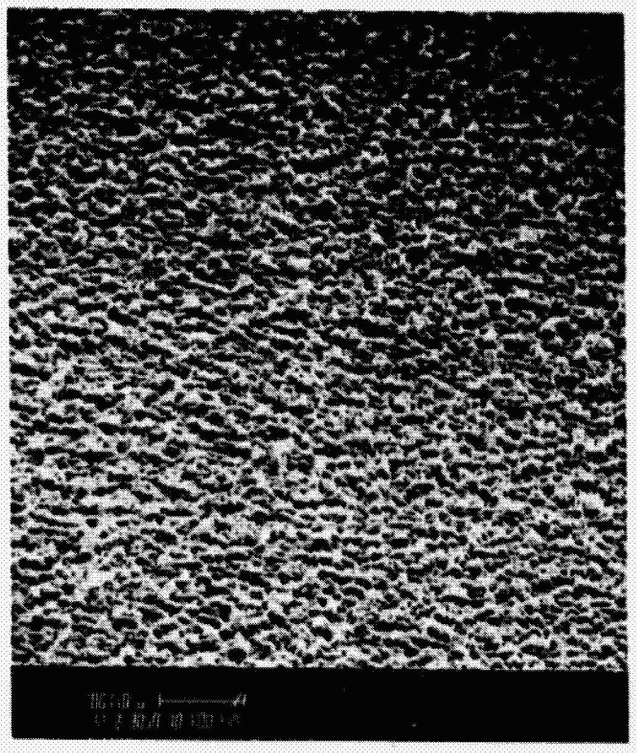

a) Smooth, chemically etched back surface, 12,000X

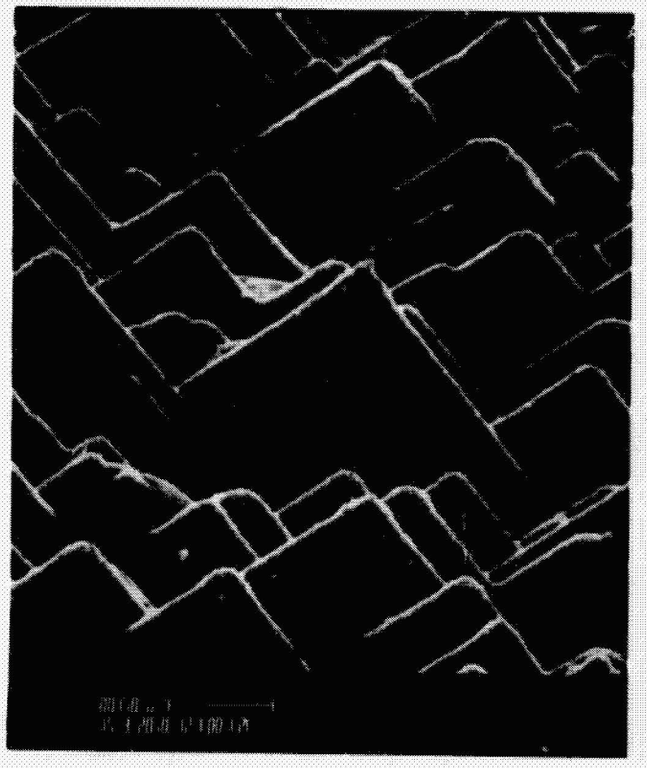

b) Texture etched front surface, 15,000X

FIGURE 3.8-4: PALLADIUM SILICIDE LAYER FORMED DURING 300°C HEAT TREATMENT OF PROCESS SEQUENCE STEP 4.

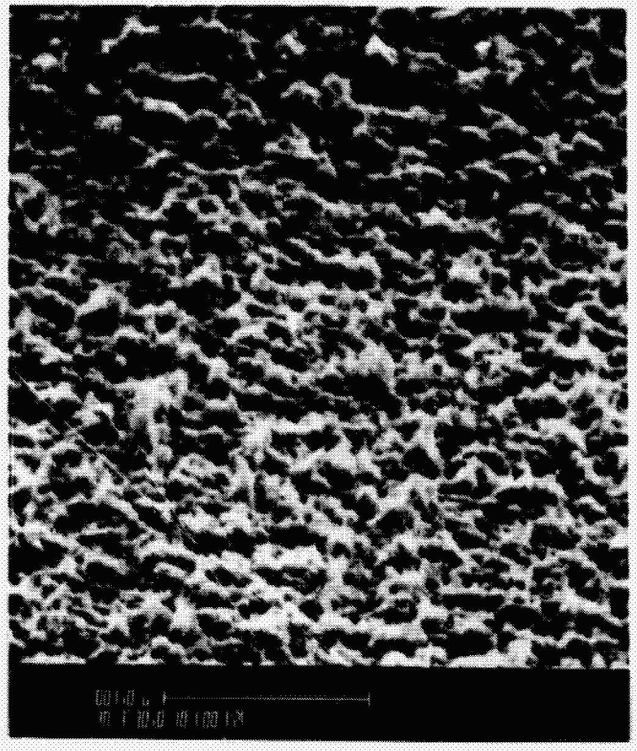

a) Smooth, chemically etched back surface, 30,000X

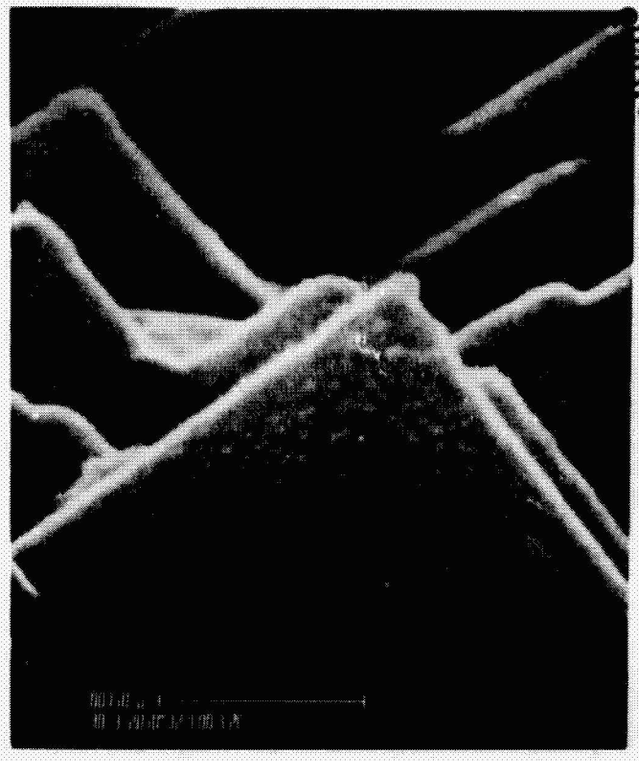

b) Texture etched front surface, 30,000X

FIGURE 3.8-5: 30,000X MAGNIFICATION OF PALLADIUM SILICIDE LAYER FORMED DURING PROCESS SEQUENCE STEP 4.

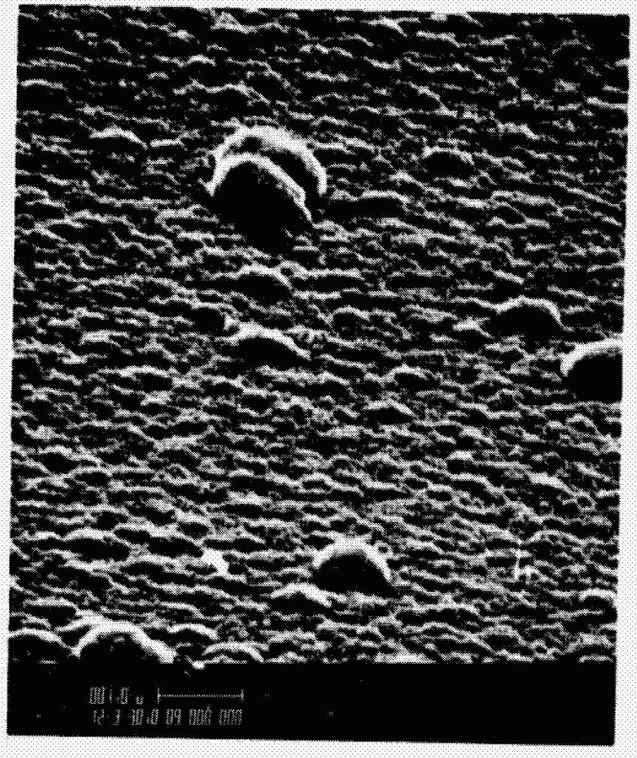

a) Smooth chemically etched back surface, 12,000X

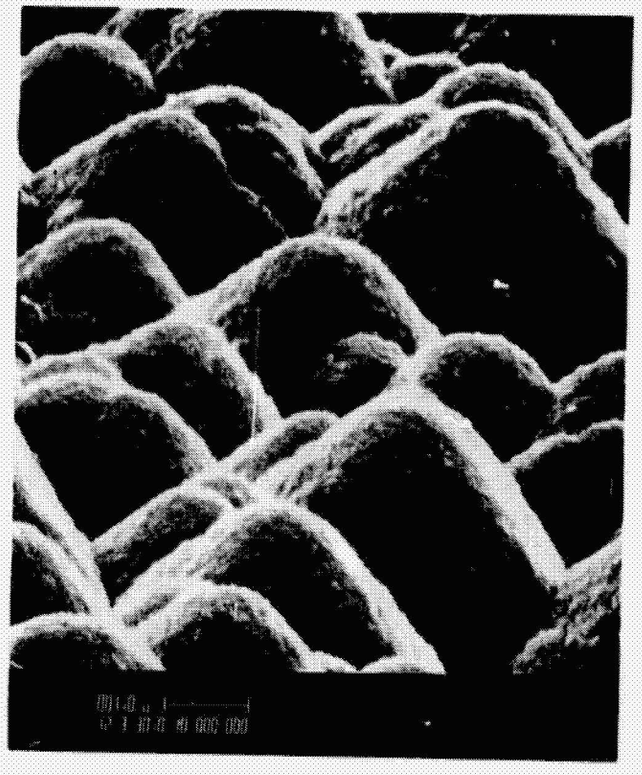

b) Texture etched front surface, 12,000X

FIGURE 3.8-6: ELECTROLESS PLATED NICKEL LAYER SEQUENCE STEP 5. ULTING FROM PROCESS

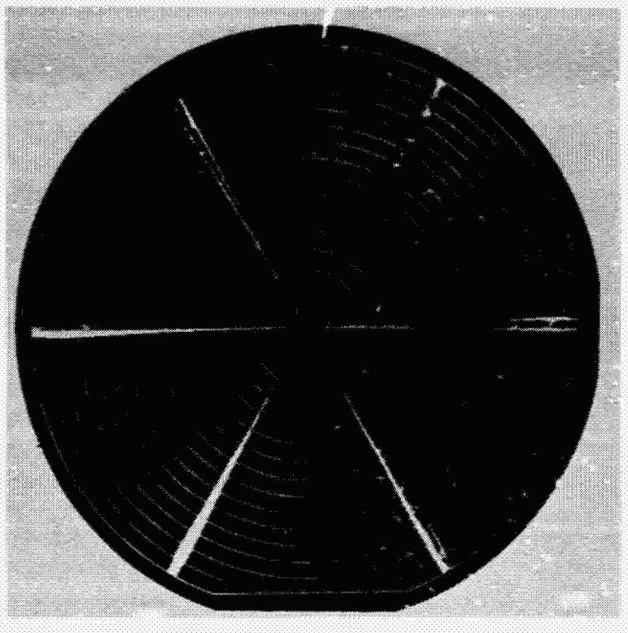

FIGURE 3.8-7: FRONT VIEW OF COMPLETED, SOLDER COATED SOLAR CELL.

3.8.3 TYPICAL ELECTRICAL AND MECHANICAL PERFORMANCE

During the development of the palladium-nickel-solder metallization system process, solar cells were batch processed in lots of at most 24 cells. All the cells of a given lot were plated simultaneously, but cells were soldered one at a time. Electrical and mechanical data are given below for a lot which is typical of solar cells processed according to the process sequence outline of Table 3.8-1.

Electrical data were taken for a lot of 22 metallized solar cells by using an x-y recorder to plot the current-voltage characteristic curve of each cell under one-sun illumination at room temperature (24°C). The illumination was from quartz-halogen lamps and was calibrated with a JPL-calibrated reference cell. The I-V curve for cell number 21 is shown in figure 3.8-8. Cell 21 is typical of the average performance of all the cells of the lot.

From each plotted I-V curve, short circuit current (I_{SC}), open circuit voltage (V_{OC}), maximum power point current (I_M), maximum power point voltage (V_M), and current at a bias of 460 mV are determined. Then cell efficiency (based on the total silicon substrate area) and curve fill factor (CFF) are calculated. These data are tabulated for each of the 22 cells in Table 3.8-2. The lot mean value and standard deviation have been calculated for each parameter. The mean values and the 2σ (twice standard standard deviation or 95% confidence level) values are given at the bottom of Table 3.8-2.

Of course, the data in this table depend primarily on the process and materials used to prepare the solar cells before the metallization process. All that can be expected of the metal system is that it does not degrade the inherent solar cell quality. In this respect, curve fill factor is probably the most significant parameter with which to monitor metal system quality.

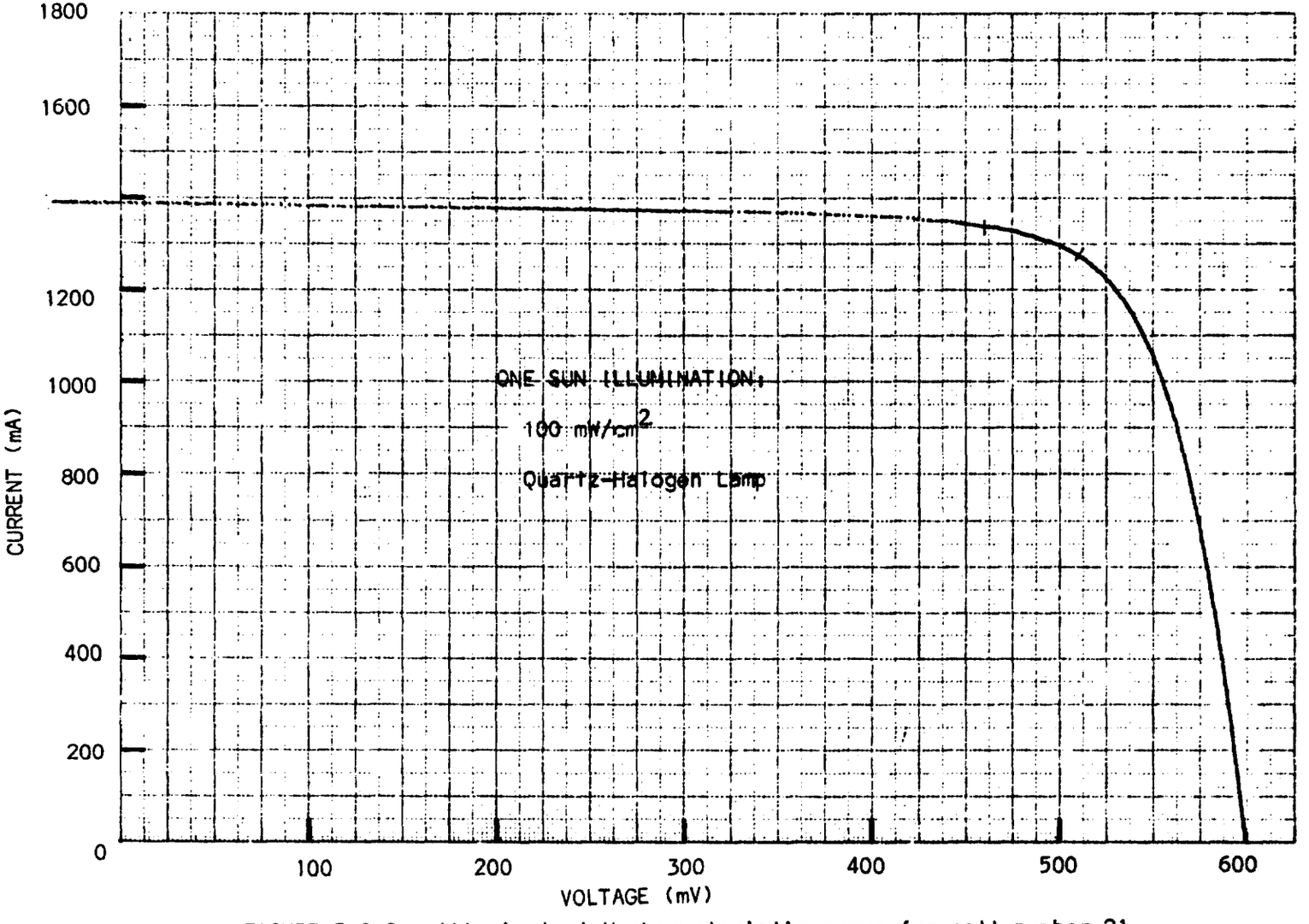

FIGURE 3.8-8: Illuminate I-V characteristic curve for cell number 21. This cell is typical of the entire 22 cell lot.

TABLE 3.8-2: DATA FOR A LOT OF 22 SOLAR CELLS METALLIZED WITH THE PALLADIUM-NICKEL-SOLDER METALLIZATION SYSTEM.

CELL NO.	I_{SC} (mA)	V_{OC} (mV)	I_M (mA)	V_M (mV)	η (%)	CFF	I @ .46V (mA)
1	1398	605	1289	514	14.61	.783	1353
2	1400	593	1261	498	13.85	.756	1325
3	1400	602	1270	507	14.20	.764	1341
4	1401	607	1291	514	14.63	.780	1360
5	1380	601	1266	507	14.15	.744	1331
6	1402	603	1295	513	14.65	.786	1365
7	1393	607	1290	515	14.65	.786	1356
8	1381	598	1274	507	14.24	.782	1340
9	1385	592	1273	498	13.98	.773	1332
10	1400	605	1246	506	13.90	.744	1310
11	1392	607	1283	513	14.51	.779	1350
12	1382	595	1280	508	14.34	.791	1342
13	1401	602	1293	515	14.68	.790	1360
14	1393	603	1288	513	14.57	.787	1352
15	1400	602	1294	513	14.64	.788	1363
16	1395	606	1282	514	14.53	.779	1351
17	1398	606	1285	519	14.71	.787	1352
18	1379	587	1263	494	13.76	.771	1319
19	1400	605	1292	519	14.79	.792	1370
20	1385	604	1275	515	14.48	.785	1341
21	1388	599	1273	510	14.32	.781	1339
22	1380	601	1247	509	14.00	.765	1311
mean	1392mA	601mV	1278mA	510mV	14.37	.778	1344mA
2σ	17mA	11mV	29mA	13mV	.63	.024	34mA
2σ%	1.2%	1.8%	2.3%	2.6%	4.4 %	3.1%	2.5%

An average value near 78% as obtained in Table 3.3-1 is very respectable and indicates little or no metallization problems. Maintaining a good fill factor requires no junction degradation by metal impurity diffusion and requires low metal contact resistance and low series resistance. Experimental measurements using both illuminated I-V curves such as Figure 3.8-8 and I-V curves taken in the dark indicate that resistive losses are only on the order of 10 millivolts at the 1400 mA current level. (These are 3 inch diameter cells.)

In addition to providing a low resistance contact which does not degrade p-n junction characteristics, the metallization must also exhibit good adhesion. The assumption throughout the term of this contract has been that a sufficient condition for metal adhesion is that pull test failures occur not only be delamination but rather by silicon fracture beneath the contact area. This condition has been achieved with the palladium-nickel-solder metallization system.

The same solar cells described by the electrical test data of Table 3.8-2 were subjected to pull strength tests. Tin coated nickel tabs were soldered to each of the six front surface contact pads on seven of the cells and soldered to the center of the back surface metal on seven other cells. These tabs were then pulled in a direction perpendicular to the solar cell substrate. The results are tabulated in Table 3.8-3. The pull strength gauge was calibrated in pounds and ounces, and readings were converted to grams. Four of the back surface tests exceeded the usable limit of force gauge (4540 g).

The pull test results demonstrate that the palladium-nickel-solder metallization system is able to maintain top quality electrical performance without sacrificing very strong mechanical adhesion. The data of Tables 3.8-2 and 3.8-3 are typical of the performance obtained when using this metallization system.

TABLE 3.8-3: PULL STRENGTH IN GRAMS FOR THE SAME CELLS LISTED IN TABLE 3.8-2. PULL TESTS WERE PERFORMED PERPENDICULAR TO THE CELL SURFACE.

CELL NO.	FRONT SURFACE CONTACT NUMBER 1	2	3	4	5	6	BACK CENTER
1	737g	2155	2438	1077	765	1758	
2							3175
3	1134	1644	1162	1332	1389	1304	
4							1389
5	1247	2098	1219	850	822	1531	
6							>4540
7	1474	2495	2013	1559	1361	1162	
8							3799
9	510	964	1247	510	907	567	
10							>4540
11	1729	1247	1049	510	1077	1276	
12							>4540
13	1332	1474	879	992	737	1134	
14							>4540
MEAN			1259g				>3787g
MINIMUM			510				1389

Pull tests were performed with 0.006" nickel straps, bent at right angles to form tabs approximately 4 mm long by 2 mm wide. Tabs were tinned and soldered by hand to the cell metallization.

3.9 NPMS COST ESTIMATES

To determine the economic feasibility of incorporating some form of the nickel-palladium metallization system into a solar cell manufacturing process for the 1986 timeframe, the preliminary process sequence outlined in Table 3.9-1 was analyzed with respect to costs early in the program. This analysis is not the final one, but it does serve to indicate the ultimate price potential for the palladium-nickel-solder metallization system. In addition, those process steps which account for a disproportionate share of the total cost have been determined from this initial analysis.

Throughout the course of contract efforts, the baseline nickel-palladium metallization system has been revised and updated. A major advantage of the ammonium fluoride type immersion palladium solution described earlier in this report is that its incorporation into the NPMS porcess sequence has allowed the scrubbing step, which was included as step 5 in the preliminary process sequence of Table 3.9-1, to be eliminated. This surface scrubbing is no longer required to guarantee consistent and repeatable performance of the plated palladium layers. In addition, the heat treatment temperatures have been lowered to 300°C, making belt furnaces even more desirable. Therefore, the preliminary process sequence used for the initial price analysis has been revised as shown in Table 3.9-2. This revised process sequence, together with some updated cost data on price-driving materials such as palladium chloride and lead-tin solder, has led to a correction in the initial IPEG price data. The correction is a favorable one, and yields a reduction of the IPEG add-on price from that obtained in the initial price analysis.

In the sections that follow, the initial IPEG price analysis is detailed and the results are tabulated. Then the process sequence corrections and materials cost corrections are discussed, and the numerical data are changed accordingly. The total add-on prices for the nickel-palladium metallization system are summarized for both the initial and revised price analyses.

TABLE 3.9-1

PRELIMINARY NPMS (NICKEL-PALLADIUM METALLIZATION SYSTEM) PROCESS SEQUENCE

Starting Point: a) Solar cell with front dielectric AR coat,
b) Pattern of desired metal contact etched into front dielectric,
c) Patterned or totally bare solar cell back surface.

STEP	PROCESS
1	Immersion palladium coat (displacement reaction), room temperature solution.
2	Heat treatment (silicide formation), 600°C in nitrogen.
3	Scrub (remove unwanted palladium salts).
4	Electroless palladium plate (autocatalytic reaction), heated solution.
5	Heat treatment (additional silicide formation), 600°C in nitrogen.
6	Electroless nickel plated (autocatalytic reaction), heated solution.
7	Solder coat, lead-tin solder.

TABLE 3.9-2

REVISED NPMS (NICKEL-PALLADIUM METALLIZATION SYSTEM) PROCESS SEQUENCE

Starting Point: a) Solar cell with dielectric AR coat

b) Pattern of desired metal contact etched into dielectric

(Back surface may be totally bare or may be patterned.)

STEP	PROCESS
1	Immersion palladium coat (displacement reaction), room temperature solution.
2	Heat treatment (silicide formation). 300°C in nitrogen.
3	Electroless palladium plate (autocatalytic reaction), heated solution.
4	Heat treatment (additional silicide formation), 300°C in nitrogen.
5	Electroless nickel plated (autocatalytic reaction), heated solution.
6	Solder coat, lead-tin solder.

3.9.1 INITIAL IPEG PRICE ANALYSIS

The method selected for performing the initial NPMS cost estimates is to follow the JPL Interim Price Estimation Guidelines (IPEG) as detailed in JPL Document 5101-33. This technique requires only the estimation of direct expense items. Included are initial capital equipment expenses (EQPT), floor space required for such equipment (SQFT), yearly direct labor wages (DLAB), yearly costs of materials and supplies (MATS), and yearly costs of utilities (UTIL) such as electricity and water. These five variables are weighted by the IPEG equation to account for all other indirect expenses, including profit.

Thus, an equation for price is formulated as shown in Figure 3.9-1. This IPEG equation will yield a price estimate in dollars per watt. Since only the metallization process is being considered in this report (and not the total solar cell fabrication sequence), the estimates result in add-on prices. Unfortunately, such an analysis can be misleading because it does not allow for the synergistic interaction of the metallization step within the totality of the solar cell array fabrication process. Thus, additional benefits of the NPMS process such as cell reliability and longevity are not factored into this cost analysis, but such benefits must, in reality, be considered.

All direct expenses presented in this analysis are deflated to 1975 dollars before they are entered into the IPEG equation. To do this, the inflation rates defined in the JPL Cost Account Catalog prepared by TB&A have been used. These are presented in Table 3.9-3. Wherever possible, labor rates, materials expenses and utilities expenses listed in the Cost Account Catalog are used in the NPMS analysis, even though some of these numbers may differ from those used at Motorola. For items used in the NPMS process which are not listed in the Cost Account Catalog, reasonable cost assumptions have been made and stated.

FIGURE 3.9-1

INTERIM PRICE ESTIMATION GUIDELINES
JPL IPEG PRICE EQUATION

$$PRICE = \frac{0.489\ EQPT + 96.9\ SQFT + 2.133\ DLAB + 1.255\ MATS + 1.255\ UTIL}{QUAN}$$

WHERE

EQPT = Direct Equipment Capital Cost

DLAB = Annual Direct Labor Salaries

MATS = Cost of Direct Materials and Supplies

UTIL = Cost Of Direct Process Utilities

SQFT = Direct Manufacturing Floor Space

QUAN = Annual Production Quantity

TABLE 3.9-3

INFLATION RATES FROM JPL
COST ACCOUNT CATALOG

CODE	CLASS	RATE (%)
A	Raw Materials	11
B	Labor	8
C	Chemicals	13
D	Commodities	8
E	Energy	12
F	Resources	15
G	Land	4
H	Facilities	9
I	Construction	8
J	Equipment	7

3.9.2 ASSUMPTIONS FOR INITIAL COST ESTIMATES

Along with the IPEG price equation, the following assumptions form the framework for the initial NPMS cost estimates.

(1) Equipment and labor are not integerized. This is the standard assumption applied to both IPEG and SAMICS cost analyses and is a fundamental weak point. Most price sensitivity to production volume is removed by this assumption. The assumption is valid only in the extreme of very large production volumes.

(2) Prices are in 1975 dollars. As stated before, inflation rates are taken from the JPL cost account catalog. In all cases, costs are adjusted to 1975 dollars before the IPEG equation is applied.

(3) Process yield is 100%. This is clearly a false assumption, but any overall yield factor can be applied at the completion of the analysis by appropriately changing the value of QUAN, the quantity of power produced.

(4) The work year is 8280 hours (8 hours per shift times 3 shifts per day times 345 days per year), as defined by JPL.

(5) Cells are fabricated on either 7.6 cm or 12 cm diameter circular substrates (ingot technology). This assumption allows evaluation of equipment, labor, and throughput requirements in terms of known, present-day technology.

(6) Cell throughput is 180 cells per hour for 7.6 cm diameter wafers and 76 cells per hour for 12 cm diameter wafers. At these throughputs, with encapsulated cell efficiencies of 14%, the annual production for either size is very close to one megawatt peak power. As a consequence of assumption number one, the direct expense figures developed in this report may simply be multiplied by the desired yearly power production (in megawatts) to obtain the direct expenses for that rate of production.

Other values of efficiency may be assumed. Figure 3.9-2 shows annual power output versus cell efficiency for 76 cells/hour throughput of 12 cm diameter cells. At an encapsulated efficiency of 14%, QUAN = 996,378 watts.

FIGURE 3.9-2

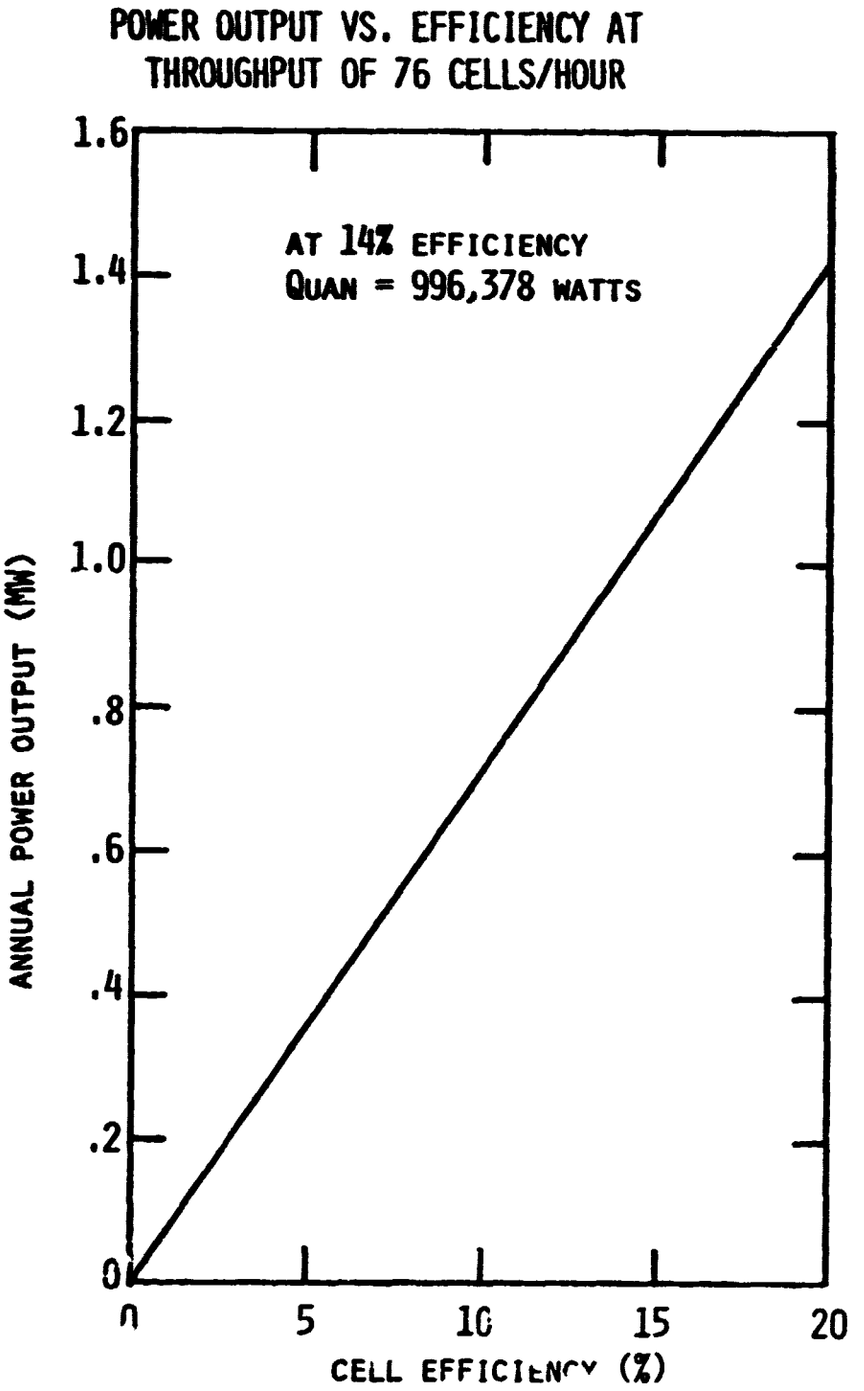
POWER OUTPUT VS. EFFICIENCY AT
THROUGHPUT OF 76 CELLS/HOUR
AT 14% EFFICIENCY
QUAN = 996,378 WATTS
ANNUAL POWER OUTPUT (MW)
1.6
1.4
1.2
1.0
.8
.6
.4
.2
0
0
5
10
15
20
CELL EFFICIENCY (%)

The same figure is almost equally valid for 7.6 cm diameter cells produced at 190 cells/hour except that the actual power quantity at 14% efficiency is QUAN = 999,146 watts.

3.9.3 DETAILED EXPENSE CALCULATIONS

The baseline NPMS process sequence discussed in Sections 3.9.1 and 3.9.2 is listed in Table 3.9.4. In this list, each major process step is further divided into substeps. Thus, step 1 has been subdivided into substeps a, b, and c. Similar divisions are made for steps 4 and 6. Each of the step subdivisions shown is treated as an operation to be costed. There are fourteen separate operations for which costing details are required. With respect to calculation of direct expenses for the IPEG price equation, several of the operations are identical, leaving only nine independent operations. In fact, three of these nine differ only in the direct materials (MATS) requirement.

Details of the expense calculations and assumptions for the nine independent operations are presented in the following sections. The step designations in the section titles refer to Table 3.9-4.

3.9.3.1 STEPS 1a, 4a, and 6a: ACID ETCH AND WATER RINSE

EQUIPMENT This step assumes a six foot laminar flow exhaust hood (such as IAS type LV6-30X) at a 1977 cost of $4,500. The hood is assumed to have six etch tanks, rinse tanks or sinks, each 7 inches wide by 6 inches deep by 20 inches long. In this application there will be three etch tanks and three rinse tanks.

Expenses for this step (and all other steps as well) depend on cell throughput. Cells are assumed to be handled in carriers of 50 wafers. The cycle time for etching and rinsing one carrier of wafers is 15 minutes. Each tank can hold four 7.6 cm cell carriers or three 12 cm cell carriers. Therefore, for 7.6 cm cells the maximum throughput is:

$$\frac{50 \text{ wafers}}{\text{carrier}} \times \frac{4 \text{ carriers}}{\text{tank}} \times \frac{3 \text{ tanks}}{\text{hood}} \times \frac{4 \text{ cycles}}{\text{hour}} = \frac{2400 \text{ wafers}}{\text{hood-hr.}}$$

TABLE 3.9-4

NICKEL-PALLADIUM METALLIZATION SYSTEM
IPEG ANALYSIS BASELINE PROCESS

1.	a.	10 Sec 10:1 H_2O:HF dip DIH_2O rinse
	b.	2 min. immersion palladium coat DIH_2O rinse
	c.	Spin dry
2.		30 minute reaction at 600°C in N_2
3.		Hydraulic, high pressure scrub (both sides)
4.	a.	DIH_2O dip
		5 sec 10:1 H_2O:HF dip
		DIH_2O rinse
	b.	15 sec immersion palladium dip
		DIH_2O
	c.	95 sec. electroless palladium plate
		DIH_2O rinse
	d.	Spin dry
5.		30 min. reaction at 600°C in N_2
6.	a.	DIH_2O dip
		5 sec 10:1 H_2O:HF dip
		DIH_2O rinse
	b.	5 min electroless nickel
		DIH_2O rinse
	c.	Spin dry
7.		Solder

For 12 cm cells the maximum throughput is:

$$\frac{50 \text{ wafers}}{\text{carrier}} \times \frac{3 \text{ carriers}}{\text{tank}} \times \frac{3 \text{ tanks}}{\text{hood}} \times \frac{4 \text{ cycles}}{\text{hour}} = \frac{1800 \text{ wafers}}{\text{hood-hr}}$$

By the assumptions of Section 3.9.2, the desired 7.6 cm cell throughput is 190 cells/hour and the 12 cm cell throughput is 76 cells/hour. These throughputs must be ratioed to the maximum throughputs in order to determine the direct equipment expenses. Therefore, for 7.6 cm cells,

$$\text{EQPT} = \frac{190 \text{ waf/hr.}}{2400 \text{ waf/hr.}} \times \frac{\$4500}{(1.07)^2} = \$311.16.$$

For 12 cm cells,

$$\text{EQPT} = \frac{76 \text{ waf/hr.}}{1800 \text{ waf/hr.}} \times \frac{\$4500}{(1.07)^2} = \$165.95.$$

These calculations assume a 7% inflation rate from Table 3.9-3.

FLOOR SPACE A total of 45 square feet is required for the hood discussed above with a reasonable work area for operators. Therefore for 7.6 cm cells,

$$\text{SQFT} = \frac{190 \text{ waf/hr.}}{2400 \text{ waf/hr.}} \times 45 \text{ ft}^2 = 3.5625 \text{ ft}^2$$

and for 12 cm cells,

$$\text{SQFT} = \frac{76 \text{ waf/hr.}}{1800 \text{ waf/hr.}} \times 45 \text{ ft}^2 = 1.9 \text{ ft}^2.$$

DIRECT LABOR A cycle time of 15 minutes per wafer carrier implies 4 cycles per hour which implies 0.5 operator per hood. At a 1976 labor rate of $8100 per year (from the cost account catalog), an 8% inflation rate, and a three shift operation, production of 7.6 cells requires

$$\text{DLAB} = \frac{190 \text{ waf/hr.}}{2400 \text{ waf/hr.}} \times \frac{0.5 \text{ op.}}{\text{shift}} \times 3 \text{ shifts} \times \frac{\$8100/\text{yr.}}{1.08} = \$890.61/\text{year}$$

while production of 12 cm cells requires

$$\text{DLAB} = \frac{76 \text{ waf/hr.}}{1800 \text{ waf/hr.}} \times \frac{0.5 \text{ op.}}{\text{shift}} \times 3 \text{ shifts} \times \frac{\$8100/\text{yr.}}{1.08} = \$474.99/\text{year}.$$

MATERIALS The materials required for this step are those for the 10:1 H_2O:HF acid rinse: HF and DIH_2O. From the cost account catalog, HF costs \$1430/2750 lb. in 1977 dollars at a 13% inflation rate. (HF weighs 9.75 lb/gal), and DIH_2O costs \$.037 per cubic foot in 1977 dollars at a 13% inflation rate. Therefore, a 10:1 H_2O:HF solution costs \$364.48 per 1000 gal in 1975 dollars. It is assumed that the dilute HF solution will be changed each shift. Therefore,

$$\frac{3 \text{ tanks}}{\text{hood}} \times \frac{3 \text{ changes}}{\text{day}} \times \frac{345 \text{ days}}{\text{yr.}} = \frac{3105 \text{ tank changes}}{\text{hood-yr.}}$$

It is assumed that solution volume per tank is enough to adequately cover the tops of the wafers in the carriers. This requires 2.106 gal/tank for 7.6 cm wafers and 3.226 gal/tank for 12 cm wafers.

Hence, for 7.6 cm cells,

$$\text{MATS} = \frac{190 \text{ waf/hr}}{2400 \text{ waf/hood-hr}} \times \frac{3105 \text{ tank changes}}{\text{hood-year}} \times \frac{2.106 \text{ gal}}{\text{tank change}} \times \frac{\$364.48}{1000 \text{ gal}}$$

$$= \$188.68/\text{year}.$$

For 12 cm cells,

$$\text{MATS} = \frac{76 \text{ waf/hr}}{1800 \text{ waf/hood-hr}} \times \frac{3105 \text{ tank changes}}{\text{hood-year}} \times \frac{3.226 \text{ gal}}{\text{tank change}} \times \frac{\$364.48}{1000 \text{ gal}}$$

$$= \$154.15/\text{year}.$$

UTILITIES The utilities requirements for one hood as described above are

electricity	1.1 KW
exhaust	450 CFM
DIH_2O	3 GPM.

The electrical power stated is the facilitization requirement. It is assumed throughout this cost analysis that steady-state operation requires only 50% of this "name-plate" power. It is assumed that the hood requires exhaust and electricity continuously, even during holidays. Therefore, electrical and

exhaust expenses are computed for 8766 hours/year. The exhaust requirement is converted to an electrical requirement by the ratio 0.46KW/1000 CFM. Thus, the electrical requirement per hood per year is:

$$[0.5\ (1.1\ KW) + 450\ CFM\ (\frac{0.46\ KW}{1000\ CFM})] \times \frac{8766\ hr}{yr} = 6635.862\ KWH/hood\text{-}yr.$$

From the cost account catalog, the electrical rate (in 1977 dollars at 12% inflation) is \$9.56/300 KWH. Hence the electricity cost for 7.6 cm cells is

$$\frac{190\ waf/hr}{2400\ waf/hood\text{-}hr} \times \frac{6635.862\ KWH}{hood\text{-}yr} \times \frac{\$9.56}{300\ KWH} \times \frac{1}{(1.12)^2} = \$13.35/year$$

and for 12 cm cells is

$$\frac{76\ waf/hr}{1800\ waf/hood\text{-}hr} \times \frac{6635.862\ KWH}{hood\text{-}yr} \times \frac{\$9.56}{300\ KWH} = \frac{1}{(1.12)^2} = \$7.12/year.$$

DI water usage per hood per year is computed to be

$$\frac{3\ gal}{hood\text{-}min} \times \frac{60\ min}{hr} \times \frac{8280\ hr}{yr} \times \frac{0.1337\ cu\ ft}{gal} = 199{,}266.48\ cu\ ft/hood\text{-}yr,$$

where DIH_2O is used only during working hours. At 1977 costs (13% inflation) of \$.037/cu. ft., the expense for 7.6 cm cells is

$$\frac{190\ waf/hr}{2400\ waf/hood\text{-}hr} \times \frac{100266.48\ cu\ ft}{hood\text{-}yr} \times \frac{\$.037}{cu\ ft} \times \frac{1}{(1.13)^2} = \$457.11/year.$$

The expense for 12 cm cells is

$$\frac{76\ waf/hr}{1800\ waf/hood\text{-}hr} \times \frac{100266.48\ cu\ ft}{hood\text{-}yr} \times \frac{\$.037}{cu\ ft} \times \frac{1}{(1.13)^2} = \$243.79/year.$$

Adding together the costs of electricity and water gives, for 7.6 cm cells,

UTIL = \$13.35/yr + \$457.11/yr = \$470.46/year

and for 12 cm cells,

UTIL = \$7.12/yr + \$243.79/yr = \$250.91/year.

The calculations for this first step have been explained in some detail to exhibit the techniques used to arrive at the inputs for the IPEG price

equation. In the presentation of subsequent steps, much of this detail will be omitted where it does not differ from this first example.

3.9.3.2 STEP 1b: IMMERSION PALLADIUM COAT AND WATER RINSE

EQUIPMENT This step assumes the same six foot laminar flow exhaust hood and set-up as in the previous step (Section 3.9.3.1) with the addition of a chemical recirculating system (such as Fluorocarbon Model 5000). The chemical recirculating system is used to agitate the immersion palladium plating bath and to pump plating solution from the working tanks through a reservoir where the condition of the solution can be monitored and the solution can be replenished. The addition of the recirculating system adds a cost of $7500 for a total 1977 cost of $12,000.

Again wafers are handled in 50 wafer cassettes and a cycle time of 15 minutes is assumed. Thus, there are 4 cycles/hr. This gives maximum throughputs per hood identical to Section 3.9.3.1. Therefore, for 7.6 cm cells,

$$EQPT = \frac{190 \text{ waf/hr}}{2400 \text{ waf/hr.}} \times \frac{\$12,000}{(1.07)^2} = \$829.77$$

and for 12 cm cells,

$$EQPT = \frac{76 \text{ waf/hr}}{1800 \text{ waf/hr.}} \times \frac{\$12,000}{(1.07)^2} = \$442.54.$$

FLOOR SPACE This is the same as Section 3.9.3.1.

DIRECT LABOR This is the same as Section 3.9.3.1

MATERIALS This category introduces an additional complexity since the amount of material used here depends on the percentage of the wafer surface to be covered with metal. Two contingencies are presented in this section and in the following sections which deal with metal application. In the first case, the

C-2

metal pattern covers 7% of the area of the solar cell front surface and 100% of the area of the cell back surface, for a total metal coverage of 107% of the wafer area. In the second case, the metal pattern covers 7% of the area of the cell front surface and has a patterned back contact which covers 14% of the area of the cell back surface, for a total metal coverage of 21% of the wafer area. Because of the cost of palladium and solder, these two contingencies will lead to significantly different total prices.

Using the formula for immersion palladium solution given Table 3.9-5, the solution costs, excluding the cost of palladium chloride, is $1.847/gal. in 1975 dollars. It is assumed that the palladium content is replenished as needed and that the solution itself is replaced once a day. Thus, solution costs are, for 7.6 cm cells,

$$\frac{1035 \text{ tank changes}}{\text{hood-yr}} \times \frac{2.106 \text{ gal}}{\text{tank change}} \times \frac{\$1.847}{\text{gal}} \times \frac{190 \text{ waf/hr}}{2400 \text{ waf/hood-hr}} = \$318.72/\text{year}$$

and for 12 cm cells,

$$\frac{1035 \text{ tank changes}}{\text{hood-yr}} \times \frac{3.226 \text{ gal}}{\text{tank change}} \times \frac{\$1.847}{\text{gal}} \times \frac{76 \text{ waf/hr}}{1800 \text{ waf/hood-hr}} = \$260.38/\text{year}.$$

Palladium costs are computed independent of the solution costs. Palladium is introduced in the bath as palladium chloride ($PdCl_2$) which has a 1976 cost of $1250 per 250 grams. The 13% chemical inflation rate will be applied. For the purpose of this analysis, it is assumed that an effective layer of 50Å of palladium is applied. For a density of 12.16 g/cm^3, this requires a weight of 6.08×10^{-6} g per cm^2 of metallized surface area.

Therefore, for 7.6 cm cells with 107% metal coverage, the palladium cost is

$$1.07 \times \frac{\pi (7.6)^2}{4} \text{ cm}^2 \times \frac{6.08 \times 10^{-6} \text{ g}}{\text{cm}^2} \times \frac{177.3 \text{ g } PdCl_2}{106.4 \text{ g Pd}} \times \frac{\$1250}{250 \text{ g } PdCl_2}$$

$$\frac{1}{1.13} \times \frac{190 \text{ waf}}{\text{hr}} \times \frac{8289 \text{ hr}}{\text{yr}} = \$3423.32/\text{year}.$$

TABLE 3.9-5

IMMERSION PALLADIUM SOLUTION

CONSTITUENT		AMOUNT
Water	H_2O	500 mℓ
Fluoboric Acid	HBF_4	500 mℓ
Hydrochloric Acid	HCl (38%)	2.5 mℓ
Palladium Chloride	$PdCl_2$	0.025 g

For 7.6 cm cells with 21% metal coverage this becomes $671.87/year. For 12 cm cells with 107% metal coverage the cost is $3413.84/year and with 21% metal coverage the cost is $670.01/year. (Remember that the 12 cm throughput is 76 wafers/hour.)

The total material cost is the sum of solution and palladium costs. Thus, for 7.6 cm cells with 107% metal,

MATS = $318.72/yr + $3423.32/yr = $3742.04/year

and with 21% metal,

MATS = $318.72/yr + $671.87/yr = $990.59/year

For 12 cm cells with 107% metal,

MATS = $260.38/yr + $3413.84/yr = $3674.22/year

and with 21% metal,

MATS = $260.38/yr + $670.01/yr = $930.39/year.

UTILITIES Since the same exhaust hood is assumed in this step as in Section 3.9.3.1 the utilities requirement differs only in the additional electricity and exhaust required for the chemical recirculating system. The total requirements for this step are

electricity	1.6 KW
exhaust	500 CFM
DIH_2O	3 GPM.

Applying the same assumptions and techniques used in Section 3.9.3.1, the total electrical requirement is 9028.98 KWH/hood-yr. This results in a 1975 cost of $18.16/year for 7.6 cm cells and $9.68/year for 12 cm cells. Adding this to the same DIH_2O costs as Section 3.9.3.1 yields, for 7.6 cm cells,

UTIL = $18.16/yr + $457.11/yr = $475.27/yr

and for 12 cm cells,

UTIL = \$9.68/yr + \$243.79/yr = \$253.47/year.

3.9.3.3 STEPS 1c, 4d, and 6c: SPIN DRY

EQUIPMENT This step assumes a centrifugal rinser-dryer such as the Fluoroware K-100 with #1150 frame and #1231 cradle (for 7.6 cm wafers). The 1977 cost of this equipment is \$2500. The spin dryer will hold six 25 wafer carriers of 7.6 cm wafers or (with a different cradle) four 25 wafer carriers of 12 cm wafers. Including loading and unloading, a 15 minute cycle time is assumed. Maximum machine throughput is, for 7.6 cm wafers,

$$\frac{25\ \text{waf}}{\text{carrier}} \times \frac{6\ \text{carriers}}{\text{machine}} \times \frac{4\ \text{cycles}}{\text{hour}} = \frac{600\ \text{waf}}{\text{mach-hr}}$$

and for 12 cm wafers,

$$\frac{25\ \text{waf}}{\text{carrier}} \times \frac{4\ \text{carriers}}{\text{machine}} \times \frac{4\ \text{cycles}}{\text{hour}} = \frac{400\ \text{waf}}{\text{mach-hr}}.$$

Therefore, for 7.6 cm cells,

$$\text{EQPT} = \frac{190\ \text{waf/hr}}{600\ \text{waf/mach-hr}} \times \frac{\$2500/\text{mach}}{(1.07)^2} = \$691.47$$

and for 12 cm cells,

$$\text{EQPT} = \frac{76\ \text{waf/hr}}{400\ \text{waf/mach-hr}} \times \frac{\$2500/\text{mach}}{(1.07)^2} = \$414.88.$$

FLOOR SPACE A total of 30 ft^2 is required for the machine above, plus work space. Therefore, for 7.6 cm cells,

$$\text{SQFT} = \frac{190\ \text{waf/hr}}{600\ \text{waf/hr}} \times 30\ ft^2 = 9.5\ ft^2$$

and for 12 cm cells,

$$\text{SQFT} = \frac{76\ \text{waf/hr}}{400\ \text{waf/hr}} \times 30\ ft^2 = 5.7\ ft^2.$$

DIRECT LABOR It is assumed that one operator can handle four machines. At the same labor rates as used in Section 3.9.3.1, for 7.6 cm cells,

$$\text{DLAB} = \frac{190 \text{ waf/hr}}{600 \text{ waf/hr}} \times \frac{0.25 \text{ op}}{\text{shift}} \times 3 \text{ shifts} \times \frac{\$8100/\text{yr}}{1.08} = \$1781.25/\text{year}$$

and for 12 cm cells,

$$\text{DLAB} = \frac{76 \text{ waf/hr}}{400 \text{ waf/hr}} \times \frac{0.25 \text{ op}}{\text{shift}} \times 3 \text{ shifts} \times \frac{\$8100/\text{yr}}{1.08} = \$1068.75/\text{year}.$$

MATERIALS The only material requirement is the nitrogen gas used during the operation of the spin dryer. Assuming that liquid nitrogen (from the JPL Cost Account Catalog) is vaporized as the source of nitrogen gas, the 1977 cost is \$.00934/cu ft (13% inflation rate). The use per machine is 13.2 ℓ/min. Therefore,

$$\frac{13.2 \text{ ℓ}}{\text{min}} \times \frac{60 \text{ min}}{\text{hr}} \times \frac{8280 \text{ hr}}{\text{yr}} \times \frac{.03532 \text{ cu ft}}{\text{ℓ}} = 231{,}620.0832 \text{ cu ft/yr per machine.}$$

For 7.6 cm cells,

$$\text{MATS} = \frac{190 \text{ waf/hr}}{600 \text{ waf/hr}} \times \frac{231620.0832 \text{ cu ft}}{\text{yr}} \times \frac{\$.00834/\text{cu ft}}{(1.13)^2} = \$479.06/\text{year}.$$

For 12 cm cells,

$$\text{MATS} = \frac{76 \text{ waf/hr}}{400 \text{ waf/hr}} \times \frac{231620.0832 \text{ cu ft}}{\text{yr}} \times \frac{\$.00834/\text{cu ft}}{(1.13)^2} = \$287.43/\text{year}.$$

UTILITIES The utilities requirement for the rinser-dryer is a 1 KW facilitization with no exhaust or water. Assuming power is required only during working hours, and, as in Section 3.9.3.1, 50% of the "nameplate" power is actually needed, the annual requirement is

$$0.5 \left(\frac{1 \text{ KW}}{\text{mach}} \right) \times \frac{8280 \text{ hr}}{\text{yr}} = \frac{4140 \text{ KWH}}{\text{mach-yr}} .$$

Hence, 7.6 cm cells require \$33.30/year and 12 cm cells require \$19.98/year.

3.9.3.4 STEPS 2 AND 5: HEAT TREATMENT AND PALLADIUM SILICIDE FORMATION

EQUIPMENT This step assumed the use of a belt furnace at a 1977 cost of $35,000. It is assumed that two carriers of 50 wafers each (either 7.6 or 12 cm) are placed on the belt simultaneously and that the throughput time is the same as the heat treatment time: 30 minutes. If two new carriers are loaded into the furnace every 30 seconds then the maximum furnace throughput is

$$\frac{100 \text{ waf}}{30 \text{ sec}} \times \frac{60 \text{ sec}}{\text{min}} \times \frac{60 \text{ min}}{\text{hr}} = 12{,}000 \text{ waf/hr.}$$

Thus, for 7.6 cm cells,

$$\text{EQPT} = \frac{190 \text{ waf/hr}}{12000 \text{ waf/hr}} \times \frac{\$35{,}000}{(1.07)^2} = \$484.03$$

and for 12 cm cells,

$$\text{EQPT} = \frac{76 \text{ waf/hr}}{12000 \text{ waf/hr}} \times \frac{\$35000}{(1.07)^2} = \$193.61.$$

FLOOR SPACE The required floor space is assumed to be 132 ft^2. Therefore SQFT = 2.09 ft^2 for 7.6 cm cells and SQFT = 0.836 ft^2 for 12 cm cells.

DIRECT LABOR One operator is required to run one furnace. At the same labor rates as used in Section 3.9.3.1, DLAB = $356.25/year for 7.6 cm cells and DLAB = $142.50/year for 12 cm cells.

MATERIALS It is assumed that a nitrogen purge in each furnace is required at a rate of 40 ℓ/min (19,872,000 ℓ/year). With the same nitrogen costs as Section 3.9.3.3, then, after adjusting for the proper throughput, the 7.6 cm cell expense is MATS = $72.58/year and for 12 cm cells, MATS = $29.03/year.

UTILITIES The utilities requirement for such a belt furnace is assumed to be an electrical facilitization of 15 kW with 100 CFM exhaust. The same assumption as used for utilities calculations in Section 3.9.3.1 apply here.

Therefore, the annual electrical requirement per furnace is

$$[0.5\ (15KW) + 100\ CFM\ (\frac{0.46\ KW}{1000\ CFM})] \times \frac{8766\ hr}{yr} = 66148.236\ KWH/year.$$

Thus, for 7.6 cm cells,

$$UTIL = \frac{190\ waf/hr}{12000\ waf/hr} \times \frac{66148.236\ KWH}{yr} \times \frac{\$9.56}{300\ KWH} \times \frac{1}{(1.12)^2} = \$26.61/year.$$

For 12 cm cells,

$$UTIL = \frac{76\ waf/hr}{12000\ waf/hr} \times \frac{66148.236\ KWH}{yr} \times \frac{\$9.56}{300\ KWH} \times \frac{1}{(1.12)^2} = \$10.64/year.$$

3.9.3.5 STEP 3: HIGH PRESSURE SCRUB

EQUIPMENT This step assumes the use or a hydraulic (DIH_2O) high pressure wafer scrubber such as the Macronetics HPC-1000 at a 1977 cost of $12,925 per track. A four track unit with a cabinet and laminar flow hood could have a total 1977 cost of $56,495. Such a four track unit has a throughput of 1000 wafers/hour for either size wafer. Since this step assumes that both sides of a wafer are scrubbed, the effective maximum throughput is 500 wafers/hour. Thus, for 7.6 cm cells,

$$EQPT = \frac{190\ waf/hr}{500\ waf/hr} \times \frac{\$56495}{(1.07)^2} = \$18,751.07$$

and for 12 cm cells,

$$EQPT = \frac{76\ waf/hr}{500\ waf/hr} \times \frac{\$56495}{(1.07)^2} = \$7,500.43.$$

FLOOR SPACE The required floor space is assumed to be 45 ft^2 per four track unit. Therefore, SQFT = 17.1 ft^2 for 7.6 cm cells and SQFT = 6.84 ft^2 for 12 cm cells.

DIRECT LABOR One operator is required to run a four track unit. Therefore, as in Section 3.9.3.1, for 7.6 cm wafers,

$$DLAB = \frac{190 \text{ waf/hr}}{500 \text{ waf/hr}} \times \frac{1 \text{ op}}{\text{shift}} \times 3 \text{ shifts} \times \frac{\$8100/\text{op-yr.}}{\$1.08} = \$8550/\text{year.}$$

For 12 cm wafers,

$$DLAB = \frac{76 \text{ waf/hr}}{500 \text{ waf/hr}} \quad \frac{1 \text{ op}}{\text{shift}} \times 3 \text{ shifts} \times \frac{\$8100/\text{op-yr.}}{\$\ 1.08} = \$3420/\text{year.}$$

MATERIALS No materials are consumed.

UTILITIES The facilities requirements are

electrical	2.1 KW
exhaust	320 CFM
DIH_2O	3.2 GPM.

The same assumptions used for utilities calculations in Section 3.9.3.1 apply here, except that the electrical requirement applies only during working hours. Therefore

$$0.5\ (2.1 \text{ KW}) \times 8280 \text{ hr/yr} + 320 \text{ CFM } (\frac{0.46 \text{ kW}}{1000 \text{ CFM}}) \times \frac{8766 \text{ hr}}{\text{yr}} = 9984.355 \text{ KWH/year.}$$

For 7.6 cm cells, electricity costs are $96.38/year and for 12 cm cells, electricity costs are $38.55/year.

Water consumption is

$$\frac{3.2 \text{ gal}}{\text{min}} \times \frac{60 \text{ min}}{\text{hr}} \times \frac{8280 \text{ hr}}{\text{yr}} \times \frac{0.1337 \text{ cu ft}}{\text{gal}} = 212550.9 \text{ cu ft/year.}$$

This adds a cost of $2340.41/year for 7.6 cm wafers and $936.16/year for 12 cm wafers. Therefore, for 7.6 cm cells,

UTIL = $2436.79/year

and for 12 cm cells,

UTIL = $974.71/year.

3.9.3.6 STEP 4b: IMMERSION PALLADIUM DIP AND WATER RINSE

With the exception of the expended materials costs, the assumptions and calculated expenses of this step are identical to those of Section 3.9.3.2 (Step 1b).

MATERIALS The cost of immersion palladium solution replacement is assumed to be identical to that calculated in Section 3.9.3.2. The plating time for this step is 15 sec while the plating time for step 1b is 120 sec. Therefore the palladium cost is assumed to be 15 sec/120 sec = 1/8 the cost calculated in Section 3.9.3.1. Hence, for 7.6 cm cells with 107% metal, adding solution and palladium costs,

MATS = $318.72/hr + $427.91/yr = $746.63/year

and with 21% metal,

MATS = $318.72/year + $83.98/yr = $402.70/year.

For 12 cm cells with 107% metal,

MATS = $260.38/yr + $426.73/yr = $687.11/year

and with 21% metal,

MATS = $260.38/yr + $83.75/yr = $344.13/year.

3.9.3.7 STEP 4c: ELECTROLESS PALLADIUM PLATE AND WATER RINSE

With the exception of the expended materials costs, the assumptions and calculated expenses of this step are identical to those of Section 3.9.3.2 (step 1b).

MATERIALS Once again, as in Section 3.9.3.1, four examples are being considered: 107% and 21% metal coverage for both 7.6 and 12 cm wafers.

Using the formula for electroless palladium solution given previously in Table 3.9-6, the solution cost, including the cost of palladium chloride,

TABLE 3.9-6

ELECTROLESS PALLADIUM SOLUTION

CONSTITUENT		AMOUNT
Water	H_2O	830 mℓ
Hydrochloric Acid	HCl (38%)	4 mℓ
Palladium Chloride	$PdCl_2$	2 g
Ammonium Chloride	NH_4Cl	27 g
Sodium Hypophosphite	$NaH_2PO_2 \cdot 2H_2O$	6 g
Ammonium Hydroxide	NH_4OH (58%)	160 mℓ

is $8.94865 per liter in 1975 dollars. It is assumed that the palladium content of the solution is used with 95% efficiency.

Materials costs are calculated for a palladium layer thickness of 800Å and an effective density of 11.98 g/cm^3. This density is slightly less than the density of elemental palladium. This assumption is made because the electroless palladium layer actually contains a small percentage of phosphorous. The amount of palladium available per liter is

$$\frac{2 \text{ g } PdCl_2}{\ell} \times \frac{106 \text{ g Pd}}{177.306 \text{ g } PdCl_2} \times 0.95 = \frac{1.140 \text{ g Pd}}{\ell} .$$

For 7.6 cm cells with 107% metal coverage, the materials cost is

$$MATS = 1.07 \times \frac{\pi(7.6)^2}{4} \frac{cm^2}{waf} \times 8 \times 10^{-6} \text{ cm} \times \frac{11.98 \text{ g}}{cm^3} \times \frac{190 \text{ waf}}{} \times \frac{8280 \text{ hr}}{hr}$$

$$\times \frac{1 \ell}{1.140 \text{ g}} \times \frac{\$8.94865}{\ell} = \$57,449.24/\text{year}.$$

For 7.6 cm cells with 21% metal coverage, this becomes MATS = $11,275.08/year. For 12 cm cells with 107% metal coverage, the cost is MATS = $57,290.10/year and with 21% metal coverage the cost is MATS = $11,243.85/year.

3.9.3.8 STEP 6b: ELECTROLESS NICKEL PLATE AND WATER RINSE

EQUIPMENT This step assumes the same equipment (laminar flow exhaust hood and chemical recirculating system) used in Section 3.9.3.2 but the cell throughput will be different. The wafers are handled in 50 wafer carriers and a cycle time of 20 minutes is assumed. Thus there are 3 cycles/hour. This gives a maximum 7.6 cm cell throughput of

$$\frac{50 \text{ waf}}{\text{carrier}} \times \frac{4 \text{ carriers}}{\text{sink}} \times \frac{3 \text{ sinks}}{\text{hood}} \times \frac{3 \text{ cycles}}{\text{hr}} = 1800 \frac{\text{wafer}}{\text{hood-hr}}$$

and a maximum 12 cm cell throughput of

$$\frac{50 \text{ waf}}{\text{carrier}} \times \frac{3 \text{ carriers}}{\text{sink}} \times \frac{3 \text{ sinks}}{\text{hood}} \times \frac{3 \text{ cycles}}{\text{hr}} = 1350 \frac{\text{waf}}{\text{hood-hr}}$$

Therefore, for 7.6 cm cells,

$$\text{EQPT} = \frac{190 \text{ waf/hr}}{1800 \text{ waf/hr}} \times \frac{\$12000}{(1.07)^2} = \$1106.36$$

and for 12 cm cells,

$$\text{EQPT} = \frac{76 \text{ waf/hr}}{1350 \text{ waf/hr}} \times \frac{\$12000}{(1.07)^2} = \$590.06.$$

FLOOR SPACE The required floor space is 45 ft^2 per hood. Therefore, SQFT = 4.75 ft^2 for 7.6 cm cells and SQFT = 2.533 ft^2 for 12 cm cells.

DIRECT LABOR Three plating cycles per hour will require 1/2 operator per hood. Assuming 3 shift operation and weighting according to wafer throughput gives DLAB = $1187.49/year for 7.6 cm cells and DLAB = $633.33/year for 12 cm cells.

MATERIALS Once again, as in Section 3.9.3.2, four examples are being considered: 107% and 21% metal coverage for both 7.6 cm and 12 cm wafers.

Using the formula for electroless nickel solution given in Table 3.9-7 the solution cost is $0.37723 per liter in 1975 dollars. It is assumed that by continuous replenishment techniques the nickel content of the solution is effectively used with 95% efficiency.

Materials costs are calculated for a nickel layer thickness of 5000Å and an effective density of 7.77 g/cm^3. The amount of nickel available per liter is

$$\frac{30 \text{ g Ni Chloride}}{\ell} \times \frac{58.71 \text{ g Ni}}{237.71 \text{ g Ni Chloride}} \times 0.95 = \frac{7.039 \text{ g Ni}}{\ell}$$

For 7.6 cm cells with 107% metal coverage, the materials cost is

TABLE 3.9-7

ELECTROLESS NICKEL SOLUTION

CONSTITUENT		AMOUNT
Water	H_2O	875 mℓ
Nickel Chloride	$NiCl_2 \cdot 6H_2O$	30 g
Ammonium Chloride	NH_4Cl	50 g
Sodium Citrate	$Na_3C_6H_5O_7 \cdot 2H_2O$	84 g
Sodium Hypophosphite	$NaH_2PO_2 \cdot 2H_2O$	10 g
Ammonium Hydroxide	NH_4OH (58%)	125 mℓ

$$\text{MATS} = 1.07 \times \frac{\pi(7.6)^2}{4} \frac{\text{cm}^2}{\text{waf}} \times 0.5 \times 10^{-4} \text{ cm} \times \frac{7.77 \text{ g}}{\text{cm}^3} \times 190 \frac{\text{waf}}{\text{hr}}$$

$$\times \frac{8280 \text{ hr}}{\text{yr}} \times \frac{1 \text{ ℓ}}{7.039 \text{ g}} \times \frac{\$0.37723}{\text{ℓ}} = \$1589.90/\text{year}.$$

For 7.6 cm cells with 21% metal coverage this becomes MATS = $312.04/year. For 12 cm cells with 107% metal coverage the cost is MATS = $1585.50/year and with 21% metal coverage the cost is MATS = $311.17/year.

UTILITIES The utilities requirement for this step is the same, per hood, as given in Section 3.9.3.2. However, the throughput per hood is different. The net result is an electricity cost (calculated as in Section 3.9.3.1) of $24.21/year for 7.6 cm cells and $12.91/year for 12 cm cells. Accounting for the different throughput rates, the DIH_2O costs are $609.48/year for 7.6 cm cells and $325.06/year for 12 cm cells. Therefore, for 7.6 cm cells,

UTIL = $24.21/year + $609.48/year = $633.69/year

and for 12 cm cells,

UTIL = $12.91/year + $325.06/year = $337.97/year.

3.9.3.9 STEP 7: SOLDER COAT

EQUIPMENT This step assumes an automatic solder system with subsystems for flux application, pre-heating, soldering, cleaning, and drying. This system is assumed to have a 1977 purchase price of $50,000 (7% inflation rate). Cell throughput calculations are made by assuming a transport speed of 10 ft/min across a solder fountain 15 inches wide. Thus 7.6 cm cells can be transported four abreast while 12 cm cells can be transported three abreast. The spacing between cell rows is assumed to be one cell diameter. Hence, 7.6 cm cells have a throughput of

$$\frac{20 \text{ rows}}{\text{min}} \times \frac{4 \text{ waf}}{\text{row}} = \frac{80 \text{ waf}}{\text{min}} = 4800 \frac{\text{waf}}{\text{hr}}$$

while 12 cm cells have a throughput of

$$\frac{12.7 \text{ rows}}{\text{min}} \times \frac{3 \text{ waf}}{\text{row}} = \frac{38.1 \text{ waf}}{\text{min}} = 4800 \frac{\text{waf}}{\text{hr}} .$$

Therefore, for 7.6 cm cells,

$$EQPT = \frac{190 \text{ waf/hr}}{4800 \text{ waf/hr}} \times \frac{\$50,000}{(1.07)^2} = \$1728.68$$

and for 12 cm cells,

$$EQPT = \frac{76 \text{ waf/hr}}{2286 \text{ waf/hr}} \times \frac{\$50,000}{(1.07)^2} = \$1451.91.$$

FLOOR SPACE One automatic solder system is assumed to require 100 ft^2 of floor space. Thus for 7.6 cm cells SQFT = 3.958 ft^2 and for 12 cm cells SQFT = 3.325 ft^2.

DIRECT LABOR Three shift operation is assumed and one operator is allocated to one automatic system. With the same labor rates as Section 3.3.3.1, DLAB = $890.61/year for 7.6 cm cells and DLAB = $748.02/year for 12 cm cells.

MATERIALS The principal materials consumed in this operation are solder and flux. A three inch diameter solar cell with a total area of metal coverage equal to 48.52 cm^2 requires 1.45 g of lead-tin solder (based on empirical measurements). This gives an effective solder weight per unit area (of metal coverage) of 0.02988 g/cm^2. Hence, 1.4504 g of solder is required for one 7.6 cm cell with 107% metal coverage and 0.28465 g of solder is required for 21% metal coverage. For a 12 cm cell, 107% requires 3.6159 g and 21% requires 0.70966 g.

The cost is assumed to be (1977 dollars) $2.97667/lb for 60 Sn/40 Pb solder. Therefore, for 7.6 cm cells with 107% metal coverage,

$$\frac{190 \text{ waf}}{\text{hr}} \times \frac{8280 \text{ hr}}{\text{yr}} \times \frac{1.4504 \text{ g}}{\text{waf}} \times \frac{1 \text{ lb}}{453.59 \text{ g}} \times \frac{\$2.97667}{\text{lb}} \times \frac{1}{(1.08)^2} = \$12,837.82/\text{year}$$

and with only 21% metal coverage the solder cost is $2519.50/year. For 12 cm wafers, the solder cost is $12,802.07/year for 107% and $2512.55/year for 21%.

Flux is assumed to cost $6.75/gal in 53 gal drums at 1978 prices (chemical inflation rate of 13%). One gallon will coat 200 ft^2 of wafer surface or 185,806 cm^2. Since wafers are completely covered with flux, flux usage is independent of metal coverage. For 7.6 cm cells the flux cost will be $3593.68/year and for 12 cm cells the cost will be $3583.73/year.

Adding flux and solder costs gives, for 7.6 cm cells with 107% metal coverage,

MATS = $12,837.82/yr + $3593.68/yr = $16,431.50/year

and for 21% metal coverage,

MATS = $2519.50/yr + $3593.68/yr = $6113.18/year.

For 12 cm cells with 107% metal coverage,

MATS = $12,802.07/yr + $3583.73/yr = $16,385.80/year

and for 21% metal coverage,

MATS = $2512.55/yr + $3583.73/yr = $6096.28/year.

UTILITIES The utilities requirements for the automatic solder system are assumed to be

electrical	15 KW
exhaust	4000 CFM
DIH_2O	10 GPM.

The exhaust is assumed to run continuously while the electricity and DIH_2O are required only during working hours. In the same manner as the calculations of Section 3.9.3.1., this gives a total electrical cost of $78.67/yr for 7.6

cm cells and $66.07/yr for 12 cm cells. The DIH_2O costs are $761.85/yr for 7.6 cm cells and $639.88/yr for 12 cm cells. Hence,

UTIL = $78.67/yr + $761.85/yr = $840.52/year

for 7.6 cm cells and

UTIL = $66.07/yr + $639.88/yr = $705.95/year

for 12 cm cells.

3.9.4 INITIAL PRICE ANALYSIS RESULTS

In Section 3.9.3, each process substep from Table 3.9-4 has been analyzed to determine the associated direct expenses for equipment, labor, materials, and utilities and to determine the required floor space and number of operators. This has been done for a nominal one megawatt annual production level for both 7.6 cm and 12 cm diameter circular solar cells. For each cell size, two metallization styles are analyzed. One style incorporates a patterned front contact with a back contact which covers the rear surface completely ("10% metal"). The other style incorporates a patterned front contact as well ("2% metal").

The expense data for the substeps of Table 3.9-4 have been tabulated for each of the seven major process steps and for the total NPMS process sequence. These results are presented in Tables 3.9-8 and 3.9-9 for 7.6 cm and 12 cm diameter cells, respectively. In both tables, the materials expense column is divided to show the differences between 2% total metal coverage and 10% total metal coverage. These differences occur only for the materials expenses.

When the weighting coefficients for the IPEG price equation are applied to the direct expenses of Tables 3.9-8 and 3.9-9, the add-on contribution to solar cell price is obtained for each expense and process step. These prices

TABLE 3.9.8

NPMS DIRECT EXPENSES

7.6 cm DIAMETER SUBSTRATES

PROCESS STEP	EQPT ($)	SQFT (ft^2)	DLAB (F/yr)	MATS ($/yr) 21% METAL	MATS ($/yr) 107% METAL	UTIL ($/yr)	NO. OF OPERATORS (prsn-yrs)
1	1832.40	16.625	3562.47	1658.33	4409.78	979.03	.4752
2	484.03	2.09	356.25	72.58	72.58	26.61	.04749
3	18751.07	17.1	8550.00	0	0	2436.79	1.14
4	2662.17	20.1875	4453.08	12345.52	58863.61	1454.30	.594
5	484.03	2.09	356.25	72.58	72.58	26.42	.04749
6	2108.99	17.8125	3859.35	979.78	2257.64	1137.45	.5148
7	1728.68	3.958	890.61	6113.18	16431.50	840.52	.1188
TOTAL	28051.37	79.863	22028.01	21241.97	82107.69	6901.31	2.93778

(a) Expenses are for 190 cells/hr X 8280 hr/yr = 1,573,200 cells
(b) Dollars are expressed in 1975 values.

TABLE 3.9-9

NPMS DIRECT EXPENSES

12 cm DIAMETER SUBSTRATES

PROCESS STEP	EQPT ($)	SQFT (ft^2)	DLAB ($/yr)	MATS ($/yr)		UTIL ($/yr)	NO. OF OPERATORS
				21% METAL	107% METAL		
1	1023.37	9.5	2018.73	1371.97	4115.80	524.36	.2691
2	193.51	.836	142.50	29.03	29.03	10.64	.01899
3	7500.43	6.84	3420.00	0	0	974.71	.456
4	1465.91	11.4	2493.72	12029.56	58418.79	777.83	.3325
5	193.61	.836	142.50	29.03	29.03	10.64	.01899
6	1170.89	10.133	2177.07	752.75	2027.08	608.86	.2901
7	1451.91	3.325	748.02	6096.28	16385.80	705.95	.0996
TOTAL	12999.73	42.87	11142.54	20308.62	81005.53	3602.35	1.48518

(a) Expenses are for 76 cells/hr X 8280 hr/yr = 629,280 cells
(b) Dollars are expressed in 1975 values.

are shown in Table 3.9-10 for 7.6 cm cells and Table 3.9-11 for 12 cm cells. The values listed are prices for a nominal one megawatt annual production (which assumes a 14% encapsulated cell efficiency). Summations are given for the total price of each process step for both cell metal coverage assumptions, for the total price associated with each expense category for the entire process, and for the grand total of the whole NPMS process for both metal coverages.

With the assumption that encapsulated cell efficiency is 14%, the prices given in 1975 dollars in Tables 3.9-10 and 3.9-11 can be converted to add-on prices in cents per watt. These data are presented in Table 3.9-12 for 7.6 cm cells and Table 3.9-13 for 12 cm cells.

Several observations can be made regarding the data of Tables 3.9-12 and 3.9-13. There is a large difference between total prices for 10% metal coverage (patterned front and solid back) and for 21% metal coverage (patterned front and patterned back). This is true for both 7.6 cm cells and 12 cm cells and is primarily due to materials expenses for electroless palladium plating (step 4) and solder coating (step 7). In fact, for the case of a solid back metal contact, the materials expenses above for step 4 and step 7 account for 52% of the price of 7.6 cm cells and 67% of the price of 12 cm cells. Of these percentages, 78% is due to the materials expense in step 4, electroless palladium plating

A third step which Tables 3.9-12 and 3.9-13 prove to be an expensive one is step 3, high pressure scrubbing of the wafer surface. The dominant expense item for this step is the direct labor cost. The reason for this is the low throughput of present day scrubbing machines.

TABLE 3.9-10

NPMS PRICES IN 1975 DOLLARS

7.6 cm DIAMETER SUBSTRATES

PROCESS STEP	0.489 EQPT	96.9 SQFT	2.133 DLAB	1.255 MATS		1.255 UTIL	STEP TOTAL	
				21% METAL	107% METAL		21% METAL	107% METAL
1	896.04	1610.96	7598.75	2081.20	5543.27	1228.68	13415.63	16368.70
2	236.69	202.52	759.88	91.09	91.09	33.40	1323.58	1323.58
3	9169.27	1656.99	18237.15	0	0	3058.17	32121.58	32121.58
4	1301.80	1956.17	9498.42	15493.63	73873.83	1825.15	30075.17	88455.37
5	236.69	202.52	759.88	91.09	91.09	33.40	1323.58	1323.58
6	1031.30	1726.03	8231.99	1229.62	2833.34	1427.59	13646.44	15250.16
7	845.32	383.53	1899.67	7672.04	20621.53	1054.85	11855.41	24804.90
TOTAL	12717.12	7738.72	46985.75	26658.67	103045.15	8661.14	103761.40	180147.88

Prices are for 190 cells/hr X 8280 hr/yr = 1,537,200 cells.

TABLE 3.9-11

NPMS PRICES IN 1975 DOLLARS

12 cm DIAMETER SUBSTRATES

PROCESS STEP	0.489 EQPT	96.9 SQFT	2.133 DLAB	1.255 MATS		1.255 UTIL	STEP TOTAL	
				21% METAL	107% METAL		21% METAL	107% METAL
1	500.43	920.55	4305.95	1721.82	5165.33	658.07	8106.92	11550.33
2	94.68	81.01	303.95	36.43	36.43	13.37	529.42	529.42
3	3667.71	662.80	7294.86	0	0	1223.26	12848.03	12848.63
4	716.83	1104.66	5319.10	15097.10	73315.58	976.18	23213.87	81432.35
5	04.68	81.01	303.95	36.43	36.43	13.35	529.42	529.42
6	572.57	981.89	4643.69	944.79	2543.99	764.12	7906.97	9506.26
7	709.98	322.19	1595.53	7650.83	20564.18	885.97	11164.50	24077.85
TOTAL	6356.87	4154.10	23767.04	25487.32	101661.94	4520.95	64286.28	140460.90

Prices are for 76 cells/hr X 8280 hr/yr = 629,280 cells

TABLE 3.9-12

NPMS PRICES IN CENTS/WATTS (1975)

7.6 cm DIAMETER SUBSTRATES

PROCESS STEP	0.489 EQPT QUAN	96.9 SQFT QUAN	2.133 DLAB QUAN	1.225 MATS QUAN		1.225 UTIL QUAN	STEP TOTAL	
				21% METAL	107% METAL		21% METAL	107% METAL
1	.09	.16	.76	.21	.55	.12	1.34	1.67
2	.02	.02	.08	.01	.01	.00	.13	.13
3	.92	.17	1.83	0	0	.31	3.21	3.21
4	.13	.20	.95	1.55	7.39	.18	3.01	8.85
5	.02	.02	.08	.01	.01	.00	.13	.13
6	.10	.17	.82	.12	.28	.14	1.37	1.53
7	.08	.04	.10	.77	2.06	.11	1.19	2.48
TOTAL	1.37	.77	4.70	2.67	10.31	.87	10.39	18.03

Prices are for 999,146 watts of 14% efficient (encapsulated) cells.

TABLE 3.9-13

NPMS PRICES IN CENTS/WATT (1975)

12 cm DIAMETER SUBSTRATES

PROCESS STEP	0.489 EQPT QUAN	96.9 SQFT QUAN	2.133 DLAB QUAN	1.255 MATS QUAN		1.255 UTIL QUAN	STEP TOTAL	
				21% METAL	107% METAL		21% METAL	107% METAL
1	.05	.09	.43	.17	.52	.07	.81	1.16
2	.01	.01	.03	.00	.00	.00	.05	.05
3	.37	.07	.73	0	0	.12	1.29	1.29
4	.07	.11	.53	1.52	7.36	.10	2.33	8.17
5	.01	.01	.03	.00	.00	.00	.05	.05
6	.06	.10	.47	.09	.26	.08	.79	.95
7	.07	.03	.16	.77	2.06	.09	1.12	2.42
TOTAL	.64	.42	2.39	2.56	10.20	.45	6.45	14.10

Prices are for 996,378 watts of 14% efficient (encapsulated) cells.

From an overall view, costs of materials and direct labor prove to be the driving forces. The price contributions of capital equipment, floor space, and utilities represent 17% to 29% of the price of 7.6 cm cells and only 11% to 23% of the price of 12 cm cells.

3.9.5 REVISED IPEG PRICE ANALYSIS

A detailed exercise of the JPL Interim Price Estimation Guidelines (IPEG) analysis for the preliminary NPMS process sequence of Table 3.9-1 has been presented in the previous sections. As discussed in the introduction of Section 3.9, elimination of the scrubbing step will impact the results of that analysis. Moreover, it was determined that one of the prime cost drivers was the cost of palladium chloride, the source of palladium in the immersion and electroless palladium solutions. It had been previously assumed that $PdCl_2$ was available at a cost of $5.00/gram (in 1976 dollars). Later investigations have led to a source of $PdCl_2$ available at a cost of $1.66/gram (in 1978 dollars). This will significantly impact the initial IPEG analysis. Accordingly, this lower cost can be factored into the initial computations. On the other hand, the cost of tin has been rapidly increasing on the open market and this has caused the cost of lead-tin solder to rise rapidly. The original cost assumption of $2.98/lb (1977 dollars) for the 60 Sn/40 Pb solder has been replaced by $4.33/lb. (1978 dollars). This higher cost for solder has also been utilized in revising the previous computations.

The summary of the revised IPEG analysis is presented in Tables 3.9-14, 3.9-15, and 3.9-16. The process steps in these tables correspond to the revised NPMS process sequence of Table 3.9-2. As in the original IPEG analysis, four separate cell geometries were considered: 7.6 cm diameter and 12 cm diameter

TABLE 3.9-14

FMS PRICES IN CENTS/WATTS (1975)

7.6 cm DIAMETER SUBSTRATES

PROCESS STEP	0.489 EQPT QUAN	96.9 SQFT QUAN	2.133 DLAB QUAN	1.255 MATS QUAN		1.255 UTIL QUAN	STEP TOTAL	
				21% METAL	107% METAL		21% METAL	107% METAL
1	.09	.16	.76	.15	.24	.12	1.28	1.37
2	.02	.02	.08	.01	.01	.00	.18	.13
3	.13	.20	.95	.51	2.07	.18	1.97	3.53
4	.02	.02	.08	.01	.01	.00	.13	.13
5	.10	.17	.82	.12	.28	.14	1.37	1.53
6	.08	.04	.19	.88	2.62	.11	1.30	3.04
TOTAL	.46	.61	2.88	1.67	5.23	.56	6.17	9.74

Prices are for 999,146 watts of 14% efficient (encapsulated) cells.

TABLE 3.9-15

NPMS PRICES IN CENTS/WATT (1975)

12 cm DIAMETER SUBSTRATES

PROCESS STEP	0.489 EQPT QUAN	96.9 SQFT QUAN	2.133 DLAB QUAN	1.255 MATS QUAN		1.255 UTIL QUAN	STEP TOTAL QUAN	
				21% METAL	107% METAL		21% METAL	107% METAL
1	.05	.09	.43	.11	.20	.07	.75	.84
2	.01	.01	.03	.00	.00	.00	.05	.05
3	.07	.11	.53	.47	2.04	.10	1.29	2.85
4	.01	.01	.03	.00	.00	.00	.05	.05
5	.06	.10	.47	.09	.26	.08	.79	.95
6	.07	.03	.16	.88	2.62	.09	1.23	2.93
TOTAL	.27	.35	1.65	1.56	5.12	.33	4.17	7.73

Prices are for 996,378 watts of 14% efficient (encapsulated) cells.

TABLE 3.9-16

REVISED NPMS ADD-ON PRICES (CENTS/WATT)

(For comparison, prices in parentheses are results of the initial analysis of Section 3.9-4).

SUBSTRATE DIAMETER	TOTAL CELL METAL COVERAGE (AS % OF FRONT SURFACE AREA) 10%	2%
7.6 cm	9.74 (18.03)	6.17 (10.39)
12 cm	7.73 (14.10)	4.17 (6.45)

JPL IPEG Analysis

Reference: 1975 Dollars

14% Encapsulated Cell Efficiency

circular substrates each with either full metal coverage of the cell back or with patterned back metal covering only 14% of the back surface area. Tables 3.9-14 and 3.9-15 give the add-on NPMS prices in 1975 cents/watt for each expense category of each process step as well as the totals for each category and each step. Table 3.9-14 is for the 7.6 cm solar cell and Table 3.9-15 is for the 12 cm solar cell. Table 3.9-16 summarizes the total add-on price for each of the four examples cited. For comparison, the results of the previous analysis are shown in parentheses. As can be seen, the present modifications have resulted in dramatic cost reductions for the NPMS system, enhancing its probability for meeting advanced cost goals.

With respect to the prices presented in the previous tables, it must be emphasized that the inputs to the IPEG analysis were prepared in a very conservative manner. For example, the input with significant influence on computed prices is the throughput or cycle time for each process step. The prices reported above could be reduced substantially by assuming shorter cycle times in several steps. For example, a total cycle time of 15 minutes was assumed for process step 1a (from Table 3.9-4), while that step includes only a 10 second etch and a water rinse. A less conservative approach might reduce that 15 minute cycle time by a factor of two or three. Such conservatism tends to make the cost figures "worst case" numbers.

There are a number of examples of this conservatism throughout the IPEG analysis which has been presented. It is believed, however, that this approach is more realistic than most. It should be recognized that the IPEG procedure itself is any thing but conservative. By careful use of input data, the IPEG optimism and input conservatism should balance each other, and then output prices may bear some resemblance to reality.

4.0 CONCLUSIONS

The technical and patent literature discussing palladium silicide formation and palladium-silicon contacts is strongly supportive of the use of palladium for solar cell metallization systems.

The application of metal contacts by chemical plating techniques, particularly using immersion and electroless plating solutions, provides a very desirable means for metallizing both regular and irregular silicon solar cell surfaces.

The success of the plated palladium-nickel-solder metal contacts judged by adherence, reliability, and uniformity during processing depends very strongly on maintaining a microscopically clean silicon surface immediately prior to the first plating (Pd) application.

Various pre-plating cleaning and surface treatment techniques have been evaluated, and several candidate processes appear to be acceptable. The most consistent cleaning process studied to date has constituted a sequence of oxygen plasma ashing and aqua regia etching; this has minimized the effects of variable processing techniques prior to metallization. However, in most cases a simple etch in a dilute hydrofluoric acid solution is sufficient.

Numerous formulations for an immersion palladium plating solution have been examined. In the course of these studies, a model has been developed to describe the effects of immersion (displacement) palladium plating reactions exhibited by these formulations. A much improved immersion palladium bath has resulted from this work. In fact, it is believed that a thin and very adherent displacement palladium layer can now be routinely formed on silicon solar cell surfaces.

Nitrogen (N_2) is an adequate ambient for heat treatment of palladium films to form palladium silicide (Pd_2Si). Forming gas is not required and is, in fact, likely to introduce additional problems if used.

The new ammonium fluoride immersion palladium solution permits effective use of low temperature annealing cycles. Results of heat treating layers formed with this solution seem to agree with behavior cited in the literature for vacuum deposited palladium films.

Electroless plating of solar cells in the dark permits simultaneous plating of front and back metal layers of acceptable thicknesses.

Excellent results have been obtained using the plated palladium-nickel-solder metallization system for both textured front surface and non-textured solar cells. This system can be used to give an adherent, low resistance metallization for solar cells. No p-n junction degradation is apparent. Good fill factors, inherent to the p-n junction device, have been maintained.

The results of the costing exercise, using the JPL IPEG price analysis, are very encouraging. This analysis shows that the primary price drivers are the materials costs for electroless palladium plating and solder coating, and the labor costs for the chemical plating steps. In spite of this, the total add-on price for the current process sequence is reasonable. For 12 cm diameter cells with conventional metal patterns the price is about 8 cents per watt. If the back metal contact were patterned to reduce materials consumption, this price would be lowered to about 4 cents per watt.

5.0 RECOMMENDATIONS

It is recommended that a plated metallization system be adopted for solar cell production and be scaled to production levels by the solar cell industry. On a laboratory scale, the palladium-nickel-solder metallization system has proven to be capable of producing high quality ohmic contacts. Low contact resistance and good metal conductivity are maintained. Strength of adhesion is such that the typical failure mechanism upon perpendicular pull testing is silicon fracture beneath the contact.

A document, "Material, Supply, and Process Specifications and Procedures for Metallization of Large Silicon Wafers with the Palladium-Nickel-Solder Metallization System," has been prepared and will be available from JPL upon request. It is recommended that this process specification serve as the starting point for adaptation of the metallization system to any particular manufacturer's solar cell fabrication sequence.

It is recommended that several actions be pursued for future improvement and development toward the goal of additional cost reduction. Several possibilities exist for either independent or simultaneous improvements. Palladium layer thickness may be reduced to lower material costs. The first palladium application and heat treatment, or the second palladium and heat treatment, may be eliminated. The metallization sequence may be reorganized to effect a single heat treatment after all plating is completed. Lead-tin solder may be replaced with lower cost conductors such as copper.

6.0 NEW TECHNOLOGY

The following new technology item has been developed on this program:

Description: Improved, ammonium fluoride based, immersion palladium solution.

Innovator: Terry G. Sparks

Progress Reports: Technical Progress Report No. 5, April 1978.

Pages: 19 - 24.

7.0 NPMS ANNOTATED BIBLIOGRAPHY

A. GENERAL REFERENCES

1. Feldstein, N., "Electroless Plating in the Semiconductor Industry," Solid State Technology, 16, 87 (Dec. 1973).
   Review of the use of electroless metal plating, including nickel, on semiconductors.

2. Graham, A.K., ed., Electroplating Engineering Handbook, Third Edition, Van Nostrand Reinhold Company, New York, 1971.
   General reference work for plating techniques. Part I, Chapter 15 discusses electroless plating solutions.

3. Lowenheim, F.A., ed., Modern Electroplating, Third Edition, John Wiley & Sons, Inc., New York, 1974.
   Excellent general reference for chemical plating techniques and solutions, including electroless nickel and palladium. In particular, see chapters 12, 14, and 31.

4. Rhoda, R.N., "Electroless Plating with Precious Metals," Plating, 50, 307 (April 1963)

   A review of general processes for displacement and electroless plating of procious metals.

5. Saubestre, E.B., "Electroless Platind Today," Metal Finishing, 50, 67 (June 1962); 60, 49 (July 1962); 60, 45 (August).

   A series of articles reviewing techniques and deposited properties of all electroless plating reported to that date. Also includes discussion of pretreatments and plating of semiconductor material.

B. METAL-SILICIDE CONTACTS AND CONTACT FORMATION

6. Anand, Y., "Zero-Bias Schottky Barrier Detector Diodes," U.S. 3,968,272 (cl. 427-84; B05D5/12), July 6, 1976. Appl. 436,431, Jan. 25, 1974.
   A Schottky diode using metal (Pd, Pt, Hf) silicide-silicon barrier.

7. Austen, H.E., and R.D. Fisher, "Internal Stress of Electroless Metal Films on Single Crystal Silicon," J. Electrochem. Soc. 116, 185 (1969).
   Stress measurements for electroless Ni and Co films as a function of thickness.

8. Bower, R.W., and J.W. Mayer, "Growth Kinetics Observed in the Formation of Metal Silicides on Silicon," Appl. Phys. Lett., 20 (9), 359 - 361, (1972).
   Brief discussion of silicide growth from evaporated metal films.

B. METAL-SILICIDE CONTACTS AND CONTACT FORMATION (continued)

9. Bower, R.W., D. Sigurd, and R.E. Scott, "Formation Kinetics and Structure of Pd_2Si Films on Si," Solid-State Electron., 16 (12), 1461 - 1471, (1973).
   Rates of palladium silicide formation from evaporated Pd layers on different Si crystal orientations.

10. Bower, R.W., et. al., "Analysis of Semiconductor Structures by Nuclear and Electrical Techniques: Silicide Formation," Air Force Cambridge Research Laboratories Report No. AFCRL-TR-74-0247, April 30, 1974.
   Metal silicide formation studies including Ni_2Si, NiSi, and $NiSi_2$.

11. Buckley, W.D., "Electrodes for Amorphous Semiconductor Switch Devices," U.S. 3,877,049 (Cl. 357-2; H01L), Apr. 8, 1975. Appl. 419,633, Nov. 28, 1973.
   Palladium silicide used as a switch contact.

12. Buckley, W. D., and S.C. Moss, "Structure and Electrical Characteristics of Epitaxial Palladium Silicide Contacts on Single Crystal Silicon and Diffused P-N Diodes," Solid-State Electron., 15 (12), 1331, (1972).
   Analysis of Pd_2Si formed at several different temperatures, with attention to preservation of Si crystal structure.

13. Calandrello, N.A., J. Hill, and J. Ryan, "Forming Semiconductor Contacts," Brit. 1,010,398 (Cl. H01L, 17/46), Nov. 17, 1965. U.S. Appl. Feb. 6, 1963.
   Contact to silicon is made by plating Au or Pd on silicon, then plating Ni, then heating to alloy the layers. Ni is applied again to thicken the top metal layer. The metal layers are then solder dipped.

14. Castrucci, P.P., and R.P. Pecoraro, "Palladium Ohmic Contact to Silicon Semiconductor," U.S. 3,431,472 (Cl. 317-324; H01L), Mar. 4, 1969. Appl. Oct. 17, 1967.
   Contact formation by Pd deposition followed by sintering to form Pd_2Si.

15. Chu, W.K., S.S. Lau, J-W. Mayer, and M-A, Nicolet, "Analysis of Semiconductor Structures by Nuclear and Electrical Techniques: Silicide Formation." Air Force Cambridge Research Laboratories Report No. AFCRL-TR-75-0092, Jan. 31, 1975.
   Metal silicide formation studies including Ni_2Si and Pd_2Si.

16. Chuss, J.T., "Applying Metallic Coatings," Fr. 1,486,263 (Cl. H01L), June 23, 1967. U.S. Appl. July 9, 1965.
   Deposition of palladium on Si wafers by means of electroless plating solutions followed by electroless nickel.

17. Dorendorf, H., H. Eger, H. Weidlich, and H. Glawischnig, "Silicon Planar Transistor," Ger. Offen. 2,044,467 (Cl. H01L), Mar. 23, 1972. Appl. P 20 44 467.1, Sept. 8, 1970.
   A device using Al over Pt_2Si or Pd_2Si contacts. The contacts are formed from 50 - 100Å of evaporated or sputtered metal.

B. METAL-SILICIDE CONTACTS AND CONTACT FORMATION (continued)

18. Drobek, J., R. C. Sun, and T.C. Tisone, "Interdiffusion and Compound Formation in Thin Films of Pd or Pt on Si Single Crystals," Phys. Stat. Sol. (A), 8 (1), 243 - 248, (1971).
Silicide formation interpreted from electron microscope observations.

19. Dudko, G.N., A.G. Pilipenko, and V.I. Tarakanov, "Structure of Films and Phase Changes in the Palladium-Silicon Contact Zone," Isv. Vyssh. Ucheb. Zaved., Fiz., 17 (5), 21 (1974).
Improvements in Pd_2Si contact conductance by altering the silicide crystal structure by annealing.

20. Hutchins, G.A., and A. Shepela, "The Growth and Transformation of Pd_2Si on (111), (110) and (100) Si," Thin Solid Films, 18 (2), 343 - 363, (1973).
Thorough discussion of Pd_2Si formation at different temperatures and on differently oriented Si crystals.

21. Iwasa, H., M. Yokozawa, and I. Teramoto, "Electroless Nickel Plating on Silicon," J. Electrochem. Soc., 115 (5), 485 (1968).
Differences in plating rates for n- and p- type silicon on wafers with p-n junctions.

22. Kahng, D., and M.P. Lepselter, "Barrier Diode with Metal Contact," U.S. 3,290,127 (Cl. 29-195), Dec. 6, 1966. Appl. March 30, 1964.
Device illustrates use of palladium silicide as an electrical contact.

23. Kircher, C.J., "Metallurgical Properties and Electrical Characteristics of Palladium Silicide-Silicon Contacts," Solid-State Electron., 14 (6), 507 - 513, 1971.
General characterization of Pd_2Si contacts.

24. Lau, S.S., and D. Sigurd, "An Investigation of the Structure of Pd_2Si Formed on Si," J. Electrochem. Soc., 121 (11), 1538 - 1540, (1974).
Crystal size and formation kinetics of Pd_2Si formed from Pd films on silicon.

25. Lee, D.H., R.R. Hart, D.A. Kiewit, and O.J. Marsh, "Alloying of Thin Palladium Films with Single Crystal and Amorphous Silicon," Phys. Stat. Sol. (A), 15 (2), 645 - 651, (1973).
Conditions under which palladium silicide will form.

26. Mayer, A., "Forming Ohmic Contacts on Metal-Insulator-Semiconductor Components," Ger. Offen. 2,128,360 (Cl. H01L), Jan. 13, 1972. U.S. Appl. 50,506, June 29, 1970.
Deposition of Pt or Pd from an acid solution onto Si substrate and formation of a silicide by heating the substrate.

27. Mayer, J.W., and K.N. Tu, "Analysis of Thin-Film Structures with Nuclear Backscattering and X-ray Diffraction," J. Vac. Sci. Technol., 11 (1), 86 (1974).
Includes general review of contemporary studies of silicide formation.

B. METAL-SILICIDE CONTACTS AND CONTACT FORMATION (continued)

28. Michelot, P., "Electrical Contacts on the Surface of Semiconductors," Fr. 1,197,979, Dec. 3, 1959.
Formation of a silicide by heating the substrate during metal deposition by evaporation.

29. Nakamura, K., J.O. Olowolafe, S.S. Lau, M.A. Nicolet, J.W. Mayer, and R. Shima, "Interaction of Metal Layers with Polycrystalline Si," J. Appl. Phys., 47 (4), 1278 - 1283, (1976).
Details of silicide formation on polycrystalline substrates.

30. Nuzillat, G., and C. Arnodo, "Adjusting the Threshold Voltage of Field Effect Transistors," Ger. Offen. 2,533, 460 (Cl. H01L), Feb. 5, 1976.
Description of a device with a gate composed of palladium silicide.

31. RCA Corp., "Semiconductor Ohmic Contact," Brit. 1,321, 034 (cl. H01L), June 20, 1973. U.S. Appl. 151,340, Apr. 5, 1971.
Contacts of platinum silicide are formed.

32. Shepela, A., "The Specific Contact Resistance of Pd_2Si Contacts on n- and p- Si," Solid-State Electron., 16 (4), 477 (1973).
Effects of dopants and resistivity on contact resistance.

33. Sullivan, M.V., and J.H. Eigler, "Electroless Nickel Plating for Making Ohmics Contacts," J. Electrochem. Soc., 104 (4), 226 (1957).
A technique for plating nickel to silicon plus measurements of plating rate, contact adhesion, and contact resistance.

34. Tanaka, Y., and H. Hattori, "Semiconductor Devices," Fr. Demande 2,183,111 (Cl. H01L), Jan. 18, 1974. Japan Appl. 72 44,141, May 2, 1972.
Contacts of platinum silicide were produced using chemically deposited platinum, heating to form the silicide, and over-plating with electroless nickel.

35. Teramoto, I., H. Iwasa, and H. Tai, "Contact Resistance of Electroless Nickel on Silicon," J. Electrochem. Soc., 115 (9), 912 (1968).
Contact resistance as a function of silicon resistivity and heat treatment.

36. Tu, K.N., "Selective Growth of Metal-Rich Silicide of Near-Noble Metals," Appl. Phys. Lett., 27 (4), 221 (1975).
A discussion of metal diffusion in the formation of metal silicides.

37. Tu, K.N., W.K. Chu, and J.W. Mayer, "Structure and Growth Kinetics of Ni_2Si on Silicon," Thin Solid Films, 25, 403 (1975).
Formation mechanisms and rates for low temperature (200°C - 325°C) nickel silicide.

B. METAL-SILICIDE CONTACTS AND CONTACT FORMATION (continued)

The following articles are from the Proceeding of the Symposium of Thin Film Pheonomena -- Interfaces and Interactions, ed: J. Baglin and J. Poate, The Electrochemical Society Proceddings, Vol. 78-2 (Princetone, N. J.).

38. Bene, R.W., and R. M. Walser, "A Membrane Model for Interphases", p. 21.

    Thermodynamic discussion of interface region to justify the phase formation of Si-Pd at less than 1/2 of the lowest eutectic temperature.

39. Canali, C., G. Majni, and G. Ottaviani, "Near-nobel Metal Film/ Semiconductor Interactions: Compound Formation", P. 38.

    Study of Si/Pt and Ge/Pd alloying showed that the first phase is metal rich (Pt_2Si) but as the metal is reacted a Si rich phase is formed (PtSi).

40. Finstad, T.G., "Diffusion Effects and Silicide Formation with Ni and Pt Thin Films Double Layers on Si", p. 44.

    Study of alloying effects of Si/Ni/Pt and Si/Pt/Ni metallization systems.

41. Ho, P.S., U. Koster, J. E. Lewis, and S. Libertini, "Material Reactions in Al/Pd_2Si/Si Junctions", p. 66.

    Study of thermal induced instability of Al/Pd_2Si/Si contacts.

42. Phillips, J. C. "Chemistry and Structure of Transition Metal Silicide-Silicon Interfaces", p 3.

    Examination of atomic model of silicide to silicon interfaces for Ni and Pd silicides.

43. Roth, J.A., "Intrinsic Properties of the Silicide/Silicon and Silicide/ Vacuum Interfaces," p. 29.

    Study of bonding structure of Pd-Si interface showing presences of covalent bonding and a silicon layer of Pd_2Si when annealed in a vacuum.

C. CHEMICAL PLATING SOLUTIONS

44. Brenner, A., and G. Riddell, J. Res. National Bur. Stan., 37, 32 (1946); Proc. Am. Electroplating Soc., 33, 23 (1946).
    Original references for electroless nickel plating.

C. CHEMICAL PLATING SOLUTIONS (continued)

45. Cohen, R. L., R. L. Meek, and K. W. West, "Sensitization with Palladium-Tin Colloids, I & II", Plating and Surface Finishing, 63, 52 (May 1976); 63, 47 (June 1976).

Discussion of Sn-Pd sensitization for electroless plating.

46. Feldstein, N., and T. S. Lancsek, "A New Technique for Investigating the Electrochemical Behavior of Electroless Plating Baths and the Mechanism of Electroless Nickel Plating," Journal of Electrochemical Society, 118, 869 (June 1971).

Investigation of control for electroless nickel plating process.

47. Graham, A. H., R. W. Lindsay, and S. J. Read, "The Structure and Mechanical Properties of Electroless Nickel", Journal of the Electrochemical Society, 112, 401 (April 1965).

Comprehensive study of Ni-P alloy structure and properties of electroless plated layers after various heat treatment cycles.

48. Gutzeit, G., Plating, 46, 1158, 1275, 1377 (1959); Plating, 47, 63 (1960).

Probable chemical reactions for electroless Ni plating.

49. Honda, T., and Y. Usami, "Electroless Palladium Plating," Japan. 71 01,241 (Cl. C 23c), Jan. 13, 1971. Appl. Aug. 30, 1968.
An electroless palladium solution containing hydrazine sulfate.

50. Johnson, R. W., "Immersion Plating of the Platinum Group Metals" Journal of the Electrochemical Society, 108, 632 (July 1961).

Discussion of palladium dispalcement plating on copper.

51. Korovin, N.V., S.B. Kalmykova, and S. Yu. Vereschinskii, "Solution for Chemical Palladium Plating," U.S.S.R. 291,991 (Cl. C23c), Jan. 6, 1971. Appl. Sept. 15, 1969.
A solution for the chemical Pd plating of metals containing sodium hypophosphite.

52. Matijevic, E., A. M. Poskanzer, and P. Zuman, "The Characterization of the Stannous Chloride/Palladium Chloride Catalysts for Electroless Plating", Plating and Surface Finishing, 62, 958 (October 1975).

Study of colloidal solution of SN/Pd catalyst plating for electroless plating.

53. Marton, J.O., and M. Schlesinger, "The Nucleation, Growth, and Structure of Thin Ni-P Films", Journal of the Electrochemical Society, 115, 16 (January 1968).

Study of nucleation mechanism of electroless nickel on Sn/Pd activation sites.

C. CHEMICAL PLATING SOLUTIONS (continued)

54. deMinjer, C. H., and P. F. v.d. Boom, "The Nucleation with $SnCl_2$-$PdCl_2$ Solutions of Glass Before Electroless Plating", Journal of the Electrochemical Society, 119, 1644 (December 1972).

Study of the $SNCl_2/PdCl_2$ chemical activation kinetics for electroless plating.

55. Murski, K., "Practical Electroless Nickel Plating," Metal Finishing, 68, 38 (1970).
Defines operational parameters and control techniques for electroless nickel plating.

56. Feldstein, F., and R.F. Weightman, "Electroless Palladium Deposition," Plating, 56, 1158 (1969).
Detailed discussion of electroless palladium solutions utilizing sodium hypophosphite.

57. Ranell, A., and A. Holtzman, "Mixed Stannous Chloride-Palladium Chloride Activators: A Study of Their Formation and Nature", Plating, 61, 336 (April 1974).

An investigation of Sn-Pd system activation of electroless plating on dielectrics.

58. Reinhardt, R.A., and K.J. Graham, "Equilibrium and Kinetics of Some Simple Complexes of Palladium (II)." U.S. NTIS, AD Rep., AD A030089, 1976.
Chemical data on complexes and reactions present in electroless plating baths.

59. Rhoda, R.N., "Barrel Plating by Means of Electroless Palladium," J. Electrochem. Soc., 108, 707 (1961).
Discussion of plating metallic substrates with electroless palladium solution utilizing hydrazine.

60. Sard, R., "The Nucleation, Growth, and Structure of Electroless Copper Deposits', Journal of the Electrochemical Society, 117, 864 (July 1970).

Use of $SnCl_2$ sensitization and $PdCl_2$ activation method to initiate electroless plating.

61. Gorgienko, A., "Bath for the Electroless Deposition of Palladium," U.S. 3,418, 143, Dec. 24, 1968. Appl. 660,588, Aug. 15, 1967.
A palladium solution utilizing hypophosphite ion.

62. Vereschinskii, S. Yu., S.B. Kalmykova, and N.V. Korovin, "Electroless Palladium Plating Process," Zashch. Metal, 9 (1), 227 (1973).
Depositing Pd on various metals, graphite, and glass using a solution containing sodium hypophosphite.

63. Zayots, A.I., I.A. Stepanova, and A.V. Gorodyskii, "Chemical Reduction of Palladium by Sodium Hypophosphite," Zashch. Metal., 9, (1), 116 (1973).
Solution composition and conditions for depositing palladium on nickel.